การตรึงพีเอ็นเอ-ดีเอ็นเอไฮบริดบนวัฏภาคของแข็งเพื่อตรวจสอบลำดับเบสของดีเอ็นเอ

นางสาวปรัชญพร ก่อแก้ว

วิทยานิพนธ์นี้เป็นส่วนหนึ่งของการศึกษาตามหลักสูตรปริญญาวิทยาศาสตรมหาบัณฑิต
สาขาเคมี ภาควิชาเคมี
คณะวิทยาศาสตร์ จุฬาลงกรณ์มหาวิทยาลัย
ปีการศึกษา 2550

SOLID-PHASE CAPTURE OF PNA-DNA HYBRIDS FOR DETERMINATION OF DNA BASE SEQUENCES

Miss Pratchayaporn Korkaew

A Thesis Submitted in Partial Fulfillment of the Requirements
for the Degree of Master in Chemistry
Department of Chemistry
Faculty of Science
Chulalongkorn University
Academic Year 2007

Thesis Title	SOLID-PHASE CAPTURE OF PNA-DNA HYBRIDS FOR DETERMINATION OF DNA BASE SEQUENCE
By	Miss Pratchayaporn Korkaew
Field of Study	Chemistry
Thesis Advisor	Associate Professor Tirayut Vilaivan, D. Phil.

Accepted by the Faculty of Science, Chulalongkorn University in Partial Fulfillment of the Requirements for Master's Degree

S. Hannongbua ..... Dean of the Faculty of Science

(Professor Supot Hannongbua, Ph. D.)

THESIS COMMITTEE

..... Chairman

(Professor Sophon Roengsumran, Ph. D.)

Tirayut Vilai ..... Thesis Advisor

(Associate Professor Tirayut Vilaivan, D. Phil.)

Warinthorn Chavasiri ..... Member

(Assistant Professor Warinthorn Chavasiri, Ph. D.)

Uthai Wichai ..... Member

(Uthai Wichai, Ph. D.)

ปรัชญพร ก่อแก้ว : การตรึงพีเอ็นเอ-ดีเอ็นเอไฮบริดบนวัฏภาคของแข็งเพื่อตรวจสอบลำดับเบสของดีเอ็นเอ: (SOLID-PHASE CAPTURE OF PNA-DNA HYBRIDS FOR DETERMINATION OF DNA BASE SEQUENCES) : อ.ที่ปรึกษา : รศ. ดร. ธีรยุทธ วิไลวัลย์; 119 หน้า.

งานวิจัยนี้มุ่งเน้นการสังเคราะห์เพพไทด์นิวคลีอิกแอซิดที่ติดฉลากด้วยสารเรืองแสงและการนำพีเอ็นเอดังกล่าวไปใช้ในการตรวจวัดลำดับเบสของดีเอ็นเอ พีเอ็นเอที่ใช้ในงานวิจัยครั้งนี้เป็นพีเอ็นเอชนิดเบต้า-พิโรลิดินิลพีเอ็นเอ ซึ่งแสดงความสามารถในการจับยึดกับดีเอ็นเอได้อย่างแข็งแรงและมีความจำเพาะเจาะจงสูง สารเรืองแสงที่ใช้ในงานวิจัยนี้ คือ เททระโรดามีน และฟลูออเรสซีน ซึ่งสามารถต่อเข้าที่ปลายด้านอะมิโนของพีเอ็นเอได้บนวัฏภาคของแข็ง พีเอ็นเอที่ติดฉลากด้วยสารเรืองแสงนี้สามารถนำไปวิเคราะห์ลำดับเบสของดีเอ็นเอโดยใช้ร่วมกับตัวดูดซับชนิดแลกเปลี่ยนไอออน วิธีการดังกล่าวอาศัยหลักการดูดซับอย่างจำเพาะเจาะจงของพีเอ็นเอ-ดีเอ็นเอไฮบริดซึ่งมีประจุลบบนตัวดูดซับซึ่งมีประจุบวกและตรวจวัดพีเอ็นเอที่ถูกดูดซับโดยใช้กล้องจุล - ทรรศน์เรืองแสง วิธีนี้สามารถบอกความแตกต่างของดีเอ็นเอเป้าหมายที่มีความยาว 9-13 เบสและมีลำดับแตกต่างกันเพียง 1 ตำแหน่งได้

ภาควิชา.....เคมี.....ลายมือชื่อนิสิต.....ปรัช.....

สาขาวิชา.....เคมี.....ลายมือชื่ออาจารย์ที่ปรึกษา.....ธีรยุทธ วิไลวัลย์.....

ปีการศึกษา.....2550.....

4872358423 : MAJOR CHEMISTRY
KEY WORD : POLYAMIDE NUCLEIC ACID / PNA / DNA
PRATCHAYAPORN KORKAEW : SOLID-PHASE CAPTURE OF PNA-DNA HYBRIDS FOR DETERMINATION OF DNA BASE SEQUENCES. THESIS ADVISOR : ASSOC. PROF. TIRAYUT VILAIVAN, D.Phil., 119 pp

This research emphasize on the synthesis of a new fluorescent labeled peptide nucleic acid (PNA) and its applications as a probe for detection of DNA sequence. The PNA used in this study was a new β-pyrrolidinyl peptide nucleic acid which can bind to DNA with high affinity and specificity. Two fluorescent labeling groups, namely tetramethylrodamine and fluorescein, have been successfully attached at N-termini of PNA oligomers using solid phase strategy. The labeled PNAs in combination with anion exchange supports have been used for analyzing DNA sequences. This method relies on a selective absorption of negatively charged PNA·DNA hybrids onto the positively charged ion exchange support. The presence of PNA·DNA hybrid on solid support can be directly detected by using fluorescent microscopy. This method is capable of detecting a single mismatched base out of 9-13 base DNA targets.

Department.....Chemistry.....Student's signature.....Pratm.....
Field of study.....Chemistry.....Advisor's signature.....Tirayut Vilaivan.....
Academic year.....2007.....

ACKNOWLEDGEMENTS

I would like to reveal my sincere gratitude to Associate Professor Dr. Tirayut Vilaivan, my thesis advisor, for guidance, suggestions and assistance throughout this research. I'm also grateful to thesis examiners: Professor Dr. Sophon Roengsumran, Assistant Professor Dr. Warinthorn Chavasiri, Dr. Uthai Wichai for all valuable comments and suggestions regarding this thesis.

I would like to thank the following: Organic Synthesis Research Unit; Department of Chemistry for the use of facilities, equipment, glassware and chemicals; Thailand-Japan Technology Transfer Project (TJTTP); Miss Lawan Boonprakong, Miss Phakawan Musikapong of the Oral Biology Research center Faculty of Dentistry, Chulalongkorn University for a generous use of Fluorescence Microscope; Mr. Jeerawat Nakkuntod, and Dr. Nattiya Hirankarn of Lupus Research Unit, Department of Microbiology, Faculty of Medicine, Chulalongkorn University for support the DNA samples; Dr. Choladda Srisuwannaket, Dr. Chaturong Suprapprom, Miss Boonjira Boonta, Miss Roejarek Kanjanawarut, Miss Cheeraporn Ananthanawat, and other PNA team member for synthesis of some intermediate compounds and provide a helpful consultant facility, Miss Boonjira Boonta for valuable encouragement and taking care of me, Miss Woraluk Mansawat, Miss Wanna Bannarukkul, Mr. Nuttawut Yothapan for NMR experiments; members of TV & WB group for their friendship, advice and their helpful; my friends for their advice, understanding and social experience through my study period

I would like to pay obeisance to my parent who had supported me with consecutive sincere throughout the research courses; Finally, my success is a very long journey not a destination.

CONTENTS

LIST OF TABLES

Pages

LIST OF FIGURES

Pages

LIST OF ABBREVIATIONS

δ	chemical shift
μL	microliter
μmol	micromole
$[\alpha]_D$	specific rotation
A	adenine
A^{Bz}	N^4-benzoyladenine
Ac	acetyl
AcCl	acetyl chrolide
Ac_2O	acetic anhydride
AcOH	acetic acid
aq	aqueous
Boc	*tert*-butoxycarbonyl
br	broad
Bz	benzoyl
c	concentration
C	cytosine
calcd	calculated
C^{Bz}	N^4-benzoylcytosine
CCA	α-cyano-4-hydroxy cinnamic acid
$CDCl_3$	deuterated chloroform
d	doublet
D_2O	deuterium oxide
DCC	dicyclohexyl carbodiimde
DCM	dichloromethane
DCU	dicyclohexylurea
DIAD	diisopropylazodicarboxylate
DIC	diisopropyl carbodiimide
DIEA	*N*,*N*′-dimethylaminopyridine
DMAP	4-dimethylaminopyridine
DMF	*N*,*N*′-dimethylformamide
DMSO-d_6	deuterated dimethylsulfoxide

DNA	deoxyribonucleic acid
DNS	dansyl chloride
Dpm	diphenylmethyl
EDC·HCl	*N*-(3-dimethylaminopropyl)-*N′*-ethyl-carbodiimide hydrochloride
equiv	equivalent (s)
FAB^+	positive ion fast atom bombardment (mass spectrometry)
Fmoc	9-fluorenylmethoxycarbonyl
FmocCl	9-fluorenylmethyl chloroformate
FmocOSu	9-fluorenylsuccinimidyl carbonate
FRET	fluorescence resonance energy transfer
g	gram
G	guanine
G^{Ibu}	N^2-isobutyrylgaunine
h	hour
HATU	*O*-(7-azabenzotriazol-1-yl)-*N*,*N*,*N′*,*N′*-tetramethyluronium hexafluorophosphate
HOAt	1-hydroxy-7-azabenzotriazole
HOBt	1-hydroxybenzotriazole
HPLC	high performance liquid chromatography
Ibu	isobutyryl
J	coupling constant
Lys	lysine
m	multiplet
MALDI-TOF	matrix-assisted laser desorption/ionization-time of flight
MeCN	acetonitile
MeOH	methanol
MeOTs	methyl tosylate
mg	milligram
MHz	megahertz
min	minute
mL	milliliter
mM	millimolar
mmol	millimole
mp	melting point

mRNA	messenger ribonucleic acid
MS	mass spectrometry
nm	namometer
NMR	nuclear magnetic resonance
Npe	2-(4-nitrophenyl)ethyl
^{o}C	degree celcius
OD_{xxx}	optical density at xxx nm (= A_{xxx})
Pfp	pentafluorophenyl
PfpOH	pentafluorophenol
PfpOTfa	pentafluorophenyl trifluoroacetic acid
PG	an unspecified protecting group
Ph	phenyl
PNA	peptide nucleic acid or polyamide nucleic acid
ppm	part per million
PTC	phase transfer catalyst
R_f	retention factor
RNA	ribonucleic acid
s	singlet
t	triplet
T	thymine
T^{Bz}	N^3-benzoylthymine
TEA	triethylamine
TFA	trifluoroacetic acid
THF	tetrahydrofuran
TLC	thin layer chromatography
TMR	tetramethylrhodamin
T_m	melting temperature
t_R	retention time
Ts	*p*-toluenesulfonyl (=tosyl)
UV	ultraviolet

CHAPTER I

INTRODUCTION

1.1 Peptide Nucleic Acids (PNA)

Deoxyribonucleic acid (DNA) [1] is a molecule that store and transfer genetic information to next generations in all living organisms. DNA consists of repeating unit of nucleotides that connect by phosphodiester linkage. The presence of phosphate groups in backbone make structure of DNA possess negative charge. Peptide nucleic acid was a neutral analogue of PNA first discovered by Nielsen and co-worker in 1991 [2]. It is a DNA analog in which a 2-aminoethyl-glycine unit generally replaced the normal phosphodiester backbone of DNA, resulting in an achiral and uncharged mimic. A methylene carbonyl linker connects natural nuclebase to this backbone at the amino nitrogen as shown in **Figure 1.1**

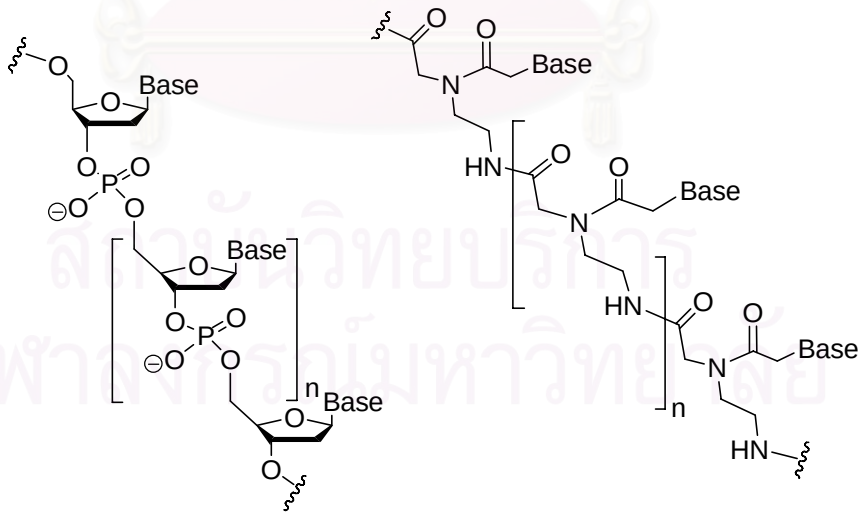

DNA *aeg*PNA (**1**)

Figure 1.1 Chemical structures of a DNA molecule and an *aeg*PNA molecule

1.2 PNA-DNA Hybridization

PNA forms hybrids with high affinity with its complementary DNA/RNA. The hybrids are more stable than that of natural DNA·DNA hybrid. Moreover, the hybridization between PNA and DNA/RNA strictly follows the Watson-Crick base pairing rule as in DNA and RNA hybridizations .(**Figure 1.2**) [3] In addition, PNA can also hybrize to double-stranded DNA by a new strand invasion mechanism to form D-loop or P-loop structures as show in (**Figure 1.3**). [4]

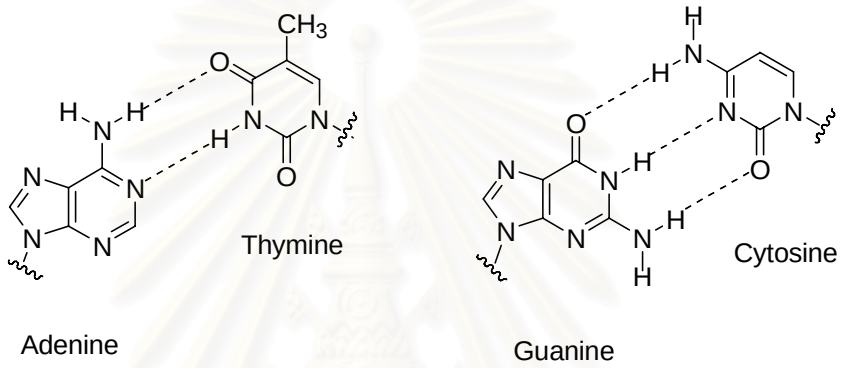

Figure 1.2 Paring between complementary nucleobase by Watson-Click base pairing.

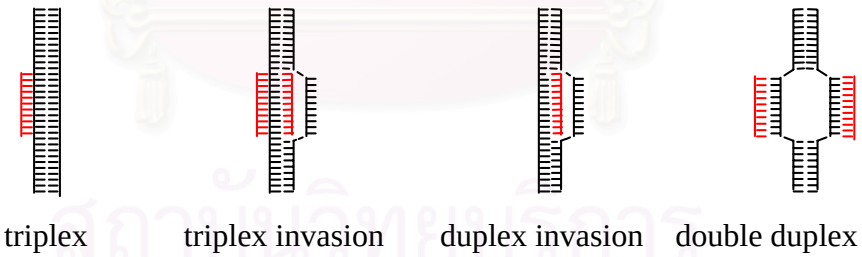

Figure 1.3 Schematic of *aeg*PNA binding mode for double stranded DNA.

In the triplex invasion complex, the second strand of PNA was bound to the dsDNA by a Hoogsteen base-pairing **(Figure 1.4)**. It also shows specific hydrogen bonding between amide N-H of the PNA backbone and the phosphate oxygen of the DNA backbone thereby further contributing to the high stability. The hybrids between PNA with DNA or RNA are more stable than the corresponding DNA·DNA or

DNA·RNA complexes. The thermal stability follows the order PNA·PNA > PNA·RNA > PNA·DNA (> RNA·DNA >DNA·DNA). [5]

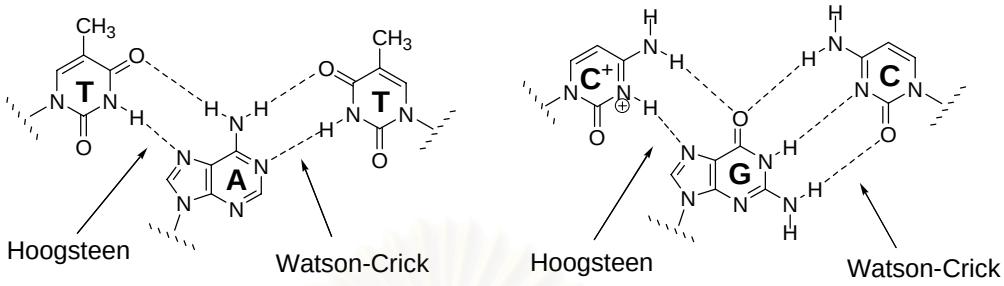

Figure 1.4 Hydrogen bonding *via* Watson-Crick and Hoogsteen base pairing.

The *aeg*PNA is known to bind with DNA in both parallel and antiparallel directions. [6] However, the binding in antiparallel orientation has a marginally higher stability. In case of PNA_2·DNA triplexes, the first PNA strand binds with DNA in antiparallel orientation resulting from Watson-Crick base pairing, and the second PNA strand binds the PNA·DNA duplex via Hoogsteen hydrogen bonding in parallel direction to the DNA stand. [7]

1.3 Modification of PNA

This original PNA reported by Nielsen in 1991 [2] shows many important features such as the ability to hybridize with DNA target with high affinity and specificity. Furthermore, PNA are not substrates for common enzymes such as nuclease and proteases. These special features of PNA make it potentially useful in antisense/antigene therapeutics. However the main drawbacks of PNA are the rather poor water solubility [8] and poor cellular uptake [9] in addition to the poor discrimination between parallel and antiparallel binding direction. Consequently, various attempts have been made by many research groups to modify the structure of parent *aeg*PNA to improve some properties such as binding properties, direction selectivity, base paring specificity, water solubility and cellular uptake. [10]

Recently, Vilaivan and co-workers [11] have proposed a new conformationally rigid pyrrolidine PNA based on prolyl-2-aminocyclopentane carboxylic acid (ACPC) backbones (**Figure 1.5**). This PNA shows a number of

unique properties. For example it can form a very stable 1:1 complex with complementary DNA with high sequence specificity. When the sequence is homopyrimidine, this PNA system hybridize with DNA target in duplex rather than triplex as in Nielsen's PNA. It also binds to DNA only in antiparallel direction.

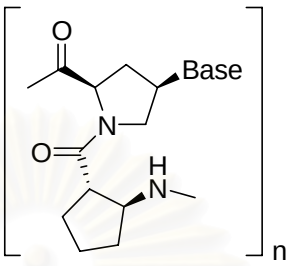

Figure 1.5 Structure of Vilaivan's ssACPC PNA. [11]

1.4 Application of peptide nucleic acid

PNA can be used to develop in a number of biotechnological and medical applications including device for genetic sequence determination, modulation of PCR analysis, microarray hybridization as well as antisense and antigene technology. Most of applications of PNA involve the use of the original Nielsen's aegPNA system since it is the only one that is presently commercially available.

1.4.1 Antigene and antisense application of PNA

Due to the strength of binding to of DNA and RNA, PNA has an obvious potential apply in therapeutics particularly as antigene and antisence drugs. PNA can be designed to recognize to complementary DNA sequences in a particular gene of interest with the aim that they should interfere with the transcription of that gene (so called antigene strategy). Whereas, PNA can also be designed to recognize and hybridize to complementary sequences in mRNA and thereby inhibit its translation (antisense strategy) as shown in **(Figure 1.6.)**. [12] The basic mechanism of antisense effects by oligonucleotides is considered to be ribonuclease H (RNase H) mediates cleavage of RNA strand in oligonucleotide-RNA heteroduplex. Since PNA·RNA duplexes are not substrates for a RNAse-H, antisene inhibition of translation by PNA

is therefore mechanistically different from that of phosphorothiotes oligonucleotides. Consequently, sensitive targets for phosphothioate oligonuecleotides are not necessarily expected to be good targets for PNA. Indeed, sensitive RNA targets for PNA oligomers have been proposed to be the targets at which the PNA can physically interfere with mRNA functions. [12]

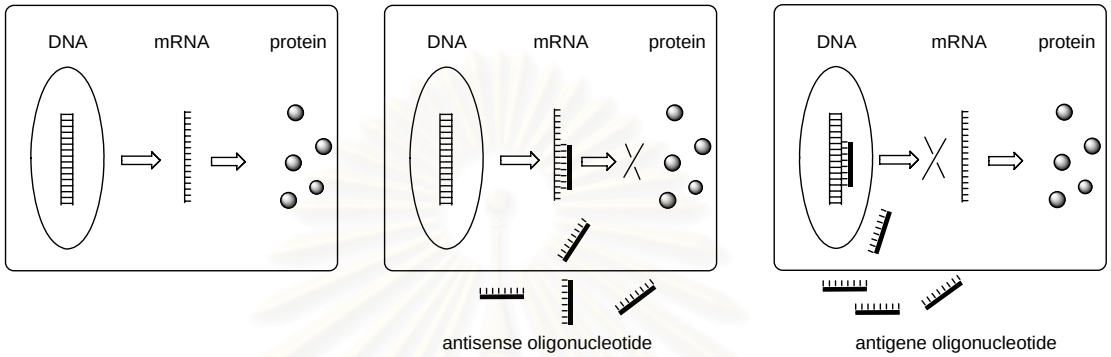

Figure 1.6 Schematic representations of the antisense inhibition and antigene inhibition. An antisene agent (e.g. PNA) binds to an mRNA containing the complementary sequence and can inhibit the expression of a protein at the level of translation. On the other hand, an antigene agent binds directly to a complementary sequence in the DNA and thereby inhibit transcription of the gene to the mRNA. [12]

1.4.2 PNAs as tools in biotechnology

Over the past years, fluorescence-based methods of investigation have become gradually more important in many different areas, most of all in biochemical analysis, nucleic biosensors and diagnostics for DNA sequence analysis. Above all this is due to the high sensitivity of fluorescence detection. [13]

The fluorescent probe is regularly covalent bond with the molecule analysis (**Figure 1.7**). Also, certain intercalation dyes do not fluoresce until they have been included into the DNA double helix.

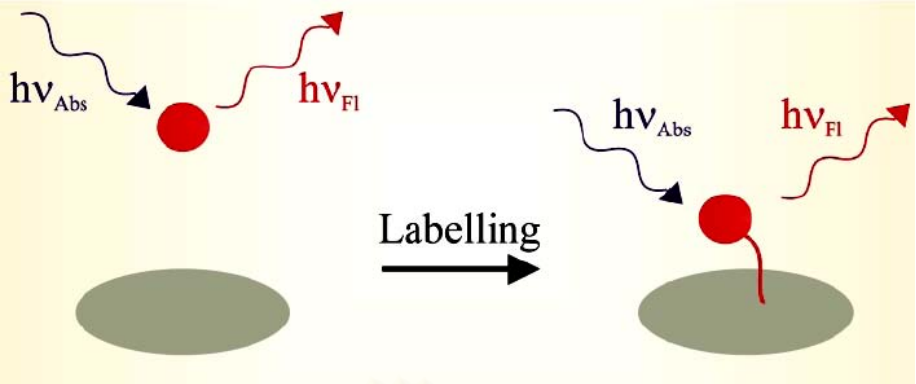

Figure 1.7 Fluorescent labeling. After coupling the fluorescent dye to the target molecule, its presence can be showed via the fluorescence of the probe. [13]

PNA showed a number of promising application in biotechnology. The polymerase chain reaction (PCR) has been widely used for various molecular genetic application including the amplification of variable number of tandem repeat (VNTR) loci for the purpose of genetic typing. Small PNA oligomers are used to block the template, and the latter becomes unavailable for intra- and inter-strand interaction during resuscitation. On the other hand, the primer extension is not blocked; during this extension, the polymerase displaces the PNA molecules from the template and the primer is extended toward completion of reaction. [12] In 1999, Whitcombe and co-worker [14] reported a system for detection of DNA sequence by using self-probing mechanism which rely on energy transfer between fluorophore and a proximal quencher molecule. In the same year, Nikiforov and Jeong [15] reported a new method for detection of DNA sequences using PNA probes (9-13 mer) labeled with fluorescent dye in combination with cationic polylysine. The method has been applied to the typing of single-nucleotide polymorphism in PCR product.

The principle of Fluorescence resonance energy transfer (FRET) is often used for detecting specific interactions between biological molecules. In this technique, two fluorophores donor and acceptors fluorophores are required. The efficacy of the donor-acceptor energy transfer is reversely proportional to the sixth power of the distance between the fluorophores residues. Therefore, upon excitation at the donor absorption region and registration of the acceptor's emission, the efficiency of the energy transfer is extremely sensitive to changes in the distance between the two

fluorophores. The techniques have been used in several studies of DNA hybridization. [16]

In 2002, Bazan et al. [17, 18] proposed a new method for DNA sequence using fluorescent labeled PNA coupled with cationic conjugated polymer (CCP). The light-harvesting properties of CCP were used to sensitize the emission of a dye on the PNA probe by FRET from CCP to the fluorphore (C*) labeled PNA. Signal transduction was controlled by binding between the PNA probe and the DNA target. The overall scheme is shown in **Figure 1.8**

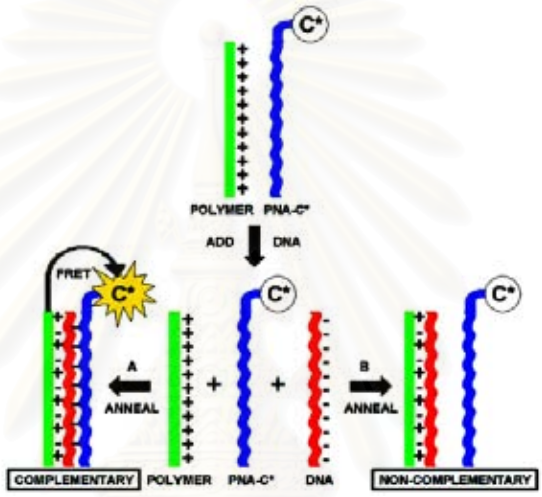

Figure 1.8 Schematic representation for the use of a water-soluble CP with specific PNA-C* optical reporter probe to detect a complementary. [18]

Furthermore, in the next year, they also studied polythiophene another conjugated polymer for detection of DNA in combination with fluorescent labeled PNA probe. In addition, they also developed a method for detection of DNA sequence analysis employing fluorescent labeled PNA probe coupled with CCP and ethidium bromide (ED) which acted an intercalator. In the presence of the complementary DNA, FRET from CCP to generating the fluorophore labeled PNA occurred, which then continued to ED fluorescent. [19-22]

1.4.3 PNA as a probe in nucleic acid biosensor

In the past**,** DNA probe was primarily used as nucleic biosensors for DNA sequence analysis **(Figure 1.9)**. Recently, PNA has been used as a probe in stead of

DNA improve the quality of assay. In these sensors, single-stranded PNA probes are often conjugate with optical (such as fluorescence labeled analy), electrochemical, or mass-sensitive transducers to detect the complementary (or mismatch) DNA strand in the sample. PNA can also labeled and used as a tag, encoding the structure of the attached molecule, by a defined base sequence. Brand, *et al*. [23] reported a preparation of peptide nucleic acid (PNA) microarrays by probe synthesis and selective coupling of full-length molecules. Such microarrays were used for direct detection of the hybridization of unlabelled DNA by time-of-fight secondary ion mass spectrometry (TOF-SIMS).

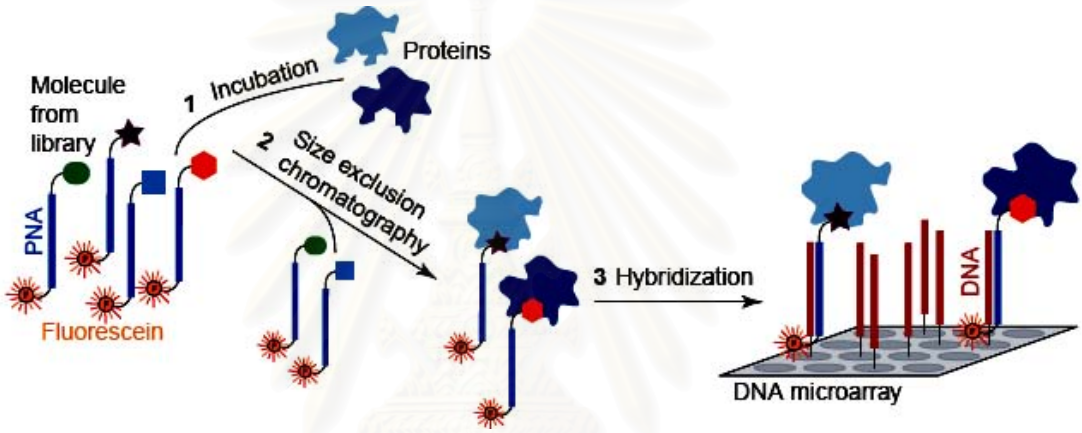

Figure 1.9 Molecule sorting on spatially addressable microarrays. [24]

The remarkable decreasing in stability in the presence of one-base mismatch in PNA·DNA duplexes marks PNA a very useful tool for detection of single nucleotide polymorphisms (SNP). For example, a detection system has been developed by Komiyama *et al*. in 2003 [25] When the target site in DNA sample is perfectly complemented to the PNA probe, the PNA·DNA hybrid is stable against enzymatic digestion by S1 nuclease. On the other hand, when the hybrid contains one or more mismatch bases, it will be completely digested as a result of its lower stability compared to the fully matched hybrid. The difference between the (matched) PNA·DNA hybrid and the (mismatched) single stranded PNA plus free nucleotides were observed after staining with a 3-3'-diethylthiadicarbocyanine dye which changes its color upon binding to PNA·DNA duplex as shown in **Figure 1.10**.

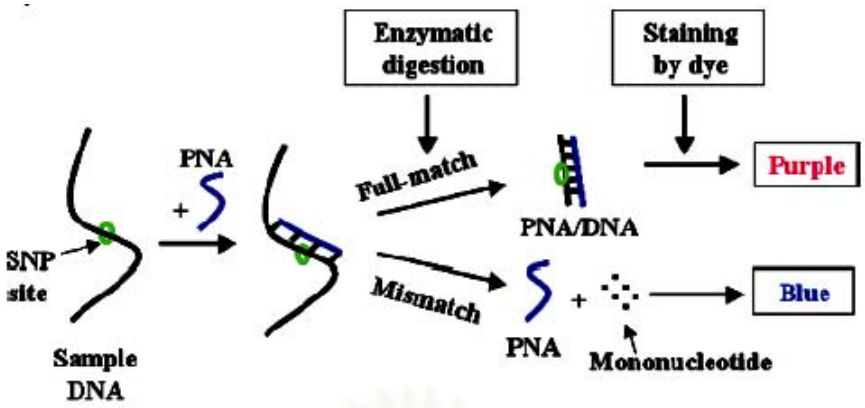

Figure 1.10 Strategy for SNP detection by the PNA/Nuclease/Dye system. [25]

In recent year, fluorescent labeled PNAs have been widely used as diagnostic probes for nucleic acid sequence studies. In 2000, Svanvik and coworkers [26] used PNA to which the cyanine dyes thiazole orange (TO) as a probe for DNA sequence determination. This technique focused on the large fluorescence enhancement of TO upon binding of the PNA to DNA. When the PNA probe hybridize with its complementary DNA target, the dye binds to DNA to generate fluorescence, whereas the unhybridized probe gave only low fluorescence. Therefore, the labeled PNA can be used to detect the DNA sequence based on the fluorescence enhancement. The principle of the strategy is shown in **Figure 1.11**.

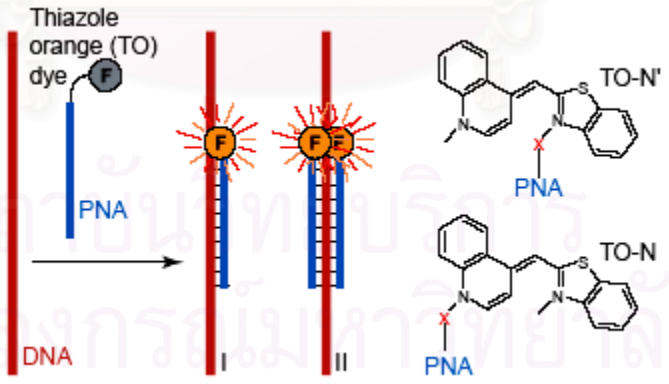

Figure 1.11 Schematic diagram showing how light-up probes work when interact with single-stranded target nucleic acids. The linker is attached to PNA TO-N and TO-N' of thiazole orange. [24]

In 2002, Kool and Sando [27] reported a system for detection of DNA sequence using DNA probe. The so-called QUAL probe is labeled with a fluorophore and a quencher (dabsylsulfonate) which is also a leaving group. The presence of a thiol-labelled DNA complementary to the probe and a DNA template leads to ligation between the probe and the thiol DNA with displacement of dabsylate. The loss of quenching was monitored by fluorescence spectroscopy.

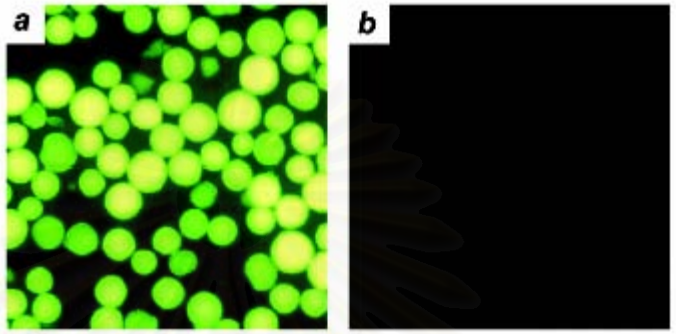

Figure 1.12 Dabsyl-mediated autoligation of DNAs on solid support. Photographs show incubation with (a) complementary (b) single mismatch target using a dabsyl/fluorescein 13mer probe. No washing was done. [27]

In 2004, the same group describe sequence determination of closely related RNA and DNA targets by multicolor quencher probes, used the same principle. [28]

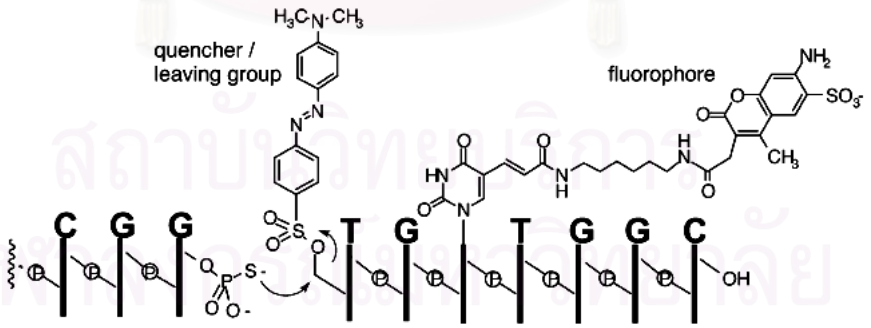

Figure 1.13 Principle of DNA-RNA sequence analysis using QUAL probe. [28]

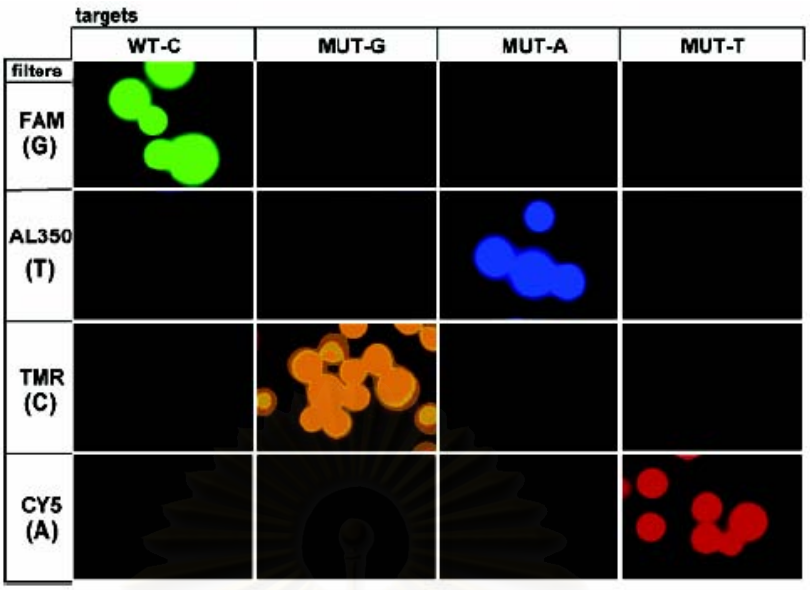

Figure 1.14 Tests of competing four-color probes having single nucleotide differences for ligation to a nucleophile probe (Ps) on PEG-polystyrene beads. [28]

Recently, quencher-free MBs have been synthesized from DNA that utilize the nucleobases as quencher. This strategy allows the inclusion of fluorophores at various points in the oligonucleotide sequence, and allows incorporation of multiple fluorophores in principle. [29]

Figure 1.15 General principle of stemless PNA molecular beacons. Fluorescence is observed upon duplex formation.[30]

The use of single-fluorophore-labelled PNA as probes for nucleic acid sequences detection was reported by Appella and coworkers in 2005. [30] The probe exhibited a fluorescent signal only in the presence of the target oligonucleotide due to the separation of the fluorophore and the nucleobase which acted as quencher.

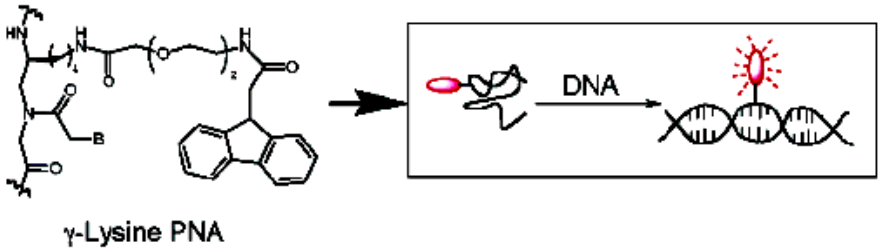

Figure 1.16 Fluorescence of PNA molecular beacons is observed upon duplex formation. [30]

In 2007, Appella and Zhang [31] used the incorporation of a cyclopentane-modified PNA into the surface-bound probe to detect DNA. One PNA is used as capture probe (PNAR) to engage complementary DNA to a surface. Another PNA, labeled with biotin, is used as a detecting probe (PNAα) **Figure 1.17**. Detection of the biotin-labeled PNAα, with commercially available avidin-horseradish peroxidase conjugate (HRP-avidin) and tetramethylbenzidine (TMB). The hybridization resulted in a colored signal visible to the naked eyes or can be measured by UV-visible spectrophotometry.

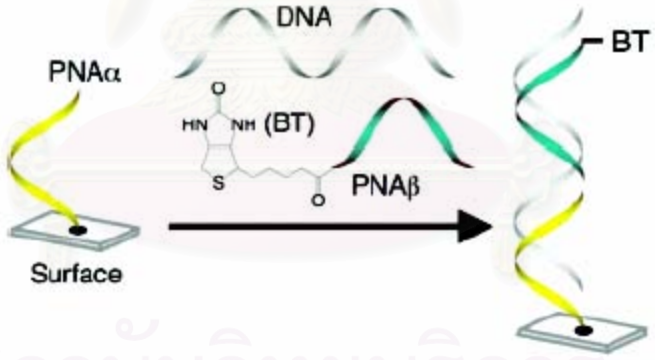

Figure 1.17 Principle of PNA-based sandwich-hybridization assay. [31]

In these techniques, some forms of purification are required to separate the unhybridized from hybridized PNA. Purification of PNA·DNA hybrids from unbond PNA in solution was usually carried out by labeling of the DNA samples with biotin. The biotin-tagged hybrids were then absorbed by a streptavidine modified capture surface such as magnetic beads. The PNA-DNA hybridization can then be determined by mass spectrometry [32] (**Figure 1.18**) or voltametry. [33] (**Figure 1.19)**

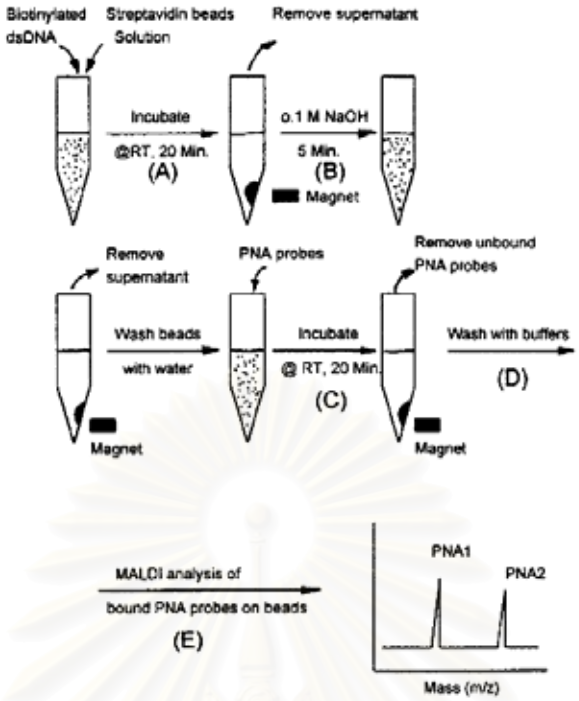

Figure 1.18 Biotin affinity capture assay for DNA. The detected molecular weight of the PNA probe indicates the sequence of the DNA sample. [32]

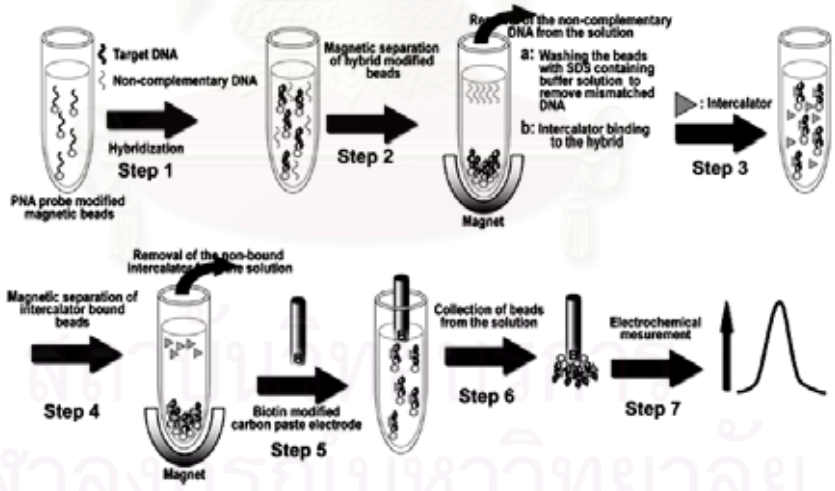

Figure 1.19 PNA modified magnetic bead-incombination with Meldola's Blue for the specific detection of Hybridization. [33]

1.5 Objective of this Research

The aim of this work is to develop a new fluorescent-based detection of PNA-DNA hybridization. This method based on the differential ionic interaction between negative charge of DNA and neutral PNA on a positively charged ion exchange support. Fluorophore-labeled PNAs can not be absorbed onto the solid support because of their electronically neutral native. In the presence of complementary DNA, the PNA can hybridize with the DNA target to from a negatively charged PNA·DNA hybrid. This DNA·PNA hybrid can then be capture by the solid support making the solid support fluorescent as shown in **Figure 1.20**

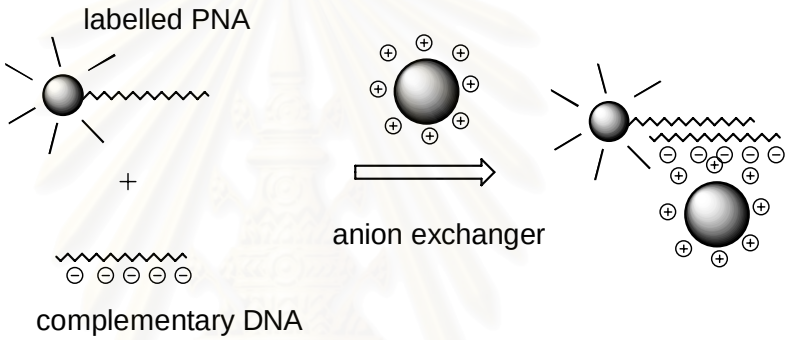

Figure 1.20 Schematic representation for Ion exchage and fluorescent technique.

The PNA that used in this study is a new beta-pyrrolidinyl PNA recently developed in the author's laboratory. This PNA showed a very high affinity and sequence specificity towards DNA. A variety of fluorescent dyes including tetramethylrhodamine, fluorescein and dansyl will be incorperated onto the PNA by solid-phase synthesis methodology. The labeled PNA will be used as a probe in DNA sequence analysis in conjunction with the anion exchange method.

CHAPTER II

EXPERIMENTAL SECTION

2.1 General procedure

2.1.1 Materials and Methods

All reactions were performed in oven-dried glasswares. The weight of all chemicals was determined on a Metler Toledo electrical balance. Evaporation of solvents was carried out on Büchi Rotavapor R-200 with a water aspirator Büchi model B-490 or a Refco Vacubrand pump. The magnetic stirrers were of Corning. The progress of the reaction was followed by thin layer chromatography (TLC) performed on Merck D.C. silica gel 60 F_{254} 0.2 mm. precoated aluminium plates cat. no. 1.05554 and visualized using UV lamp (254 nm). Silica gel 70-230 from Merck was used for column chromatography. Reverse phase HPLC experiments were performed on Water Delta 600^{TM} system equipped with gradient pump and Water 996^{TM} photodiode array detector; optionally alternate to Rheodyne 7725 manual sample loop (100 μL sample size for analytical scale). A Polaris C_{18} HPLC column, 3 μm particle size, 4.6 × 50 mm from Varian was used for both analytical and preparative purposes. Peak monitoring and data processing were investigated on the base Empower software. Fractions from HPLC were collected manually which was assisted by real-time HPLC chromatogram monitoring. The PNAs were recovered from the combined fractions by freeze drying (Freezone 77520, Benchtop Labconco). ^{1}H and ^{13}C NMR spectra were recorded in appropriate deuterated solvents on Varian Mercury-400 plus operating at 400 MHz (^{1}H) and 100 MHz (^{13}C) respectively. Chemical shifts (δ) are reported in part per million (ppm) relative to tetramethylsilane (TMS) or using the residual protonated solvent signal as a reference ($CDCl_3$ δ 7.27, DMSO-d_6 δ 2.50). Coupling constant (*J*) are proton-proton coupling unless otherwise noted and reported in hertz (Hz). Multiplicities were abbreviated as followed: singlet (s), doublet (d), triplet (t), quartet (q). Splitting patterns that could not be interpreted

or easily visualized are designated as multiplet (m) or broad (br). MALDI-TOF mass spectra of all PNA sequences were obtained on a Microflex MALDI-TOF mass spectrometry (Bruker Daltonics) using α-cyano-4-hydroxy cinnamic acid (CCA) as matrix. trifluoroacetic acid 0.1% in acetonitrile:water (1:2) was used as the diluents for preparation of MALDI-TOF samples.

All chemicals were purchased from Fluka, Merck or Aldrich Chemical Co., Ltd., and were used as received without further purification. Commercial grade solvents for column chromatography were distilled before use. Solvents for reactions and crystallization were reagent grade and used without purification. Acetonitrile for HPLC experiments was HPLC grade, obtained from BDH or Labscan and was filtered through a membrane filter (13 mm ϕ, 0.45 μm Nylon Lida) before use. Anhydrous *N*,*N*-dimethylformamide ($H_2O \leq 0.01\%$) for solid phase peptide synthesis was obtained from Fluka and dried over activated 3Å molecular sieves. The solid support for peptide synthesis (TentaGel S RAM Fmoc resin) and trifluoroacetic acid were obtained from Fluka. The protected amino acids (Fmoc-Ser^{t}Bu-ODhbt) was obtained form Calbiochem Novabiochem Co., Ltd. Amine reactive fluorescent labels (carboxyfluorescein-OSu, Atto425-OSu, Atto520-OSu, TMR-OSu and dansyl chloride) were obtained from Fluka. Trifluoroacetic acid (98%) was obtained from Fluka. Nitrogen gas was obtained from Thai Industrial Gas (TIG) with high purity up to 99.5 %. MilliQ water was obtained from ultrapure water system with Millipak® 40 filter unit 0.22 μm, Millipore (USA). Acrylamide and *N*,*N*-methylene bisacrylamide and *N*,*N*,*N*′,*N*′-tetramethylethylenediamine (TEMED) and chemicals necessary for preparing buffers for elctrophoresis were obtained from Fluka Chemical Company. Oligonucleotides were purchased from Bioservice Unit, National Science and Technology Development Agency (Thailand). (*N*-Fmoc)-*cis*-4-(thymine-1-yl)-D-proline pentafluorophenyl ester (Fmoc-T-OPfp) and (*N*-Fmoc)-*cis*-4-(N^2-isobutyrylguanin-9-yl)-D-proline pentafluorophenyl ester were prepared by Miss Boonjira Boontha and Dr.Chaturong Suparpprom. (*N*-Fmoc)-*cis*-4-(N^4-benzoylcytosin-1-yl)-D-proline (Fmoc-C^{BZ}-OPfp) and (*N*-Fmoc)-*cis*-4-(N^4-benzoyladenin-9-yl)-D-proline pentafluorophenyl ester (Fmoc-A^{BZ}-OPfp) were synthesized by Miss Cheeraporn Ananthanawat. Fmoc-*trans*-(1*S*,2*S*)-2-aminocyclopentanecarboxylic acid spacer (Fmoc-ACPC-OPfp) were prepared by Miss Roejarek Kanjanawarut.

2.2 Synthesis of 6-*O*-(carboxymethyl)fluorescein 2-ethyl ester pentafluorophenyl ester

2.2.1 ethyl 2-(6-hydroxy-3-oxo-3*H*-xanthen-9-yl)benzoate (2) [34]

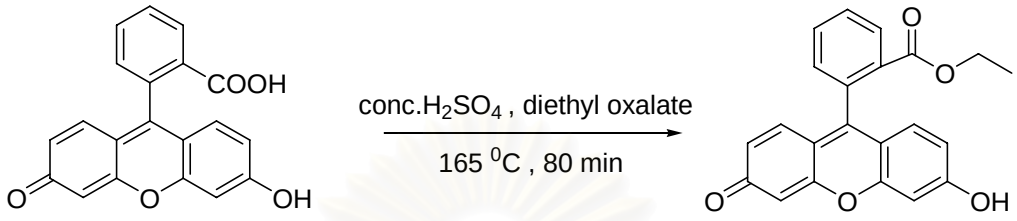

(**1**) (**2**)

Fluorescein (**1**) (1.66 g, 4.82 mmol), diethyl oxalate (8 mL) and concentrated H_2SO_4 (1 mL) were refluxed at 160-165 ^oC for 80 min. Upon cooling, the reaction mixture was taken up in a mixture of $CHCl_3$ (100 mL) and MeOH (20 mL) and extracted with saturated $NaHCO_3$ (60 mL). The solvent was removed by rotary evaporator, and the crude product was precipitated by addition of EtOH (5 ml) and ethyl acetate (55 mL). The precipitate was dissolved in boiling absolute EtOH (100 mL), whereby crystallization set in. Standing overnight at -20 ^oC gave 985.6 mg (57% yield) of the product as red-brown crystals with green luster: mp 240-242 ^oC

^1H NMR (400 MHz, $CDCl_3$): δ 8.25 (d, *J*=6.8 Hz, 1H, Ar*H*), 7.96-7.57 (m, 2H, Ar*H*), 7.49 (d, *J*=7.7 Hz, 1H, Ar*H*), 7.21 (s, 1H, O*H*), 7.04-6.70 (m, 4H, COC*H*CH), 6.50-6.45(m, 1H, Ar*H*), 6.45-6.20 (m, 1H, COC*H*C).

2.2.2 6-O-*(tert*-Butyoxycarbonylmethyl)fluorescein 2-ethyl ester (3) [34]

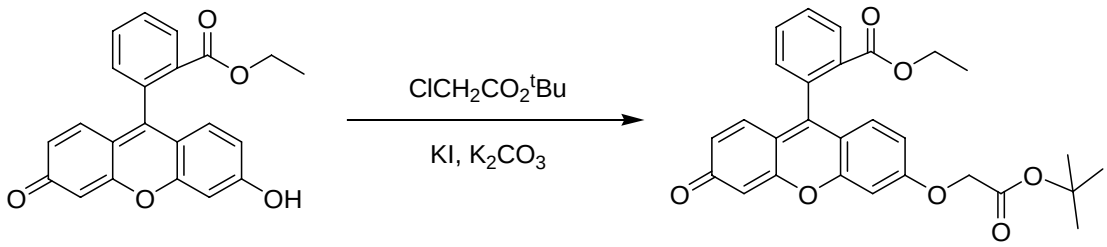

(**2**) (**3**)

Fluorescein 2-ethyl ester (**2**) (333 mg, 0.92 mmol) and tert-butyl chloroacetate (100 mL), K_2CO_3 (138 mg, 1 mmol) and KI (166 mg, 1 mmol) were refluxed at 100 ^oC for 1 h. The reaction mixture was taken up in CH_2Cl_2 (200 mL) and extracted with saturated $NaHCO_3$ (100 mL) The solvents were removed on a rotary evaporator, and the crude product column chromatography in system hexanes:ethyl acetate 1:1. The residue was dissolved in diethyl ether and left in the freezer at -20 ^oC. After cooling at -20 ^oC 3 days, the orange crystals (**3**) formed were filtered off and washed with diethyl ether: yield 307 mg (70%) : mp 131-133 ^oC

^1H NMR (400 MHz, $CDCl_3$): δ 8.25 (d, *J*=8.0 Hz, 1H, Ar*H*), 7.83-7.61 (m, 2H, Ar*H*), 7.29 (d, *J*=7.7 Hz, 1H, Ar*H*), 7.00-6.42 (m, 3H, Ar*H* and CHC*H*C), 6.79 (d, *J*=7.1 Hz, 1H, COC*H*CH), 6.58 (d, J=10 Hz, 1H, Ar*H*), 6.52 (s, 1H, COC*H*C), 4.61 (s, 2H, OCH_2CO), 4.10-3.80 (m, OCH_2CH_3), 1.50 (s, 9H, CCH_3), 0.95 (t, J=7.09 Hz, 3H, CH_2CH_3).

2.2.3 6-*O*-(Carboxymethyl)fluorescein 2-ethyl ester (4) [34]

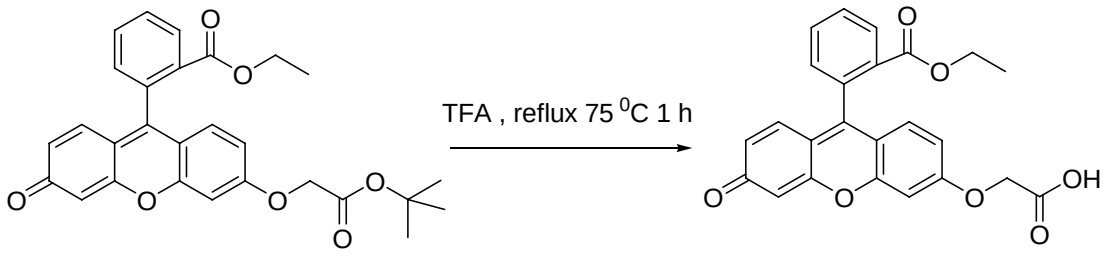

(**3**) (**4**)

6-O-(*tert*-Butyoxycarbonylmethyl)fluorescein 2-ethyl ester **(3)** (100 mg 0.47 mmol) in trifluoroacetic acid (4 mL), was refluxed at 75 ^{o}C for 1 h. Most of the trifluoroacetic acid was removed by a gentle nitrogen stream, and the product was precipitated with diethyl ether and filtered off. It was dissolved in boiling absolute EtOH (100 mL). Overnight standing at -20 ^{0}C produced orange crystals, which were filtered off, washed with ethanol, and dried at 100 ^{o}C : 230-231 ^{o}C

^{1}H NMR (400 MHz, $CDCl_3$): δ 8.29(d, *J*=6.8 Hz, 1H, Ar*H*), 7.80-7.69 (m, 2H, Ar*H*), 7.37-7.26 (m, 3H, Ar*H*), 7.21 (s, 1H, O*H*), 7.04-6.70 (m, 4H, COC*H*CH), 6.50-6.45(m, 1H, Ar*H*), 6.45-6.20 (m, 1H, COC*H*C).

2.2.4 6-*O*-(Carboxymethyl)fluorescein 2-ethyl ester pentafluorophenyl ester (5) [34]

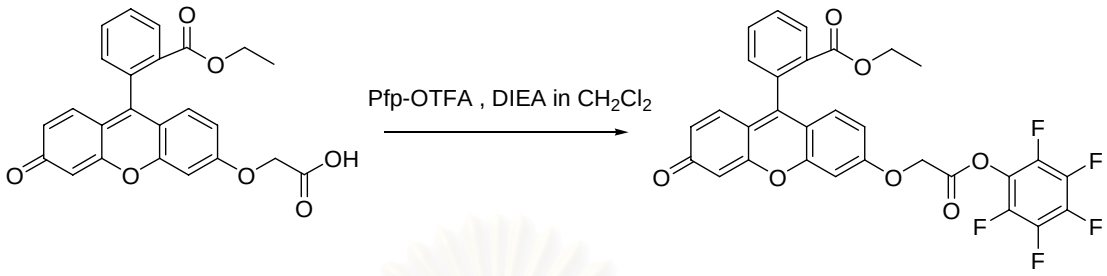

(4) **(5)**

The 6-*O*-(Carboxymethyl)fluorescein 2-ethyl ester **(4)** (100 mg, 0.239 mmol) was dissolved in dichloromethane (0.5 mL). Pentafluorophenyl trifluoroacetate (71 μL, 0.411 mmol) and diisopropylethylamine (68 μL, 0.425 mmol) were added, respectively. DMF was used as co-solvent for clear solution. The reaction mixture was stirred at room temperature until the starting material disappeared (1 h, monitored by TLC). The reaction mixture was further purified by column chromatography (hexanes:ethyl acetate 1:1) to give the activated fluorescein derivative as unstable orange crystals (117.2 mg, 84% yield) :

^{1}H NMR (400 MHz, $CDCl_3$): δ 8.31(d, *J*=7.1 Hz, 1H, Ar*H*), 7.86-7.71 (m, 2H, Ar*H*), 7.37-7.27 (m, 1H, Ar*H*), 7.21-6.94 (m, 6H, Ar*H*, COC*H*CH and C-CH-CH), 5.18 (s, 2H, OCH_2CO, O-CH_2-CH_2), 4.04 (q, *J*=7.1H_2, 2H), 1.01 (t, J=7.1H_2, 3H, CH_2-CH_3).

2.3 Synthesis of{2-[2-(Fmoc-amino)ehtoxy]ethoxy}acetic acid pentafluoro phenyl ester

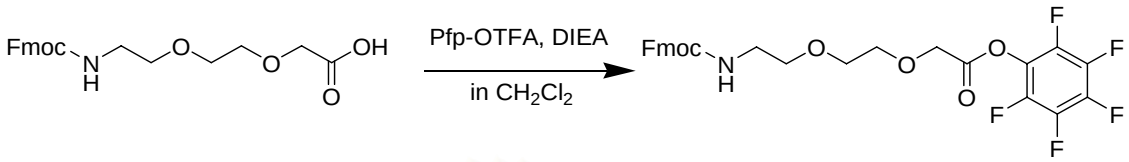

(6) **(7)**

2-[2-(Fmoc-amino)ethoxy] ethoxy acetic acid (**6**) (100 mg, 0.26 mmol) was dissolved in dichloromethane (0.5 mL). Pentafluorophenyl trifluoroacetate (69 μL, 0.39 mmol) and diisopropylethylamine (66 μL, 0.39 mmol) were added twice over a period of 30 min. The reaction mixture was stirred at room temperature until the starting material disappeared (1 h, monitored observed by TLC). The reaction mixture was further purified by column chromatography (hexanes:ethyl acetate 3:1) to give the product as white crystals (74.5 mg, 52 % yield) : mp 89.9-90.1 ^{o}C

^{1}H NMR (400 MHz, $CDCl_3$): δ 7.76(d, *J*=7.7H_2, 2H, Ar*H*), 7.58(d, *J*=7.7H_2, 2H, Ar*H*), 7.39 (t, *J*=7.5H_2, 2H, Ar*H*), 7.29(t, *J*=7.5H_2, 2H, Ar*H*), 5.25(s, 1H, N*H*), 4.51(s, 2H, O-C*H*$_2$-CO_2), 4.39 (d, *J*=6.4H2, 1H, CH-C*H*$_2$-N), 4.20 (t, J=6.4H_2,CH_2-C*H*-AR), 3.81 (s, 2H, CH_2-C*H*$_2$-O), 3.70 (s, 2H, CH_2-CH_2-O), 3.59 (s, 2H, CH_2-CH_2-O), 3.42 (s, 2H, CH_2-CH_2-N)

2.4 PNA Synthesis

2.4.1 Preparation of the reaction pipette and apparatus for solid phase synthesis

All peptide syntheses were carried out using a custom-made peptide synthesis columns equipped with sintered glass as previously described. [35] The resin was weighed into the peptide synthesis column and was pre-swollen in DMF for 1 h before use. For each reactions, the reagent was directly sucked in, ejected out or hold on using a rubber teat attached on the top of the column. All washings were performed by filling the solvent via the top of the column. The excess solvent was ejected out by squeezing the rubber teat.

2.4.2 Synthesis of PNA

The PNA sequences synthesized in this work are shown in **Table 2.1.** All PNA contains alternating *cis*-D pyrrolidine monomers and *SS*-ACPC spacer. Most of the PNA have fluorescent labels attached at the N-termini via an diethyleneglycol linker (O-linker). The neutral and hydrophilic $SerNH_2$ was included at the C-terminal to improve the solubility of the PNA.

Table 2.1 The sequences of the PNA synthesized in this work.

Code	N-Ter to C-Ter
P1	TMR-TTTTTTTTT-SerNH$_2$
P2	TMR-O-TTTTTTTTT-SerNH$_2$
P3	TMR-O-TTCCCCCTCCCAA-SerNH$_2$
P4	TMR-O-TTCCCCTTCCCAA-SerNH$_2$
P5	CarboxyFlu-O-TTTTATTTT-SerNH$_2$
P6	FITC-O-TTTTATTTT-SerNH$_2$
P7	NeutralFlu-O-TTTTATTTT-SerNH$_2$
P8	NBD-O-TTTTATTTT-SerNH$_2$
P9	Pyr-O-TTTTATTTT-SerNH$_2$
P10	Atto520-O-TTTTCTTTT-SerNH$_2$
P11	Atto425-O-TTTTGTTTT-SerNH$_2$
P12	CarboxyFlu-O-TTCCCCCTCCCAA-SerNH$_2$
P13	NeutralFlu-O-TTCCCCCTCCCAA-SerNH$_2$
P14	DNS-TTTTTTTTT-SerNH$_2$
P15	DNS-Ser-TTTTTTTTT-SerNH$_2$
P16	Ac-Ser-Lys(DNS)-TTTTTTTTT-SerNH$_2$
P17	Ac-Ser-Lys(DNS)-TTCTATGTT-SerNH$_2$

2.4.3 Solid Phase Peptide Synthesis of PNA oligomers.

The PNA **P14-P17** were synthesized according to the precedure outlined in **Figure 2.1** as described previously. [35] The remaing in PNA were synthesized by a slightly modified protocol in **Figure 2.2** as follows.

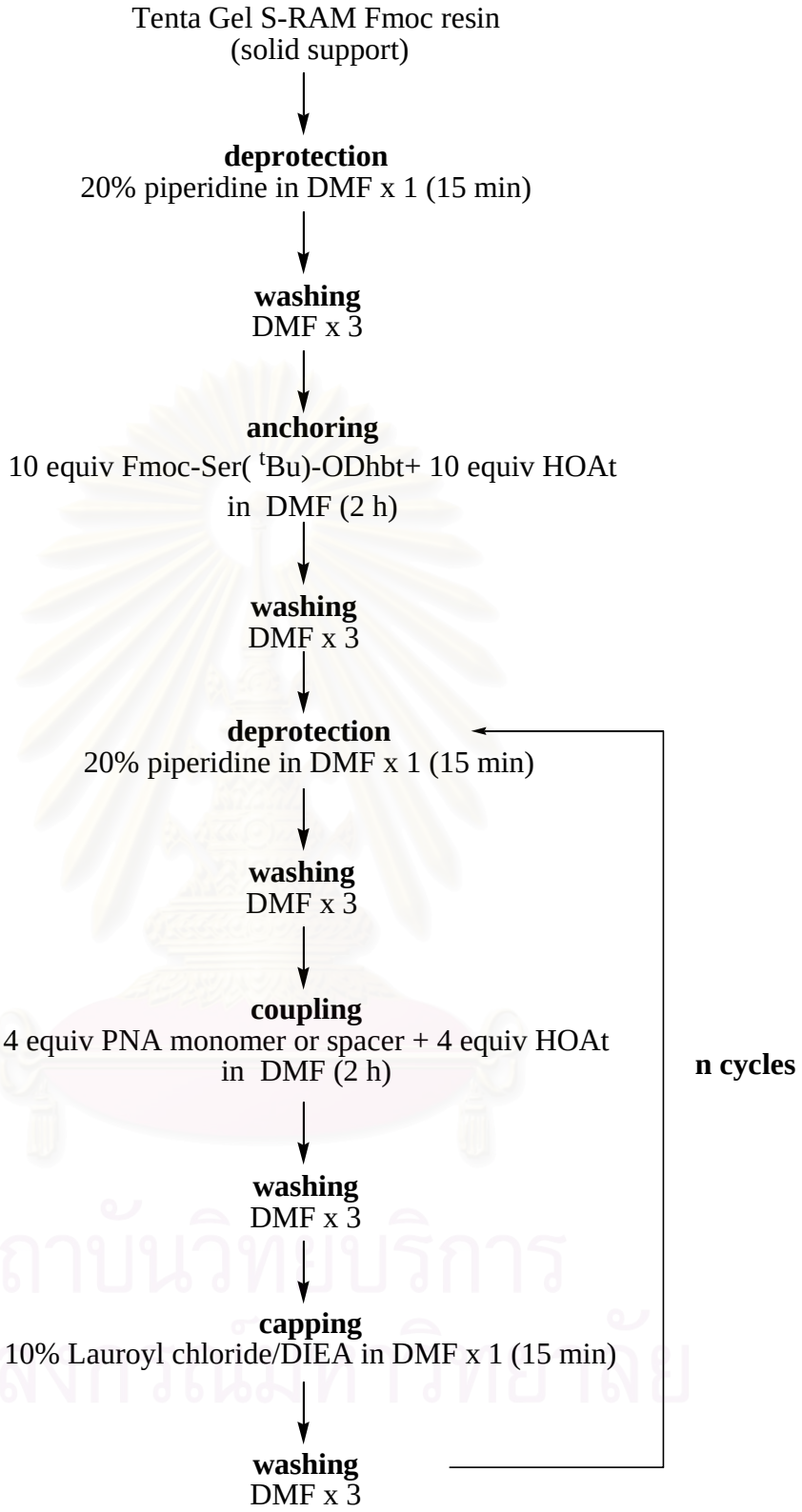

Figure 2.1 The procedure for solid phase synthesis of PNA.

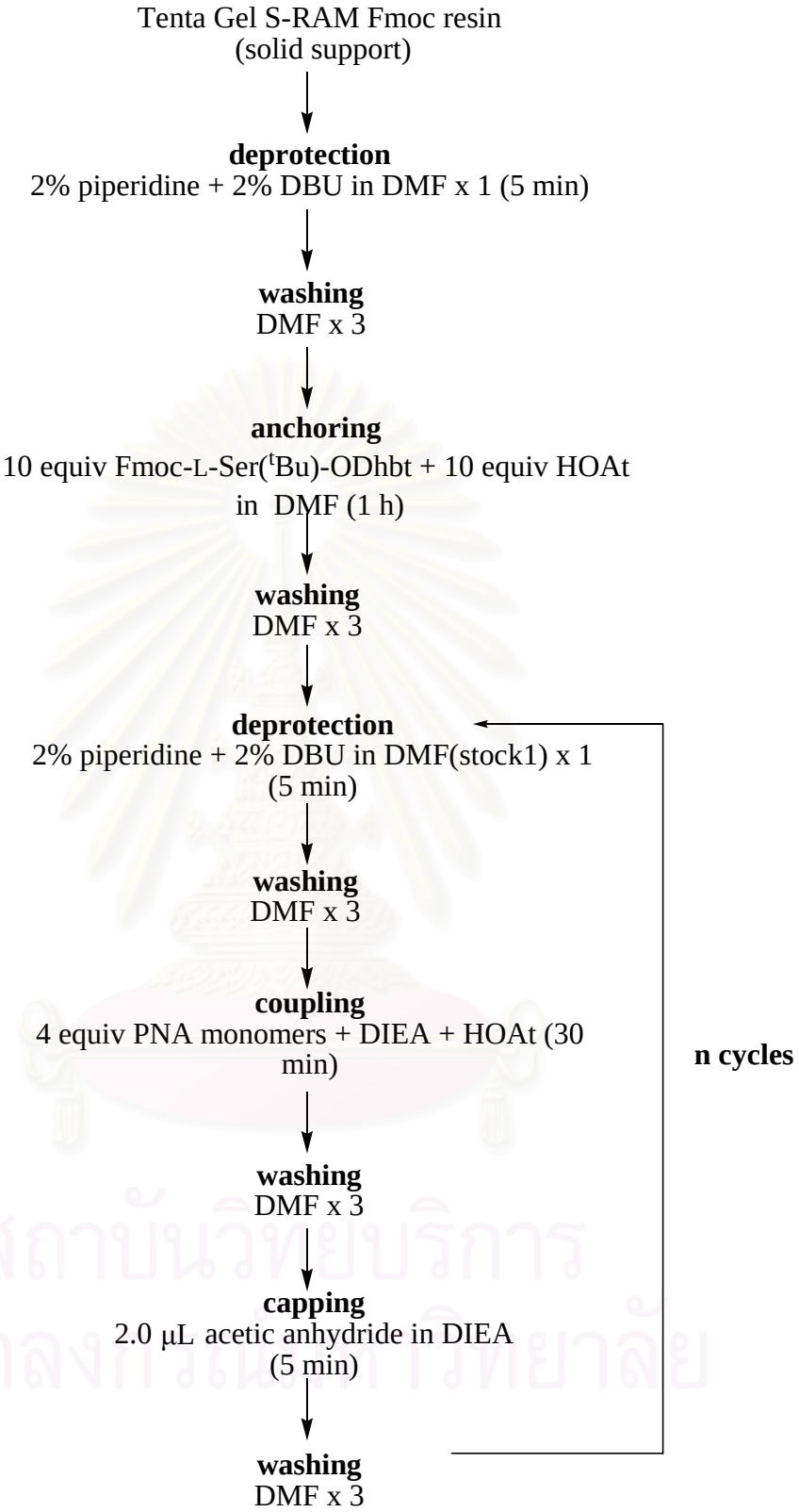

Figure 2.2 The modified procedure for solid phase synthesis of PNA.

Syntheses of PNAs were typically carried out on 1.0-1.5 μmol scale. Before commencing the synthesis, the following three stocks solutions were prepared.

Stock 1 : (deprotection) 20 μL piperidine, 20 μL DBU in 960 μL DMF.

Stock 2 : (capping and coupling) 70 μL DIEA in 930 μL DMF

Stock 3 : (activator) 5.5 mg HOAt in 100 μL DMF

The synthesis was divided into steps as follows.

i Removing of the N-terminal Fmoc protecting group

A reaction pipette prepared as described above was packed with TentaGel S RAM Fmoc resin (4.2 mg, 1.0 μmol). The resin was treated with 100 μL of deprotection solution (stock 1) for 5 min at room temperature. After the specified period of time, the reagent was squeezed off and the reaction column was washed extensively with DMF.

ii Anchoring with the first amino acid (Ser) residue

Fmoc-Ser(^{t}Bu)-ODhbt (5.28 mg, 10 μmol) and HOAt (1.36 mg, 10 μmol) were dissolved in anhydrous DMF (30 μL) and then DIEA (3.4 μL, 20 μmol) was added to this mixture. The deprotected resin carrying free amino groups was soaked in this solution with occasional agitation at room temperature for 1 h. After that, the resin was extensively washed with DMF.

iii Deprotection of the Fmoc protecting group at *N*-terminus

This followed the procedure described in step **i**. Ten μL of the used deprotecting reagent was taken out and diluted with methanol (2 mL) and then the UV-absorbance at 264 nm of dibenzofulvene-piperidine adduct was measured to determine the coupling efficiency. The first UV-absorbance of this adduct, released from the resin preloaded with Fmoc-Ser(^{t}Bu), was assumed to be 100%.

iv Coulping with of PNA monomers

The deprotected resin carrying free amino groups was further coupled with the PNA monomers. The coupling mixture consisted of the Pfp-monomers (4.0 μmol), 10 μL of stock 3 (HOAt) and 10 μL of stock 2 (DIEA). The reaction pipette was treated with this solution at room temperature for 30 min with occasional agitation followed by extensive washing with DMF.

v capping

After anchoring or coupling step, any remaining free amino residues was capped with a capping mixture consisting of 2.0 μL acetic anhydride and 30 μL stock 2 (DIEA) in a 1.5 mL eppendrof tube. After 5 minutes the reagent was squeezed off and the reaction column was washed exhaustively with DMF.

The deprotection-coupling-capping (iii-iv-v) recycle was repeated until PNA of the desired sequence and length were obtained.

2.4.4 Attachment of O-linker and fluorescent labels

The labels were generally attached to the PNA via a hydrophilic diethyleneglycol ("O") linker. This require liberation of the free amino group on the resin-attached PNA by treatment with piperidine-DBU in DMF (stock 1).

For PNA sequences consisting of adenine, cytosine and guanine, the exocyclic amino protecting groups (benzoyl and isobutyryl) were also removed by treatment with 1:1 ammonia/dioxane in a sealed test tube at 60 ^{o}C for 6 hour or overnight prior to attachment of the O-linker and labels.

The coupling of the O-linker (3.8 mg, 10 μmol) were dissolved in anhydrous DMF (30 μL). The reaction pipette was treated with this solution for 30 min with occasional agitation and followed by extensive washing with DMF.

If the label is fluorescein, the exocyclic amino protecting groups removal may be postponed until after attachment of the label. The deprotected PNA was coupled with an appropriate amine-reactive labels [5(6)-carboxy-X-rhodamine *N*-succinimi

didyl ester (TMR-OSu), 5(6)-carboxy fluorescien succinimidyl ester (Flu- OSu), fluorescein isothiocyanate (FITC), dansyl chloride, Atto425-Osu, Atto520-Osu reactive. These fluorescence labels were directly coupled under basic conditions (10 eq, DIEA 20 eq, DMF 30 uL). 6-*O*-(carboxymethyl)fluorescein 2-ethyl ester 6-pentafluorophenyl ester (10 eq) was coupled using (HOAt 10 eq, in DMF 30 uL). 4-Pyrenebutyric acid (10 eq) was first activated (HATU 10 eq, DIEA 20 eq, DMF 30 uL) before coupling. After about 4 h – overnight coupling at room temperature (followed by MALDI-TOF mass spectrometry), the resin was washed extensively with DMF. In the case of carboxyfluorescein, the resin was treated with 1:1 ammonia/dioxane to deprotect the nucleobase side-chain and to remove any non-specific ally bound fluorescein. The procedure is not recommended for labels that are sensitive to ammonia treatment such as TMR. The labeled PNAs were ready for cleavage and purified.

2.4.5 Cleavge and Purification

The resin-bound PNA was cleaved from the resin by treatment with trifluoroacetic acid (2 x 0.5 mL x 1 h) at room temperature with occasional agitation. During the time, the resin turned red, indicating that the cleavage has occurred. The removal of trifluoroacetic acid was achieved by a gentle nitrogen stream (in fume hood). The residue was treated with diethyl ether (1 mL), centrifuged and decanted to obtain the crude PNA oligomer. Finally the crude PNA was air-dried at room temperature and stored as solids at -20 °C until used.

The crude PNA was prepared for HPLC analysis by dissolving the solid in 200 μL of deionized water. Up to 10 % of acetonitrile may be added to increase solubility. The solution was filtered through a nylon membrane filter (0.45 μm). Analysis and purification was performed by reverse phase HPLC, monitoring by UV-absorbance at 260 nm and eluting with a gradient system of 0.1% TFA in acetonitrile/water. The following conditions were used for HPLC gradient system;

Solvent A = 0.1% trifluoroacetic acid in acetonitrile

Solvent B = 0.1% trifluoroacetic acid in milli Q water

The gradient set-up is as shown in **Table 2.2** and **Figure 2.2**.

Table 2.2 Gradient system for HPLC analysis of PNA.

Time (min)	Flow Rate (mL/min)	Solvent A (%)	Solvent B (%)
0	0.5	10	90
5	0.5	10	90
30	0.5	90	10
35	0.5	90	10
45	0.5	10	90
60	0.5	10	90

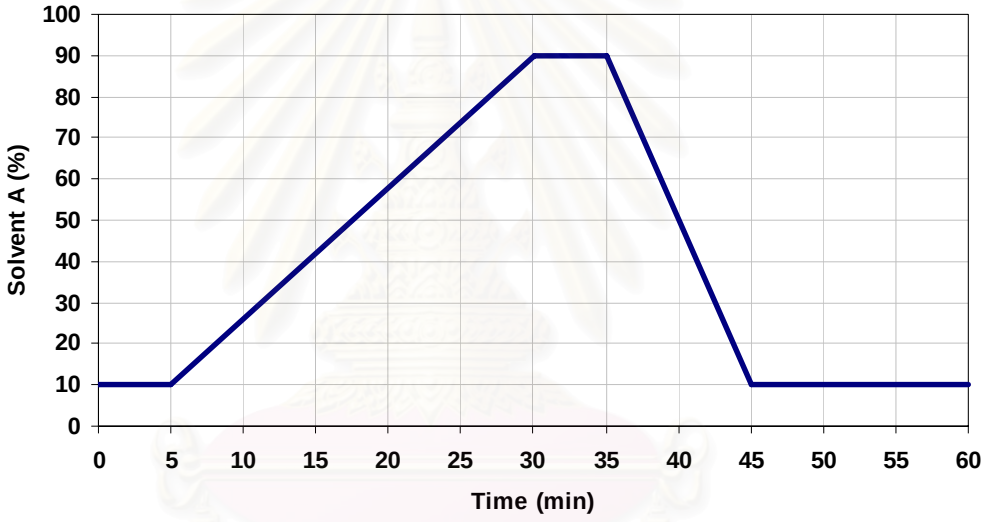

Figure 2.3 Diagram of gradient solvent in HPLC analysis of PNA.

2.4.6 Characterization

All PNAs were characterized by MALDI-TOF mass spectrometry. The mass spectra of all PNA samples were obtained on Microflex MALDI-TOF mass spectrometry (Bruker Daltonics) and recorded in a linear positive ion mode with accelerating voltage of 25 kV. All samples used matrix solution containing CCA in 0.1% trifluoroacetic acid in acetonitrile:water (1:2) solution. All spectra were processed by summing 30 individual laser shots or more. External mass calibration was performed using PNA of known molecular weight.

2.4.7 Selected examples of PNA synthesis

a) TMR-T_9-SerNH_2 (**P1**)

Synthesis of TMR-T_9-SerNH_2 (**P1**) was accomplished in the same way as described above. Starting from TentaGel S RAM Fmoc resin (4.2 mg, 1.0 μmol) and monomers in the order shown in Table.

Cycle	Monomers	Amount	A_{264}	Coupling efficiency
1	Fmoc-Ser(^{t}Bu)-ODhbt	5.4 mg (10 μmol)	0.620	100.0
2	Fmoc-T-OPfp	2.6 mg (4 μmol)	0.574	92.6
3	Fmoc-ACPC -OPfp	2.1 mg (4 μmol)	0.683	100.0
4	Fmoc-T-OPfp	2.5 mg (4 μmol)	0.643	94.2
5	Fmoc-ACPC -OPfp	2.2 mg (4 μmol)	0.640	99.5
6	Fmoc-T-OPfp	2.6 mg (4 μmol)	0.617	96.9
7	Fmoc-ACPC -OPfp	2.2 mg (4 μmol)	0.589	95.5
8	Fmoc-T-OPfp	2.5 mg (4 μmol)	0.579	98.4
9	Fmoc-ACPC -OPfp	2.3 mg (4 μmol)	0.563	97.2
10	Fmoc-T-OPfp	2.5 mg (4 μmol)	0.538	95.5
11	Fmoc-ACPC -OPfp	2.1 mg (4 μmol)	0.540	100.0
12	Fmoc-T-OPfp	2.6 mg (4 μmol)	0.500	92.6
13	Fmoc-ACPC -OPfp	2.2 mg (4 μmol)	0.516	100.0
14	Fmoc-T-OPfp	2.7 mg (4 μmol)	0.444	86.0
15	Fmoc-ACPC -OPfp	2.3 mg (4 μmol)	0.468	100.0
16	Fmoc-T-OPfp	2.4 mg (4 μmol)	0.371	79.5
17	Fmoc-ACPC -OPfp	2.3 mg (4 μmol)	0.392	100.0
18	Fmoc-T-OPfp	2.6 mg (4 μmol)	0.349	89.2
19	Fmoc-ACPC -OPfp	2.2 mg (4 μmol)	0.340	74.7
20	5(6)-Carboxy-X-rhodamine *N*-succinimididyl ester	5.2 mg (10 μmol)	-	-

b) CarboxyFlu-O-T_4AT_4-$SerNH_2$ (P5)

Synthesis of CarboxyFlu-O-T_4AT_4-$SerNH_2$ (**P5**) was accomplished in the same way as described for (**P1)** above. Starting from TentaGel S RAM Fmoc resin (4.2 mg, 1.0 μmol) and monomers in the order shown in Table.

Cycle	Monomers	Amount	A_{264}	Coupling efficiency
1	Fmoc-Ser(^{t}Bu)-ODhbt	5.4 mg (10 μmol)	0.680	100.0
2	Fmoc-T-OPfp	2.6 mg (4 μmol)	0.667	98.1
3	Fmoc-ACPC -OPfp	2.1 mg (4 μmol)	0.670	100.0
4	Fmoc-T-OPfp	2.5 mg (4 μmol)	0.594	88.6
5	Fmoc-ACPC -OPfp	2.2 mg (4 μmol)	0.574	96.6
6	Fmoc-T-OPfp	2.6 mg (4 μmol)	0.550	95.8
7	Fmoc-ACPC -OPfp	2.2 mg (4 μmol)	0.529	96.2
8	Fmoc-T-OPfp	2.5 mg (4 μmol)	0.501	94.8
9	Fmoc-ACPC -OPfp	2.3 mg (4 μmol)	0.489	97.6
10	Fmoc-A^{BZ}-OPfp	2.5 mg (4 μmol)	0.461	94.3
11	Fmoc-ACPC -OPfp	2.1 mg (4 μmol)	0.450	97.6
12	Fmoc-T-OPfp	2.6 mg (4 μmol)	0.430	95.6
13	Fmoc-ACPC -OPfp	2.2 mg (4 μmol)	0.410	95.4
14	Fmoc-T-OPfp	2.7 mg (4 μmol)	0.390	95.1
15	Fmoc-ACPC -OPfp	2.3 mg (4 μmol)	0.390	100.0
16	Fmoc-T-OPfp	2.4 mg (4 μmol)	0.381	97.7
17	Fmoc-ACPC -OPfp	2.3 mg (4 μmol)	0.375	98.4
18	Fmoc-T-OPfp	2.6 mg (4 μmol)	0.374	99.7
19	Fmoc-ACPC -OPfp	2.2 mg (4 μmol)	0.360	96.2
20	Fmoc-O-Spacer-OPfp	3.8 mg (10 μmol)	0.352	97.8
21	5(6)-Carboxyfluorescein-OSu	5.2 mg (10 μmol)	-	-

After the complete PNA sequence was assembled, it was treated with 1:1 ammonia:dioxane to remove the nucleobase side chain protecting groups. The pure PNA was obtained after cleavage from resin and purification by reverse phase HPLC.

c) Synthesis of TMR-O-TTCCCCTTCCCAA-SerNH$_2$ (TMR-O-SLE2) (P4)

Synthesis of TMR-O-TTCCCCTTCCCAA-SerNH$_2$ was accomplished in the same way as described for Fmoc-O-TTCCCCTTCCCAA-SerNH$_2$ above. Starting from TentaGel S RAM Fmoc resin (4.3 mg, 4.0 μmol) and monomers as in following Table.

Cycle	Monomers	Amount	A_{264}	Coupling efficiency
1	Fmoc-Ser(^{t}Bu)-ODhbt	5.5 mg (4 μmol)	0.768	100.0
2	Fmoc-A^{BZ}-OPfp	3.0 mg (4 μmol)	0.619	80.6
3	Fmoc-ACPC-OPfp	2.2 mg (4 μmol)	0.616	99.0
4	Fmoc-A^{BZ}-OPfp	3.0 mg (4 μmol)	0.593	96.3
5	Fmoc-ACPC-OPfp	2.1 mg (4 μmol)	0.610	100.0
6	Fmoc-C^{BZ}-OPfp	3.0 mg (4 μmol)	0.652	100.0
7	Fmoc-ACPC-OPfp	2.1 mg (4 μmol)	0.567	86.9
8	Fmoc-C^{BZ}-OPfp	2.9 mg (4 μmol)	0.598	100.0
9	Fmoc-ACPC-OPfp	2.2 mg (4 μmol)	0.595	99.5
10	Fmoc-C^{BZ}-OPfp	2.9 mg (4 μmol)	0.698	100.0
11	Fmoc-ACPC-OPfp	2.2 mg (4 μmol)	0.561	80.4
12	Fmoc-T-OPfp	2.6 mg (4 μmol)	0.644	100.0
13	Fmoc-ACPC-OPfp	2.1 mg (4 μmol)	0.654	100.0
14	Fmoc-T-OPfp	2.6 mg (4 μmol)	0.663	100.0
15	Fmoc-ACPC-OPfp	2.2 mg (4 μmol)	0.547	82.5
16	Fmoc-C^{BZ}-OPfp	3.2 mg (4 μmol)	0.546	99.8
17	Fmoc-ACPC-OPfp	2.2 mg (4 μmol)	0.457	83.7
18	Fmoc-C^{BZ}-OPfp	3.0 mg (4 μmol)	0.444	97.2
19	Fmoc-ACPC-OPfp	2.1 mg (4 μmol)	0.451	100.0

20	Fmoc-C^{BZ}-OPfp	2.9 mg (4 µmol)	0.460	100.0
21	Fmoc-ACPC-OPfp	2.1 mg (4 µmol)	0.450	97.8
22	Fmoc-C^{BZ}-OPfp	2.8 mg (4 µmol)	0.495	100.0
23	Fmoc-ACPC-OPfp	2.2 mg (4 µmol)	0.369	74.8
24	Fmoc-T-OPfp	2.6 mg (4 µmol)	0.315	85.4
25	Fmoc-ACPC-OPfp	2.0 mg (4 µmol)	0.357	100.0
26	Fmoc-T-OPfp	2.5 mg (4 µmol)	0.328	91.9
27	Fmoc-ACPC-Opfp	2.0 mg (4 µmol)	-	-
28	Fmoc-O-Spacer-OPfp	4.1 mg (4 µmol)	-	-
29	5(6)-Carboxy-X-rhodamine *N*-succinimididyl ester	4.5 mg (4 µmol)	-	-

d) Flu-O-TTCCCCCTCCCAA-SerNH$_2$ (Flu-O-SLE 1) (P12)

Synthesis of Flu-O-TTCCCCCTCCCAA-SerNH$_2$ **(P12)** was accomplished in the same way as described for TMR-T$_9$-SerNH$_2$ **(P1)** above. Starting from TentaGel S RAM Fmoc resin (4.2 mg, 1.0 µmol) and monomers in the order shown in Table.

Cycle	**Monomers**	**Amount**	**A_{264}**	**Coupling efficiency**
1	Fmoc-Ser(^{t}Bu)-ODhbt	5.3 mg (4 µmol)	0.768	100.0
2	Fmoc-A^{BZ}-OPfp	3.0 mg (4 µmol)	0.619	80.6
3	Fmoc-ACPC-OPfp	2.2 mg (4 µmol)	0.616	99.52
4	Fmoc-A^{BZ}-OPfp	3.0 mg (4 µmol)	0.593	96.3
5	Fmoc-ACPC-OPfp	2.1 mg (4 µmol)	0.610	100.0
6	Fmoc-C^{BZ}-OPfp	3.0 mg (4 µmol)	0.652	100.0
7	Fmoc-ACPC-OPfp	2.1 mg (4 µmol)	0.567	86.9
8	Fmoc-C^{BZ}-OPfp	2.9 mg (4 µmol)	0.598	100.0
9	Fmoc-ACPC-OPfp	2.2 mg (4 µmol)	0.595	99.5
10	Fmoc-C^{BZ}-OPfp	2.9 mg (4 µmol)	0.698	100.0
11	Fmoc-ACPC-OPfp	2.2 mg (4 µmol)	0.561	83.4
12	Fmoc-T^{BZ}-OPfp	2.6 mg (4 µmol)	0.644	100.0

13	Fmoc-ACPC-OPfp	2.1 mg (4 µmol)	0.654	100.0
14	Fmoc-C^{BZ}-OPfp	2.6 mg (4 µmol)	0.544	83.2
15	Fmoc-ACPC-OPfp	2.2 mg (4 µmol)	0.475	87.3
16	Fmoc-C^{BZ}-OPfp	3.0 mg (4 µmol)	0.448	94.3
17	Fmoc-ACPC-OPfp	2.2 mg (4 µmol)	0.444	99.1
18	Fmoc-C^{BZ}-OPfp	3.0 mg (4 µmol)	0.450	100
19	Fmoc-ACPC-OPfp	2.1 mg (4 µmol)	0.403	89.6
20	Fmoc-C^{BZ}-OPfp	2.9 mg (4 µmol)	0.432	100.0
21	Fmoc-ACPC-OPfp	2.1 mg (4 µmol)	0.417	100.0
22	Fmoc-C^{BZ}-OPfp	3.0 mg (4 µmol)	0.358	96.53
23	Fmoc-ACPC-OPfp	2.2 mg (4 µmol)	0.375	85.6
24	Fmoc-T-OPfp	2.6 mg (4 µmol)	0.358	100
25	Fmoc-ACPC-OPfp	2.0 mg (4 µmol)	0.313	95.5
26	Fmoc-T-OPfp	2.4 mg (4 µmol)	0.295	87.4
27	Fmoc-ACPC-OPfp	2.0 mg (4 µmol)	0.285	94.4
28	Fmoc-O-Spacer-OPfp	3.8 mg (4 µmol)	-	-
29	5(6)-Carboxyfluorescein-OSu	5.4 mg (4 µmol)	-	-

Before attachment of the O-spacer, the Fmoc group was removed followed by the nucleobase protecting group as described above. The next two couplings were then followed without capping. After cleavage from resin, the crude PNA was dissolved in 10% MeCN in water and purified by reverse phase HPLC.

2.5 Binding studies of PNA and DNA

2.5.1 T_m measurements

UV melting curves were measured at 260 nm by using a CARY 100 Bio UV-Visible spectrophotometer (Varian Ltd.) equipped with a thermal melt system. The sample for T_m measurement was prepared by mixing calculated amounts of stock oligonucleotide and PNA solutions together to give final concentration of nucleotides and sodium phosphate buffer (pH 7.0) and the final volumes were adjusted to 3.0 mL

by addition of deionized water. The samples were transferred to a 10 mm quartz cell with a Teflon stopper and equilibrated at the starting temperature for 10 min. Prior to analysis, the samples were heated from 20 to 90 ^{o}C with a rate of 1 ^{o}C/min and hold at 90 ^{o}C within 10 min, cooled from 90 to 20 ^{o}C with a rate of 1 ^{o}C/min and hold at 20 ^{o}C within 10 min, the last step were heated from 20 to 90 ^{o}C with a rate of 1 ^{o}C/min. The temperature recorded was the block temperature and was corrected.

Correct temperature and normalized absorbance are defined as follows.

$$\text{Correct. Temp.} = (0.978 \times T_{block}) - 0.6068$$

$$\text{Normalized Abs.} = Abs_{obs}/Abs_{init}$$

Only the result taken from the last heating cycle was used and was normalized by dividing the absorbance at each temperature by the initial absorbance. T_m was obtained from derivative plot after smoothing in KaleidaGraph 3.6 (Synergy Software) and analysis of the data was performed using Microsoft Excel XP (Microsoft Corp.). The independent experiments were accurate within ±0.5 °C.

2.5.2 Gel electrophoresis

Polyacrylamide gel electrophoresis experiments were performed on a electrophoresis apparatus (SCIE-PLAS, V10-SET, SCIE-PLAS Ltd.). The medium used was 15% polyacrylamide gel in 90 mM Tris-Borate-EDTA (TBE) pH 8.0 and run at a constant voltage of 150V. The samples were prepared by mixing the calculated amount of concentrated stock of fluorescent labeled PNA and DNA to give the total amount of PNA = 1 nmol. These were mixed with appropriate volume of stock TBE buffer, loading buffer (sugar in same of loading buffer) and the volume adjusted with deionized water to give the final concentration of the TBE buffer of 90 mM. The samples were loaded into the well at the top of the gel *via* microsyringe and then the system was connected to a power supply until the bromophenol blue marker dye moved about half-way through the gel. The power supply was then disconnected

and the gel was removed from the glass plate using a thin spatula and the gel was visualized by a UV transilluminator and photographs taken.

2.6 Preparation of samples for fluorescence measurement

The Q sepharose was wash with deionized water and twice with phosphate buffer pH 7.0 (10 mM) and resuspended in the phosphate buffer until used. The PNA and PNA-DNA were hybridized in the some phosphate buffer at room temperature fr 15 min. The Q-sepharose was then added (~2 μL). The hybridization mixture was incubated at room temperature for about 15 min. The Q-sepharose was then washed with several aliquots of deionized water or aqueous acetonitrile to eliminate the unhybrized PNA probes. The 1 μL of Q-sepharose bead coming the PNA·DNA hybrid was examined under fluorescent microscope and UV-transilluminator .

2.7 Fluorescence experiments

2.7.1 UV transilluminator

The washed solid supports in the eppendorf tubes were directly visualized under a long-wave UV-transilluminator (366 nm). The photograph was taken digitally without the use of filters.

2.7.2 Fluorescence microscopy

Fluorescence experiment was performed on a Fluorescence Microscope (Olympus BX 50) at the Oral Biology Research Center Faculty of Dentistry, Chulalongkorn University. About 1 uL of the washed anion exchange support was placed on a microscope slide and viewed under the microscope using an appropriate filter set for each labels as recommended by the manafacturer's manual (WIG for TMR (excitation range 520-550 nm, emission range > 580 nm), WBV for Flu (excitation range 400-440 nm and emission range > 475 nm) [36]

a)

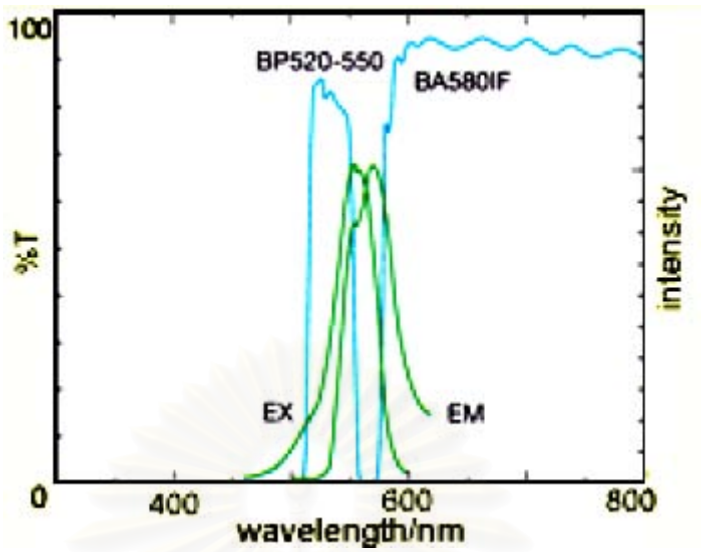

b)

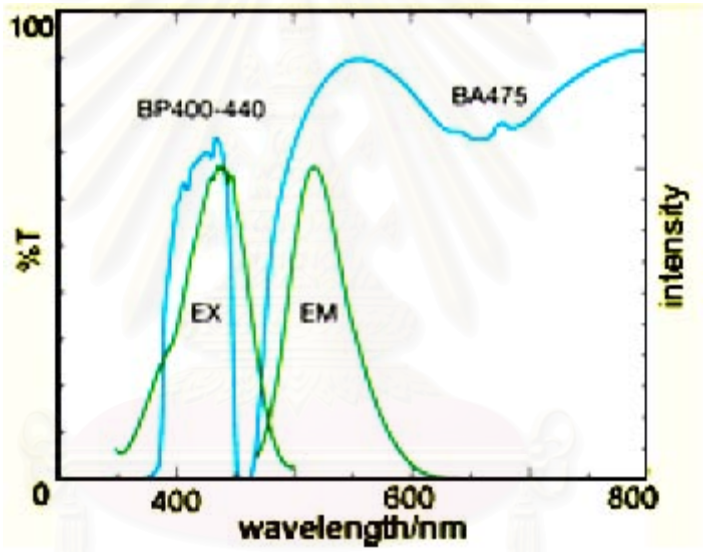

Figure 2.4 The excitation and emission range of a) WIG and b) WBV filter sets. [36]

Due to the limited filter sets available, some labels cannot be visualized efficiently in this fluorescence microscopy system. Photographs were taken using a digital camera (Olympus C5060WZ) in manual mode with all settings (ISO, shutter speed, aperture) constant for the same set of experiments.

CHAPTER III

RESULTS AND DISCUSSION

3.1 Synthesis of labeled PNA oligomers

3.1.1 Solid Phase Synthesis of PNA

One pyrrolidine monomer carrying a nucleobase and the *β*-amino acid spacer were coupled together *via* a peptide bond to become one subunit of PNA. By iterative coupling on a solid support according to the previously developed protocol [35], PNAs with desired sequences were obtained.

The microscale synthesis of PNA was carried out manually from Fmoc-protected monomers in a custom-made Pasteur pipette as described in **Chapter II.** The TentaGel S-RAM [37] resin containing a polyethylene glycol (PEG) grafted on polystyrene resin and a moderately acid labile Rink amide (RAM) linker [38] **(Figure 3.1)** was used as the solid support for all PNA syntheses. This linker is stable to piperidine, which is used in Fmoc deprotection, and can be easily cleaved with 95-100% TFA to provide peptide amides. Furthermore, the amino linker of RAM resin allows easy coupling with active esters such as Pfp ester to form amide bonds giving higher loading efficiency compared to resins containing *p*-benzyloxybenzyl alcohol linker such as Wang resin [39].

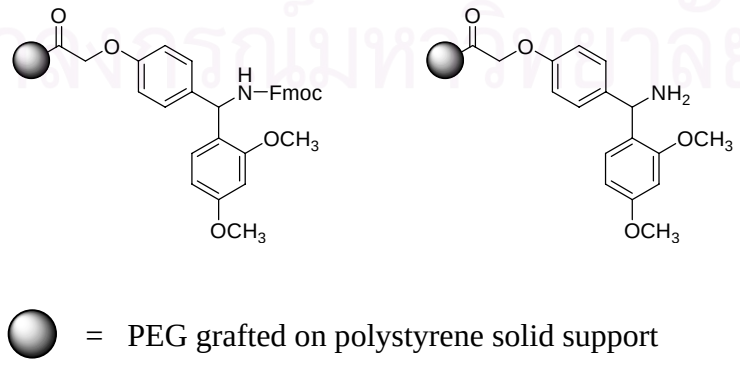

Figure 3.1 TentaGel S RAM Fmoc resin and TentaGel S RAM resin.

Synthesis of PNA (**P1**) consists of three important steps as follows.

i) Deprotection: The Fmoc protecting group must be first removed from the amino terminus of the resin and the growing PNA oligomer, which is accomplished by 2 % piperidine and 2% DBU in DMF.

ii) Coupling: The pyrrolidine monomer and the *β*-amino acid spacer in the form of their respective pentafluorophenyl (Pfp) esters were alternately coupled in the presence of HOAt as activator to the growing peptide chain attached onto the resin. This step was repeated until the required PNA sequence was obtained.

iii) Capping: The resin-bound amino group that had not been successfully coupled was capped by acetylation to prevent incomplete peptide chain from being coupled in the next cycles. This will reduce the deletion by-products that might have formed and thus facilitating subsequent purification. Capping was carried out with a solution of Ac_2O/DIEA in DMF as described in **section 2**.

The detailed synthesis cycle of PNA used in this work compared to that originally developed in this laboratory [35] is shown in **Figure 2.2**. The coupling efficiency can be monitored by measurement of the absorbance at 264 nm of dibenzofulvene-piperidine adduct released upon Fmoc-deprotection. The coupling efficiency in each step was calculated from UV-absorption. In general, coupling efficiency of 94-98% were usually achieved which translated into overall coupling efficiency of 47-74% depending on length and sequence of the PNA. Typical results are shown in **Table 3.1**.

Table 3.1 A average coupling efficiency/step and overall coupling efficiency in the synthesis of PNA sequences used in this study.

Sequence	**Scale (μmol)**	**Coupling efficiency (%)**	
		average	**overall**
H-TTTTTTTTT-$SerNH_2$	1.0	96.9	56.4
H-O-TTTTTTTTT-$SerNH_2$	2.0 (split in to 4 reactions)	95.9	46.8
H-O-TTTTATTTT-$SerNH_2$		98.1	70.5
H-O-TTTTCTTTT-$SerNH_2$		94.3	56.9

H-O-TTTTGTTTT-SerNH_2		96.9	50.2
H-O-TTCCCCCTCCCAA-SerNH_2	2.0 (split in to 2 reactions)	94.8	38.5
H-O-TTCCCCTTCCCAA-SerNH_2		95.4	42.7
H-TTTTTTTTT-SerNH_2	2.0 (split in to 3 reactions)	99.2	86.4
NH_2-Ser-TTTTTTTTT-SerNH_2		97.0	58.4
Ac-Ser-LysNH_2-TTTTTTTTT-SerNH_2		98.3	74.0
Ac-Ser-LysNH_2-TTCTATGTT-SerNH_2	1.0	97.3	60.9

3.1.2 End group modification with fluorescent labels

Several fluorescent labels including tetramethylrhodamine (TMR), fluorescein (Flu), dansyl (DNS), pyrene (Pyr), nitrobenzofurazan (NBD), Atto425, Atto520 were successfully incorporated. These were usually coupled directly to the amino group of the PNA via their respective active esters (succidimidyl ester, pentafluorophenyl ester). For pyrene, the commercially available pyrenebutyric acid was coupled using HATU/DIEA as activators**.**

Table 3.2 Structure of fluorescence properties of labels used in this study. [40-44]

Amine Reactive Label	**Label**
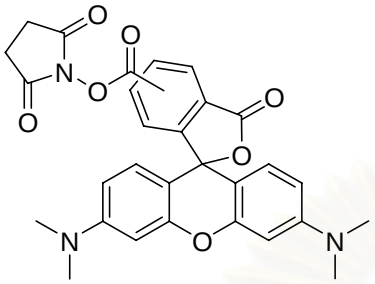	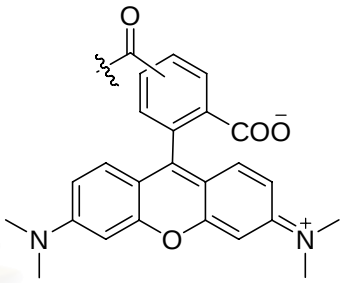
5(6)- Carboxytetramethylrhodamine (TMR) Excitation : 555 nm, Emission : 584 nm , ε : 91,000 $M^{-1}.cm^{-1}$	
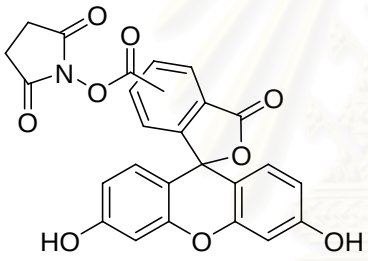	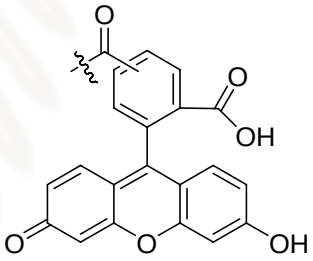
5(6)-Carboxyfluorescein (carboxyFlu) Excitation : 492 nm, Emission : 517 nm, ε : 68,000 $M^{-1}.cm^{-1}$	
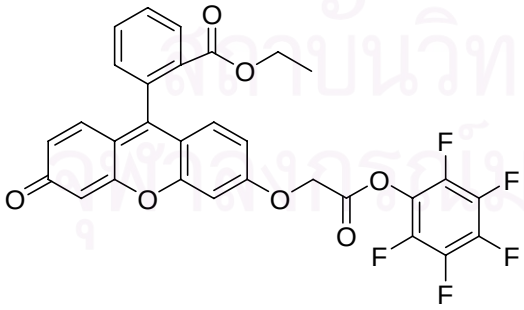	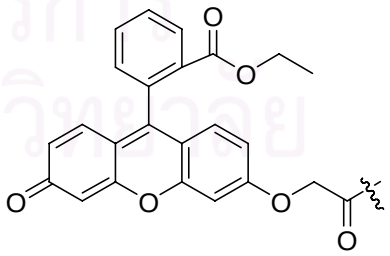
6-*O*-(Carboxymethyl)fluorescein 2-ethyl ester (Neutral Flu)) Excitation : 441 nm, Emission : 517 nm, ε : 68,000 $M^{-1}.cm^{-1}$	

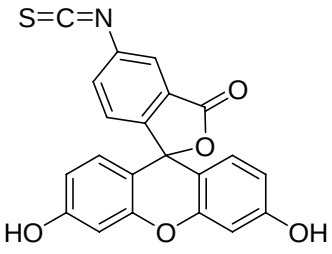

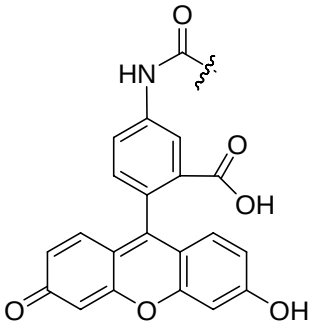

Fluorescein isothiocyanate (FITC)

Excitation : 492 nm, Emission : 518 nm, ε : 72,000 $M^{-1}.cm^{-1}$

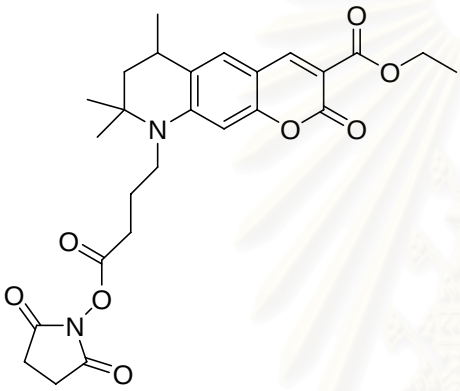

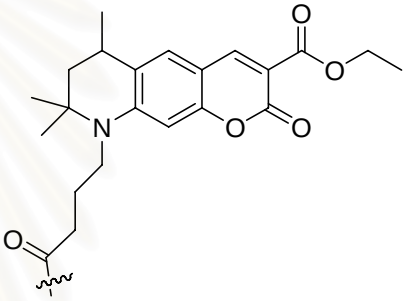

Atto425

Excitation : 437 nm, Emission : 483 nm, ε : 45,000 $M^{-1}.cm^{-1}$

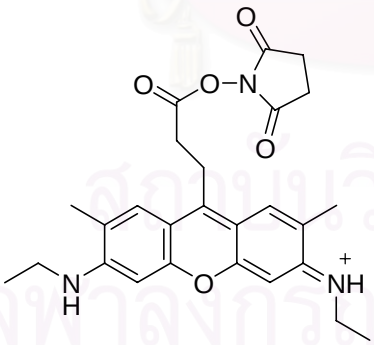

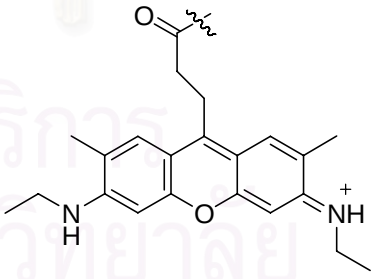

Atto520

Excitation : 520 nm, Emission : 540 nm , ε : 110,000 $M^{-1}.cm^{-1}$

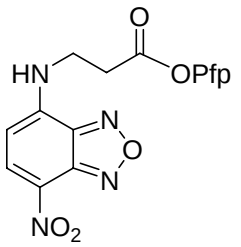

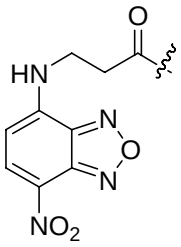

Nitrobenzofurazan (NBD)

Excitation : 420 nm, Emission : 540 nm, ε : 22,000 $M^{-1}.cm^{-1}$

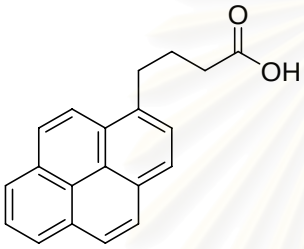

(+ HATU + DIEA)

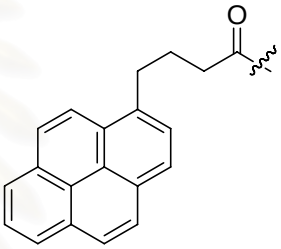

1- Pyrenebutyryl (Pyr)

Excitation : 345 nm, Emission : 376 nm, ε : 54,000 $M^{-1}.cm^{-1}$

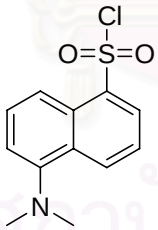

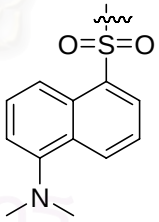

Dansyl (DNS)

Excitation : 338 nm, Emission : 492 nm , ε : 5,900 $M^{-1}.cm^{-1}$

After addition of the final residue was completed, the Fmoc group at the N-termini of the support-bound PNA was removed by treatment with the deprotection solution (2% piperidine/DBU in DMF). The PNAs were then modified with an appropriate fluorescent label at the N-termini. For PNA sequences carrying adenine, cytosine and guanine, deprotection of the exocyclic amino protecting groups (benzoyl

and isobutyryl), a side-chain is required. This involved treatment with 1:1 ammonia/dioxane in a sealed test tube at 60 ^{o}C for 6 hour or overnight [45]. The conditions are not always compatible with all fluorescent labels. The side chain deprotection was therefore carried out first for fluorescent labels that were not stable towards strongly basic conditions including TMR etc. For stable label such as fluorescein, the side-chain deprotection was postponed until after the label has been incorporated. In PNA sequences containing only thymine, no side-chain deportection was required. A hydrophilic diethyleneglycol (egl) or O-linker was also optionally incorporated between the label and the PNA to reduce possible interactions between the nucleobases and the fluorescent labels which might lead to reduced fluorescence. If the linker was included, the nucleobase side-chain deprotection was performed before introduction of the linker since it was observed that migration of the benzoyl/isobutyryl groups to the amino group of the linker was a serious competing side-reaction.

After the labels had been introduced, the labeled PNAs were released from the resin by treatment with 95 % trifluoroacetic acid. The labeled PNAs were collected as crude after removing the volatile and precipitating with diethyl ether. They were purified by C-18 reverse phase HPLC monitoring by UV-absorbance at 260 nm and at the wavelength at which the label absorb. A typical chromatogram is shown in **Figure 3.2a.** The pooled HPLC fractions were freeze-dried. The residue was redissolved in 100 μL of water and the concentration of the PNA was determined spectrophotometrically. The identity of the PNA was confirmed by MALDI-TOF mass spectrometry which showed the expected mass of the molecular ion $[M+H]^+$ or $[M+Na]^+$ as shown in **Figure 3.2b and Table 3.3**.

a)

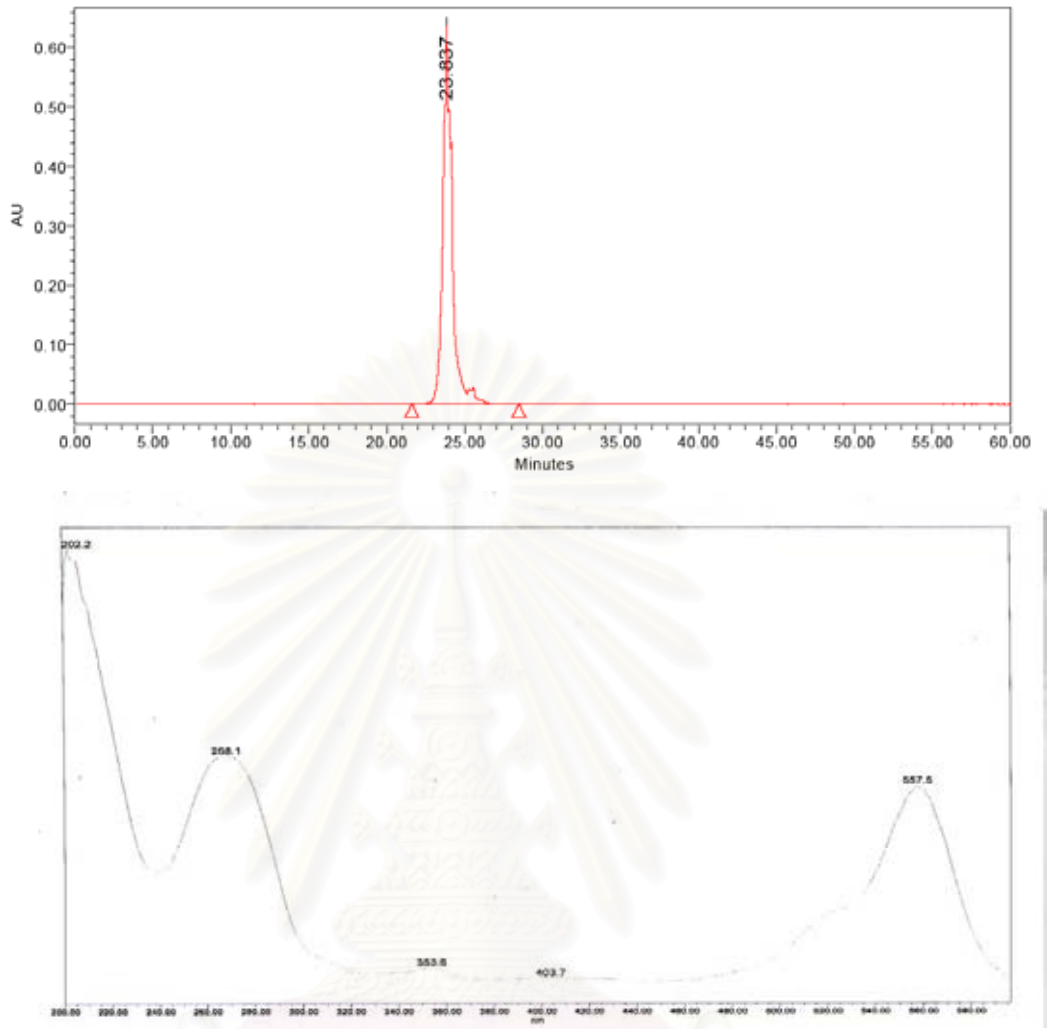

b)

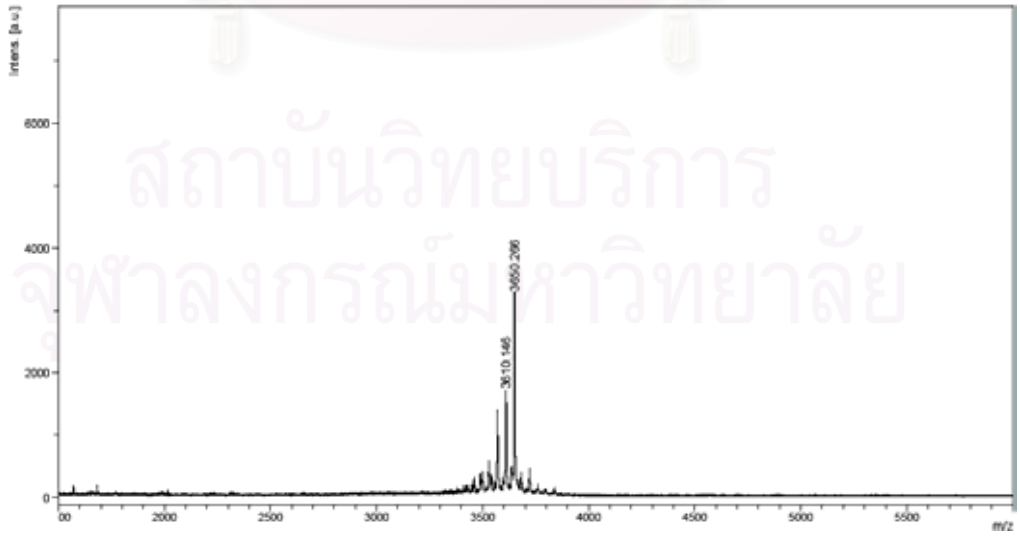

Figure 3.2 (a) HPLC chromatogram using condition displayed in **Figure 2.2** (upper and lower shown UV spectrum of TMR: 555 nm and PNA: 260 nm, respectively) and (b) MALDI-TOF MS of **P2** $M{\cdot}H^{+}$(calcd)=3653.521.

Table 3.3 Characterization data of labeled PNA sequences used in this study.

PNA	t_R[a]	M·H$^+$ (found)[b]	M·H$^+$(calcd)[c]	% error[d]
P1	Purify by c-8	3507.918	3508.448	0.015
P2	23.8	3653.750	3653.521	0.006
P3	23.0	4875.640	4880.806	0.052
P4	22.0	4890.783	4895.892	0.051
P5	24.1	3605.435	3607.429	0.020
P6	Purify by Q-S	3643.531	3638.417	0.051
P7	21.9	3648.209	3649.763	0.016
P8	33.5	3482.827	3484.424	0.016
P9	21.5	3493.639	3492.687	0.002
P10	Purify by Q-S	3577.644	3575.564	0.021
P11	23.5	3651.035	3649.824	0.033
P12	32.3	4827.902	4825.779	0.021
P13	23.5	4869.530	4868.114	0.014
P14	25.6	3350.814	3351.350	0.011
P15	22.7	3432.723	3431.441	0.037
P16	Purify by gel	3619.377	3618.690	0.018
P17	Dialysis	3638.955	3637.710	0.034

[a] Condition for reverse-phase HPLC: C-18 column 3μ particle size 4.6 x 50 mm; gradient system of 0.1% TFA in acetonitrile/water 10:90 to 90:10 in 25 min; hold time 25 min.

[b] matrix solution containing CCA in 0.1% trifluoroacetic acid in acetonitrile:water (1:2) solution

[c] Mass calculate

[d] M·H$^+$(calcd) – M·H$^+$ (found)[b]/ M·H$^+$ (found) x 100

3.2 Binding Properties of PNA

3.2.1 Hybridization of PNA with DNA by UV-melting technique

The UV-melting technique technique was used to determine the formation of PNA·DNA hybrids. [46] The maximum UV absorption of oligonucleotides revealed a strong at approximately 260 nm and a molar extinction coefficient (ε) in the order of 10^4 $dm^3mol^{-1}cm^{-1}$. This interaction is sensitive to the state of base stacking and base pairing. In general, the resulting of base-base stacking provides the decrease in ε which is known as hypochromism. [47] The hypochromism can be observed in DNA·DNA duplex as well as DNA·PNA complex. Dissociation of the duplex into single stranded oligonucleotides, e.g. by heating, makes the absorption increased which can be monitored at 260 nm. The transition from the duplex to the single stranded form takes place within a narrow temperature range (typically 10-20 ^oC). The temperature at the midpoint of the transition is called melting temperature T_m and can be taken as an indication of stability of the duplex. The higher the T_m, the more stable the duplex. In all cases (**Table 3.4**) it was confirmed that the labeled PNA retained the high affinities and specificity in DNA recognition of the unlabeled PNA.

Table 3.4 T_m values.

PNA	T_m with DNA (°C)		note
	DNA sequence 5'---------3'	Corrected T_m^* (°C)	
P1	AAAAAAAAA	74.0	perfect match
P1	AAAATAAAA	29.0	single mismatch
P2	AAAAAAAAA	76.0	perfect match
P2	AAAATAAAA	47.9	single mismatch
P3	TTGGGGGAGGGAA	62.0	perfect match
P3	TTGGGGAAGGGAA	46.6	single mismatch
P4	TTGGGGAAGGGAA	70.0	perfect match
P4	TTGGGGGAGGGAA	39.9	single mismatch
P5	AAAATAAAA	59.0	perfect match
P5	AAAAAAAAA	28.0	single mismatch

P7	AAAATAAAA	65.2	perfect match
P7	AAAAAAAAA	33.3	single mismatch
P8	AAAATAAAA	65.7	perfect match
P8	AAAAAAAAA	40.3	perfect match
P9	AAAATAAAA	60.9	perfect match
P10	AAAAGAAAA	59.2	perfect match
P11	AAAACAAAA	66.3	perfect match
P13	TTGGGGGAGGGAA	57.2	perfect match
P13	TTGGGGAAGGGAA	40.2	single mismatch
P14	AAAAAAAAA	69.0	perfect match
P16	AAAAAAAAA	69.9	perfect match

*The equation for determining the corrected temp was obtained by measuring the actual temp in the cuvette using a temperature probe and plotting against the set temperature (T_{block}) from 20-90 °C. The linear equation and relationship were obtained with Y = 0.978X-0.6068 and $r^2 > 0.99$.

3.2.2 Hybridization of PNA with DNA by gel electrophoresis

Interactions between some fluorescent labeled PNA and DNA can be monitored by polyacrylamide gel electrophoresis. The study was carried out only for TMR-labeled T_9 (**P1**) and DNS-labeled T_9 (**P14**) in the absence and presence of complementary target DNA (dA9). The resulting gel was photographed after visualization under a UV-transilluminator (black light) as shown in **Figure 3.3**.

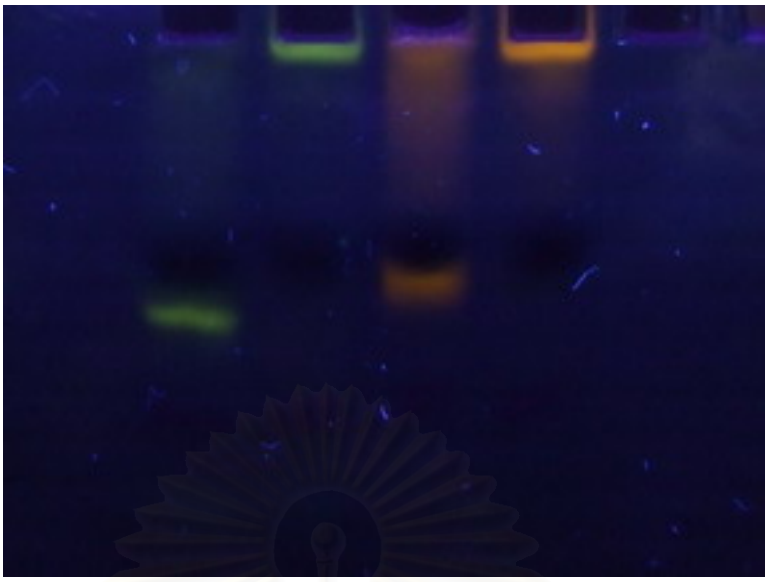

Figure 3.3 Gel hybridization experiment: Lane 1: (**P14**) **+ dA9**, Lane 2: (**P14**) + $dA_2G_4T_3$, Lane 3: (**P1**) + dA_9, Lane 4: (**P1**) + $dA_2G_4T_3$, Condition: 15% polyacrylamide gel in 90 mM Tris-Borate-EDTA (TBE) pH 8.0 and run at a constant voltage of 150 V**.**

In lane 1 and 3, (**P14**) and (**P1**) form a new negatively-charged hybrid with complementary DNA as shown by a new fast-migrating band in each case. In the presence of non-complementary DNA (lanes 2 and 4), the PNA hardly migrate at all due to their electronically neutral nature. This experiment suggests that both PNA can form stable hybrids with DNA in a sequence-specific manner.

3.3. Development of a new fluorescence-based method in detection of DNA Sequences

3.3.1 The concept

This research emphasizes on development of a new fluorescence-based technique for DNA sequence determination using fluorescent labeled PNA as a probe. The probe was used in combination with an insoluble anion exchange support. The technique relied on differential ionic interaction between neutral PNA and negative charge of DNA on positively charged ion exchanger. Because of its neutrality,

fluorophore labeled PNA can not be immobilized onto the anion exchanger by itself. In the presence of the complementary DNA, the PNA can form a negatively charged hybrid with the DNA target. This PNA·DNA hybrid can be absorbed onto the anion exchange support, causing fluorescence when visualized under UV lamp or fluorescence microscope. On the other hand, in the presence of the non-complementary DNA target, a negatively charged PNA·DNA complex can not be formed due to the high specificity of the PNA·DNA interaction. In this case, only the DNA will be absorbed by the anion exchange support and the support will not be fluorescent. The principle can be schematically illustrated in **Figure 3.4**.

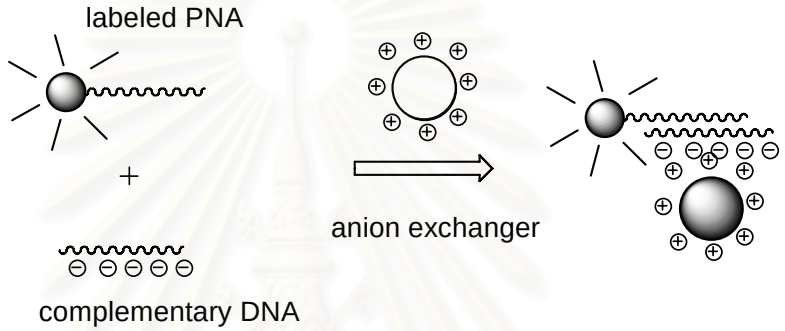

Figure 3.4 The concept of using fluorescent-labeled PNA and solid anion exchange support for determination of DNA sequences.

3.3.2 Validation of the concept by UV-VIS spectrophotometry

To proof the validity of this concept, two preliminary experiments were investigated using the quaternary ammonium modified silica (trimethylammoniumpropyl) (SAX) as a model of anion exchange support**.** The ability of the solid anion exchanger to absorb PNA and its DNA hybrids was determined in two ways.

In the first strategies, the UV-VIS spectrophotometry technique was used to determine the absorption of PNA·DNA hybrid onto the anion exchange support. No fluorescent label was used at this early stage. The PNA probe used as a model was Ac-T_9-LysNH_2. Two DNA were chosen as a model, dA_9 for complementary and dT_9 for non-complementary DNA. In the experiment, the intensity of the UV absorbance of PNA·DNA hybrid before and after adding the solid support was measured and

compared to the control solution (PNA solution with out DNA). The results are as shown in **Figure 3.5**.

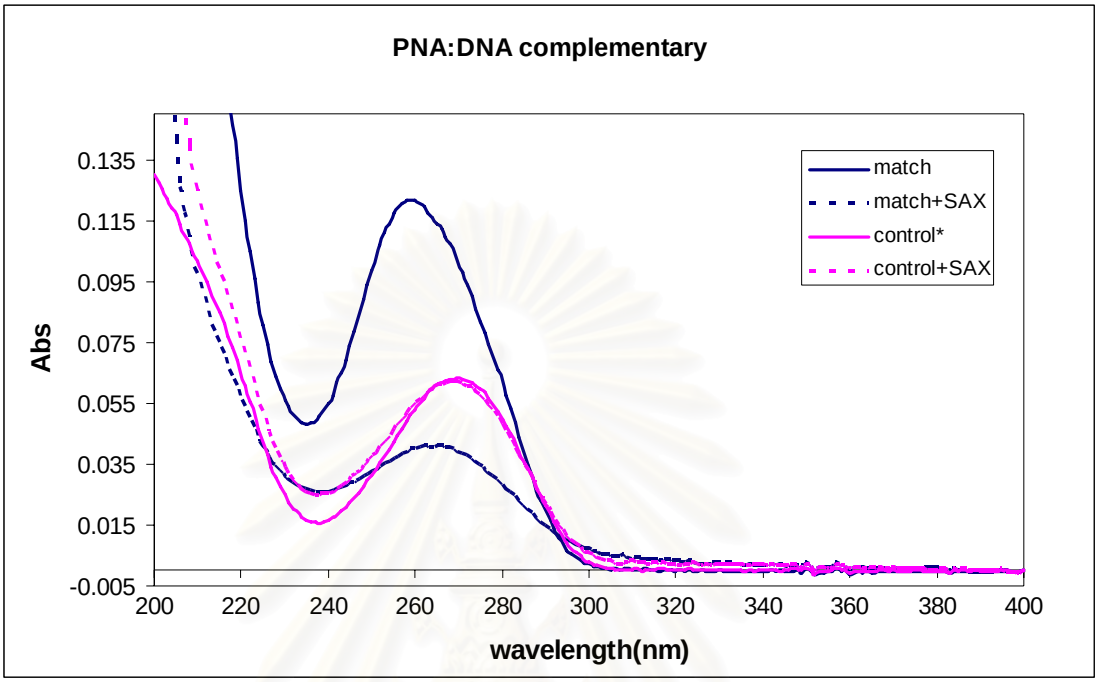

*control was only PNA in reaction

Figure 3.5 UV spectrum of control solution before and after adding the solid support.

The UV spectrum of the control solution before and after adding the solid support was almost the same (pink lines). This means that the PNA could not be absorbed onto the solid support by it self, which is consistent with the expectation. On the other hand, in the presence of complementary DNA target, the intensity of the UV spectrum of PNA·DNA complex after adding the solid support (dotted blue line) was lower than before adding the solid support (solid blue line). More importantly, the intensity was lower than when PNA alone was treated with the support. This means that some of the PNA were absorbed onto the solid support, making the intensity of the UV spectrum of the solution after adding solid support deceased.

3.3.3 Application of fluorescent labeled PNA as a probe for DNA sequence analysis.

In the second strategies, the experiments involved immobilization of fluorescent labeled PNA·DNA hybrid on solid anion exchange support. The success of the immobilization on the solid support was detected by UV lamp or fluorescence microscope. The dansyl labeled PNA **P15** was used as a model. The DNA AAAAAAAAA was used as the complementary target DNA.

All experiments were carried out at 0.5 nmol each of PNA probe and DNA target in 10 mM phosphate buffer pH 7 (total volume 30 µL). After hybridization the anion exchange support was washed with water. The result is shown in **Figure 3.6**.

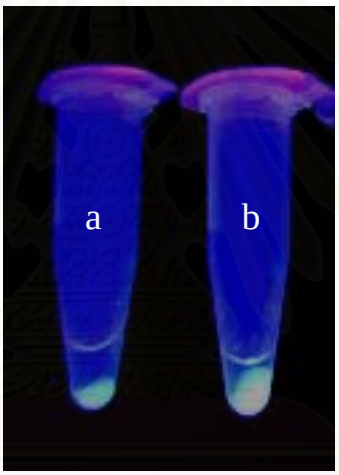

Figure 3.6 Photograph of the ion exchange support after treatment with... a) PNA alone (control) b) PNA + complementary DNA.

It is clearly shown that in the presence of complementary DNA, the solid support in tube (b) fluoresced more strongly than in tube (a) because the negatively charged fluorescent labeled PNA·DNA complex formed was absorbed more readily onto the solid support. However, it was also evidenced that the free PNA could be immobilized onto the solid support to some extent making solid support slightly fluorescent as shown in tube a.

These results confirmed that the negatively charged PNA·DNA complex can be immobilized onto the solid support in preference to the free PNA as shown by UV absorbance of the solution and by fluorescence of the support.

Encouraged by these preliminary experiments, another dansyl labeled PNA containing all four nucleobase (**P18**) was tested with the DNA AACATAGAA and AACACAGAA as complementary and single mismatched targets respectively.

All experiments were carried out at 2 nmol each of the PNA probe and the DNA target in 10 mM phosphate buffer pH 7.0. After hybridization the ion exchange support was washed with water as described previously. The result is as shown in **Figure 3.7**.

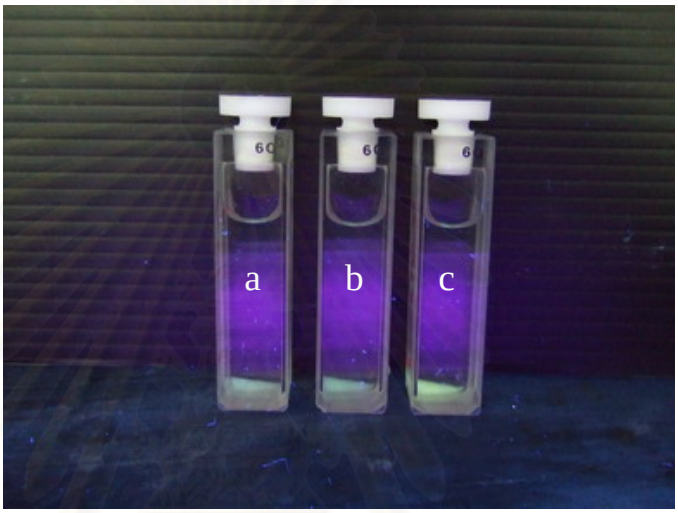

Figure 3.7 Photograph of the ion exchange support after treatment with a) PNA alone (control) b) PNA + single mismatched DNA c) PNA + complementary DNA.

In the presence of the complementary DNA, the negatively charged PNA·DNA complex was formed and was preferentially absorbed onto the solid support making the solid support fluorescent significantly as shown in cell (c). Consistent to the previous experiment, in the absence of complementary DNA targets the labeled PNA can be absorbed slightly on the ion exchange support, making the support weakly fluorescence as seen in cells (a) and (b). The single base mismatch DNA target (cell b), showed similar fluorescence to the control (cell a).

From these results, it can be concluded that dansyl labeled PNA can be used as a probe to discriminate between complementary DNA and single base mismatch DNA targets when used in combination with anion exchanger and visualized under UV lamp at 366 nm.

Although the results have validated the concept, two major problems were encountered. Firstly, due to the low molar extinction coefficient and low quantum yield of dansyl label, it was difficult to detect small quantities of the PNA probes (and DNA targets). Consequently, the several types of fluorescent dyes that exhibit better fluorescence than dansyl were studied. From the survey of several commercially available fluorescent labeling groups, it was found that the TMR labeling group show a very high molar extinction coefficient and high quantum yield than others (**Table 3.2**). Furthermore, its structure consisted of positive charge which should decrease the non-specific interaction between the labeled PNA and the anion exchanger. TMR was therefore chosen as the fluorescent labeling group of choice.

The second problem was the relatively high background absorption of the labeled PNA by the ion exchange support (SAX) even in the absence of DNA. This is believed to involve mainly hydrophobic interaction between the label and the support. To solve this problem, two strategies were employed. One was to use organic solvents to wash the support after the absorption. The other approach was to change the support to less hydrophobic materials. The results will be discussed in more details in the next section.

3.3.4 Optimization of the condition to decrease non-specific absorption

As earlier stated, the high background absorption was a major problem. The first strategy employed to reduce the background level was by washing the support with acetonitrile or by including acetonitrile to the hybridization media. TMR-labeled PNA (**P1**) was used as a model and the level of specific and non specific absorptions determined by UV absorbance measurement at 555 nm in the presence of (equimolar or excess) complementary (dA_9) and non-complementary DNA (dT_9) respectively. It was found that including acetonitrile in the hybridization experiment, not only the background absorption of the PNA, but also the absorption of the PNA when the complementary DNA was present was significantly decreased. A typical UV-experiment result is shown in **Figure 3.8**.

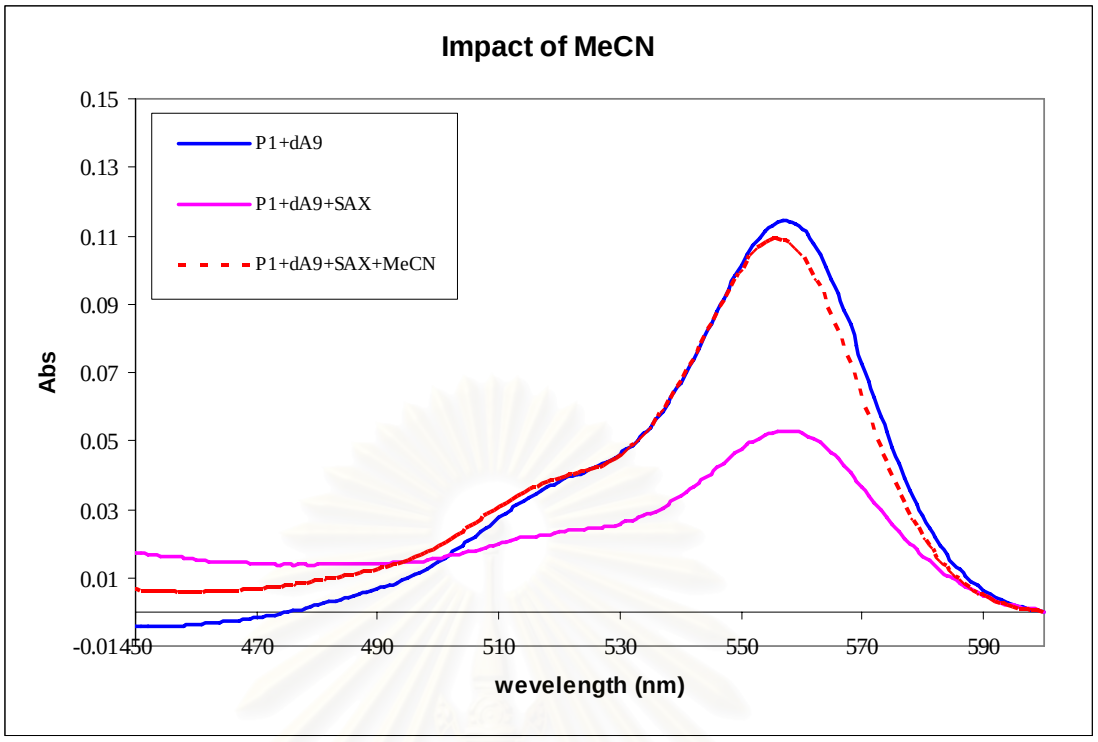

Figure 3.8 The effect of including acetonitrile in the hybridization medium.

The results suggested that the presence of acetonitrile could also destabilize the complementary PNA·DNA hybrid. The spectrum of the complementary PNA·DNA after treatment with the ion exchange support showed an increase of intensity when MeCN was added to a concentration of 10% (dot red line). Since the presence of acetonitrile can have impact on the binding affinities of PNA·DNA hybrids, it was thought that washing the support with acetonitrile containing medium might be better.

The effect of including acetonitrile in the washing medium is shown in **Table 3.5**.

Table 3.5 Compare the fluorescence of the solid supports before and after wash by 50% aqueous MeCN. (from left to right, complementary DNA (dA_9), non-complementary DNA (dT_9), single mismatch DNA (dA_8T) and control (no DNA)).

PNA	Before wash by 50%MeCN	After wash by 50%MeCN
P15	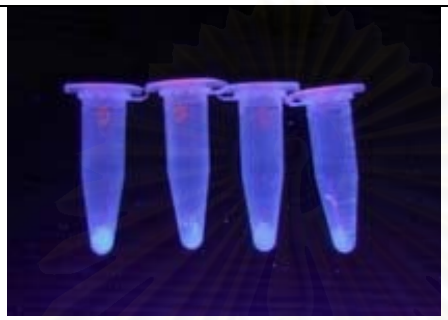	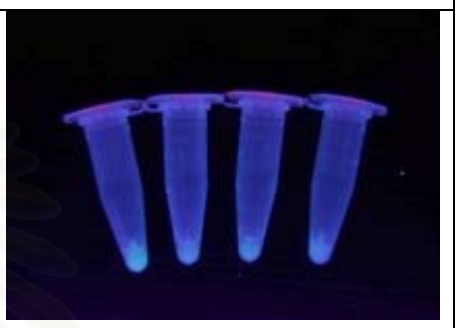
P1	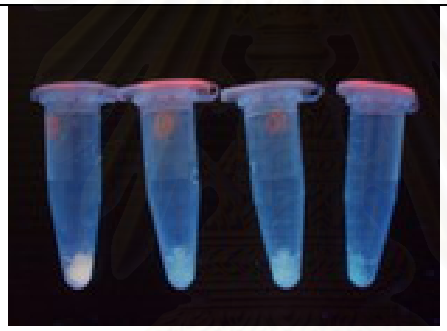	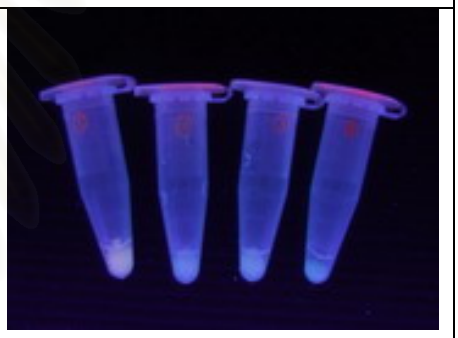

The results show that only limited success could be obtained since a distinct fluorescence of the support was observed especially with the TMR-labeled probe when the complementary DNA was present. However, the presence of acetonitrile in the washing medium can still have adverse effects on the binding affinities of PNA·DNA complex. It the washing was done far too long time, the fluorescence decreased even in complementary cases.

As the non-specific absorption is thought to involve mainly hydrophobic interactions, other less hydrophobic supports were investigated as the second strategy. Other anion exchangers tested in this study include quaternary ammonium (trimethylaminopropyl) (SAX), ethylenediamine-N-propyl (PSA), diethylaminoethyl cellulose (DEAE cellulose), diethylaminoethyl sepharose (DEAE sepharose), quaternary ammonium sepharose (Q sepharose) and chitosan. The structures of all anion exchangers are shown in **Table 3.6**. Each of anion exchanger exhibited the

different ionic capacity (number of charged substitute group per gram dry ion exchanger or per ml swollen gel) as shown in **Table 3.7.** [48-50]

Table 3.6 Structures of anion exchanger used. [48-50]

<table>
<tr><td> 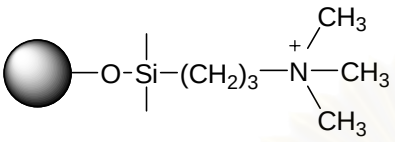 </td><td> 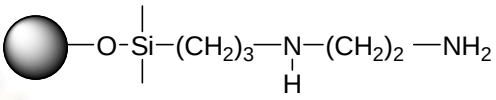 </td></tr>
<tr><td>trimethylammoniumpropyl silica (SAX)</td><td>N-aminoethylaminopropyl silica (PSA)</td></tr>
<tr><td> 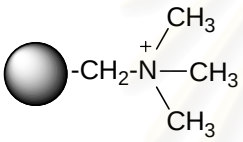 </td><td> 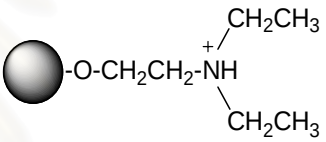 </td></tr>
<tr><td>Quaternary ammonium sepharose (Q sepharose)</td><td>Diethylaminoethyl sepharose (DEAE sepharose)</td></tr>
<tr><td colspan="2"> 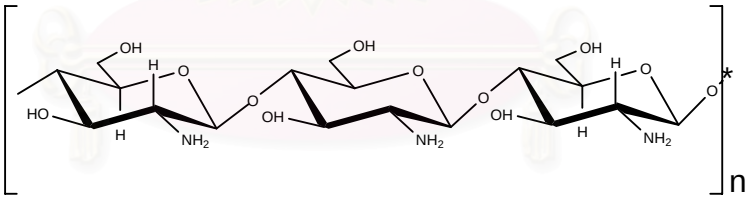 </td></tr>
<tr><td colspan="2">2-amino-2-deoxy-D-glucose (chitosan).</td></tr>
<tr><td colspan="2"> 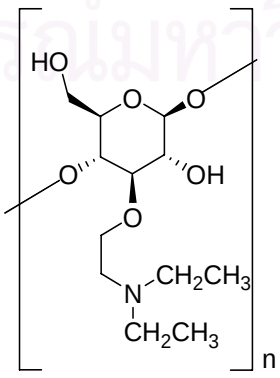 </td></tr>
<tr><td colspan="2">Diethylaminoethyl cellulose (DEAE cellulose)</td></tr>
</table>

Table 3.7 Ionic capacity of each of anion exchanger. [48-50]

Anion exchanger	Type of anion exchanger	Total ionic capacity
SAX	Strong	850 μmol/g
PSA	Weak	1100-1400 μmol/g
Q sepharose	Strong	180-250 μmol/mL gel
DEAE sepharose	Weak	110-160 μmol/mL gel
DEAE cellulose	Weak	1000 μmol/g
chitosan	Weak	2500-2800 μmol/g

In all experiments, the PNA was mixed with the target DNA in phosphate buffer (10 nm, 2 mL) and followed by addition of the anion exchanger (about 10 mg). The intensity of the spectrum of the PNA·DNA complex solution with both its complementary and non complementary DNA before and after addition of the solid support was detected at 555 nm, which is the maximum absorption of the TMR label. Ideally, the absorbance should remain the same in the presence of non-complementary DNA before and after the ion exchanger was added since no absorption of the PNA should take place. In practice, some absorption was observed and this figure will be taken as background absorption. A good support should exhibit minimal background absorption. On the other hand, in the presence of complementary DNA, the signal at 555 nm should be decreased most. The appropriate solid support should provide maximum difference between complementary and non-complementary cases. Some typical results are as shown in **Figure 3.9** and **Table 3.8**.

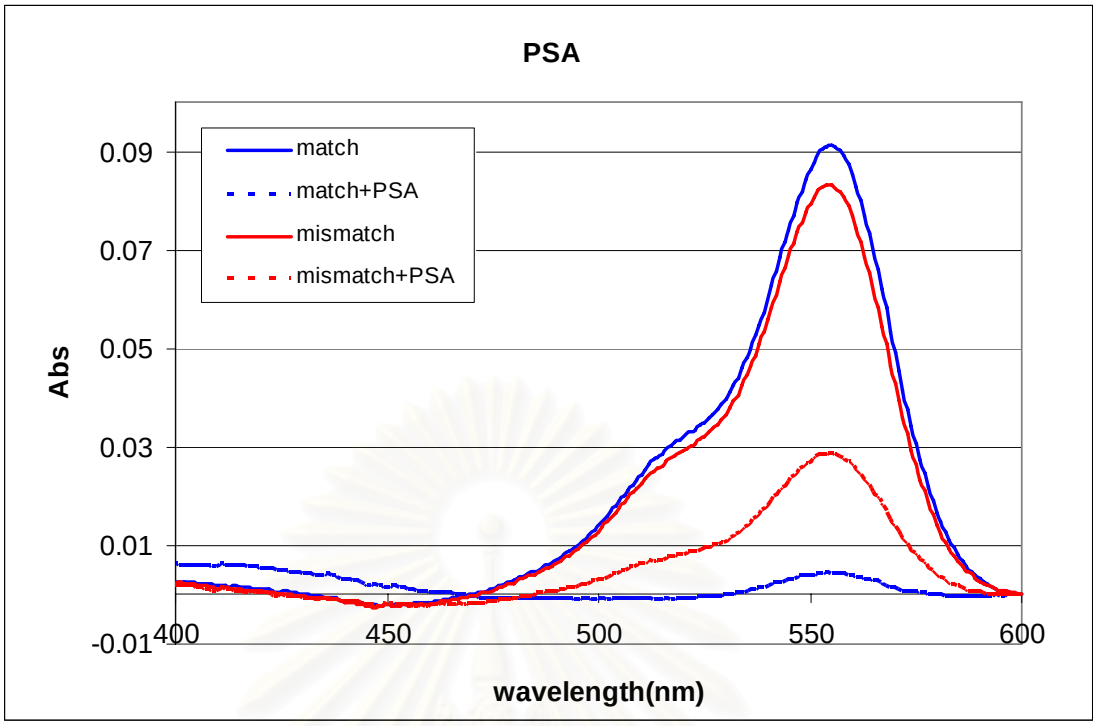
PSA
match
match+PSA
mismatch
mismatch+PSA
Abs
0.09
0.07
0.05
0.03
0.01
-0.01
400
450
500
550
600
wavelength(nm)

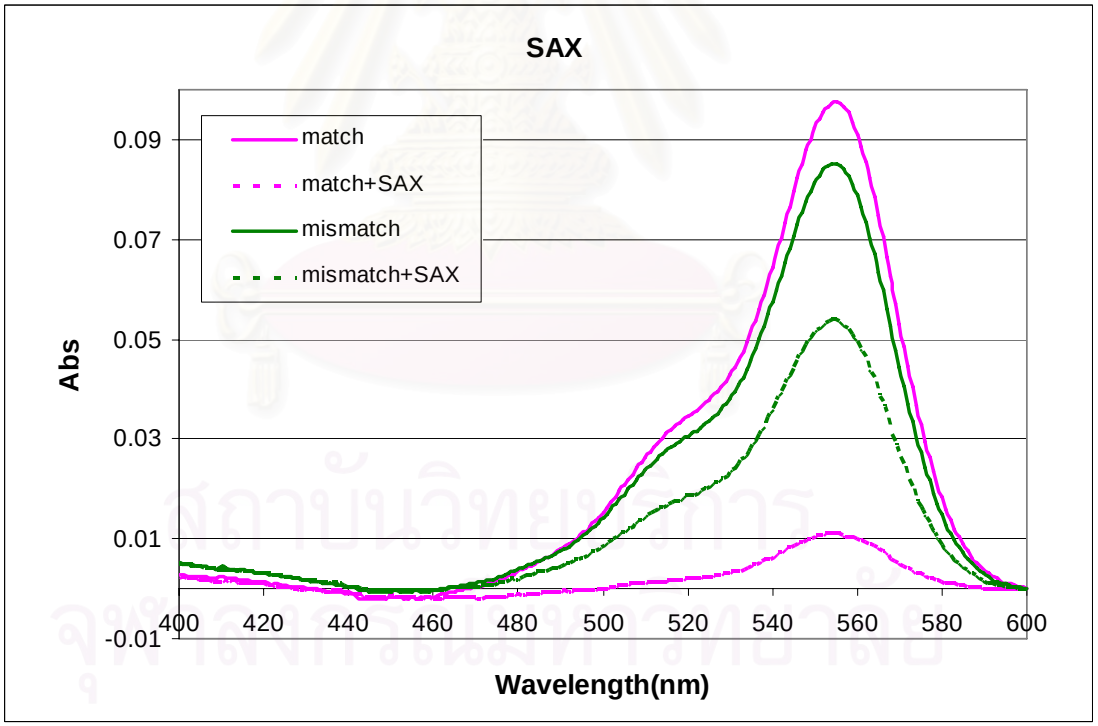
SAX
match
match+SAX
mismatch
mismatch+SAX
Abs
0.09
0.07
0.05
0.03
0.01
-0.01
400
420
440
460
480
500
520
540
560
580
600
Wavelength(nm)

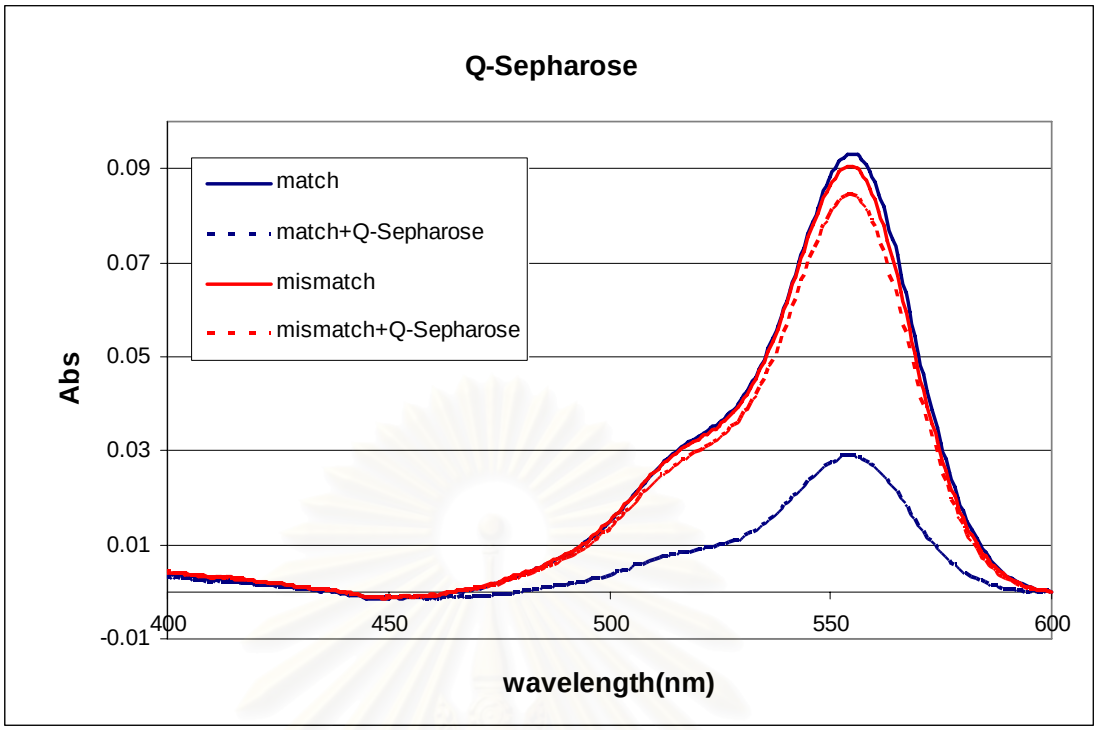
Q-Sepharose
match
match+Q-Sepharose
mismatch
mismatch+Q-Sepharose
Abs
0.09
0.07
0.05
0.03
0.01
-0.01
400
450
500
550
600
wavelength(nm)

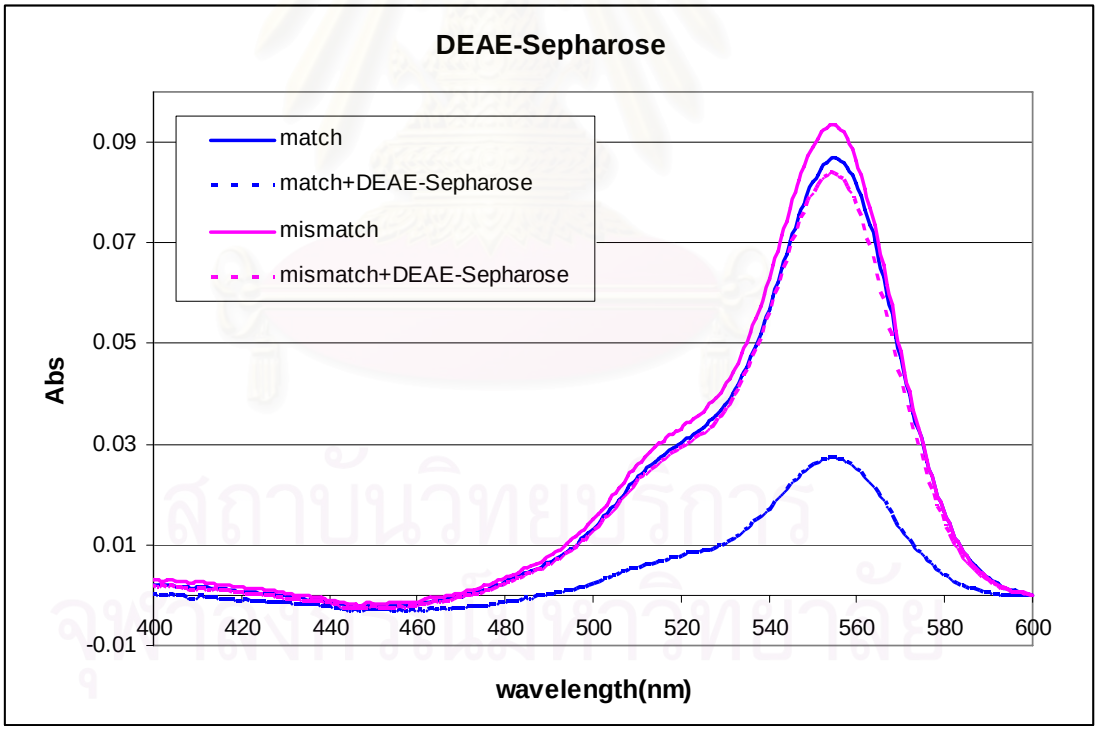
DEAE-Sepharose
match
match+DEAE-Sepharose
mismatch
mismatch+DEAE-Sepharose
Abs
0.09
0.07
0.05
0.03
0.01
-0.01
400
420
440
460
480
500
520
540
560
580
600
wavelength(nm)

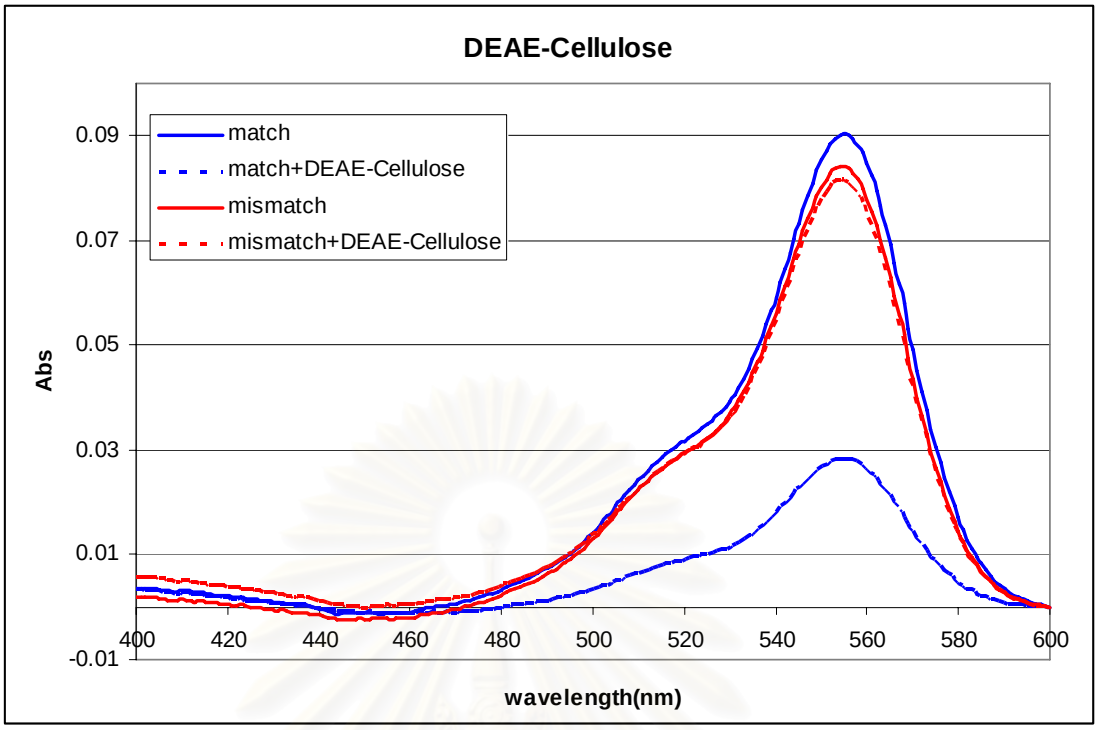

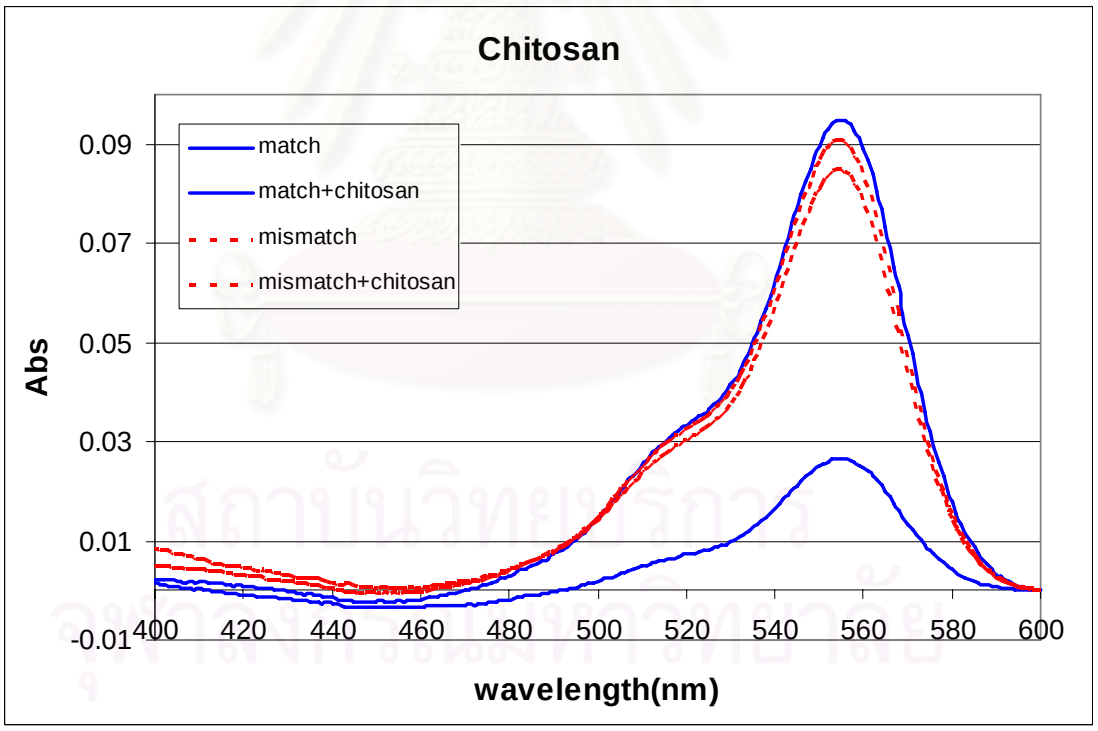

Figure 3.9 UV spectra of a mixture between TMR-PNA (**P1**) and complementary or non-complementary DNAbefore and after addition of various anion exchange supports.

Table 3.8 The intensity of UV absorbance at 555 nm in each experiment.

Anion exchanger	A_{555} of match	A_{555} of match + anion exchanger	A_{555} of mismatch	A_{555} of mismatch + anion exchanger
SAX	0.0975	0.0110	0.0850	0.0539
PSA	0.0912	0.0043	0.0830	0.0287
Q sepharose	0.0931	0.0288	0.0905	0.0844
DEAE sepharose	0.0869	0.0273	0.0935	0.0839
DEAE cellulose	0.0903	0.0284	0.0842	0.0817
Chitosan	0.0949	0.0264	0.0909	0.0850

From the results shown in Table 3.9 above, percent of difference between match and mismatch of each anion exchanger can be calculated according to the equations (1) and (2) shown below.

$$\% \text{ absorbed (match)} = 100 - \left\{ \frac{Abs_{555 \text{ of match + anion exchanger}}}{Abs_{555 \text{ of match without anion exchanger}}} \times 100 \right\} \quad (1)$$

$$\% \text{ absorbed (mismatch)} = 100 - \left\{ \frac{Abs_{555 \text{ of mismatch + anion exchange}}}{Abs_{555 \text{ of match without anion exchanger}}} \times 100 \right\} \quad (2)$$

$$\% \text{ Difference} = \% \text{ absorbed match} - \% \text{ absorbed (mismatch)}$$

The resulting data are shown in **Table 3.9**.

Table 3.9 Percent of difference between match and mismatch of each anion exchanger.

Anion exchanger	% absorbed (match)	% absorbed (mismatch)	%Difference
SAX	88.7	36.5	52.2
PSA	95.2	65.4	29.8
Q sepharose	69.0	6.7	**62.3**

DEAE sepharose	68.6	10.3	58.3
DEAE cellulose	68.5	2.9	65.5
Chitosan	72.2	6.5	65.7

A good of solid support would be have high percent of absorbed (match) and low percent of absorbed (mismatch or background). Form these experiments, it was found that Q sepharose, DEAE cellulose and chitosan showed a better efficiency than others ion exchangers in terms of minimal background absorption. The wide range of operating pH of Q-sepharose (all pH range) compared to DEAE-sepharose (pH < 9-10) and chitosan (pH < 7-8) were also significant advantages. As a result, Q sepharose was selected for further use as the anion exchanger for detection DNA sequences.

3.3.5 Detection of PNA·DNA hybridization using Q sepharose and fluorescence microscopy.

In this experiment, the TMR-T_9-SerNH_2 (**P1**) was used as a probe, dA_9 as complementary DNA, dA_8T as single mismatch DNA and dT_9 as non-complementary DNA. The hybridization was carried out with 0.5 nmol of PNA probe and DNA target in 10 mM phosphate buffer pH 7 (30 µL). After 15 min of incubation at room temperature, the Q-sepharose (approximately 2 mg) was added and left for another 15 min. After washing with water, the ion exchange support was viewed under UV transilluminator and fluorescent microscope. A clear differentiation between complementary and non complementary was achieved. The result was shown in **Figure 3.10**.

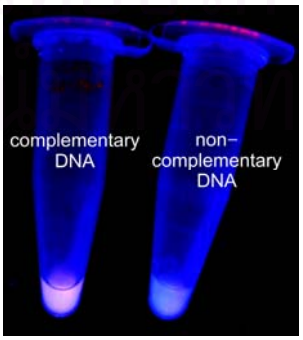

Figure 3.10 Complementary and non-complementary at 500 pmol of (**P1)** under UV-Transilluminator

3.3.5.1 Detetion limit of the technique using TMR-labeled T_9 PNA probe

The experiment above showed that the TMR-PNA probe (**P1**) can be used to differentiate complementary and non-complementary DNA in the presence of Q-sepharose as the anion exchange support. The quantity of the probe and sample required were far too high (500 pmol) for practical purposes.

In order to improve the sensitivity and to find the detection limit of the technique, fluorescent microscopy was used to examine the solid supports obtained from above. Since the fluorescent microscope used is equipped with a filter set that match with TMR label (WIG), The TMR-labeled PNA (**P2)** having an O-linker at the N terminus and was chosen for further optimization. A clear difference between the presence of complementary (dA_9) and single mismatched DNA targets (dA_4TA_4) was observed under fluorescence microscope at 500 pmol (equimolar quantites of probes and targets). In order to find the detection limit, the amounts of the PNA and DNA probes were systematically decreased from 500 to 1 pmol. The results are as shown in **Table 3.10** (All photographs were taken using identical parameters: shutter speed – 1 second, F stop - 4.8; ISO - 80. Identical filter sets were used in all experiments.).

Table 3.10 Detection limit in differentiation between dA_9 and A_8T using the PNA probe **P2**.

Quantity	Complementary	Single mismatch
500 pmol	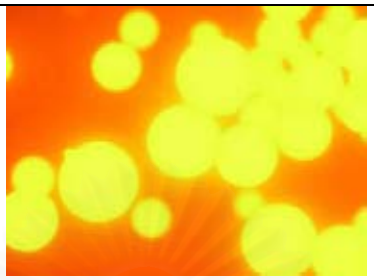	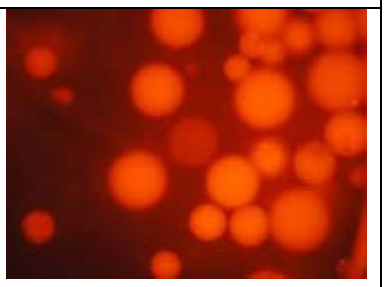
100 pmol	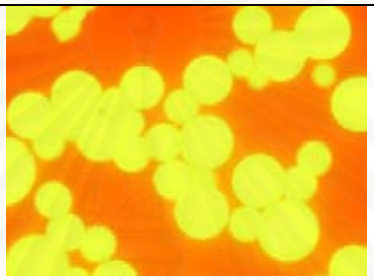	
10 pmol		
5 pmol		
1 pmol	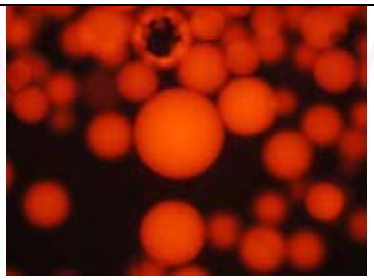	

The results in **Table 3.10** showed that it is possible to detect the difference between complementary and single mismatch DNA targets using TMR-labeled T_9

PNA probe (**P2**) in the concentration range between 1 to 500 pmol (total volume of 30 µL). The sensitivity in this case is far better than the use of UV-transilluminator which requires at least 100 pmol of PNA probes and DNA samples to be visible by naked eyes. The detection limit of 1 pmol, although not very low compared to enzyme-based techniques, is sufficient for detection of DNA sequences in routine PCR samples having the target DNA in picomole ranges. Most importantly, at all concentrations, very clear differences between complementary and single mismatch DNA were observed. This indicate a very high specificity of the detection technique, which can be attributed to the specificity of the PNA probe

Next the hybridization specificity in mixed base PNA sequences were determined. The sequences chosen correspond to a SNP position-1082 in human IL-10 promoter region which consist of two possibilities (g or a). Two TMR-labeled PNA probes **P3** and **P4** with sequences of TTCCCCCTCCCAA and TTCCCCTTCCCAA were designed to detect this SNP. One probe (**P3**) had the sequence correspond to IL10-1082(g) and the other to IL10-1082(a) genotypes. Two target DNAs were used 5'-TTGGGGGAGGGAA-3' and 5'-TTGGGGAAGGGAA-3' as model. A non complementary 5'-AATGGGATTTTGT-3' was also included as control. The fluorescent images of the support after the usual hybridization-absorption-washing are shown in **Table 3.11**.

Table 3.11 Fluorescence image of experiments using the PNA probe TMR-O-SLE 1 (**P3**)

Quantity	Control	Complementary	Single mismatch	Non-complementary
100 pmol		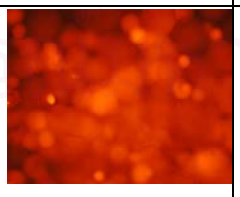	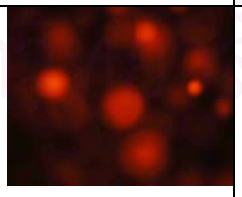	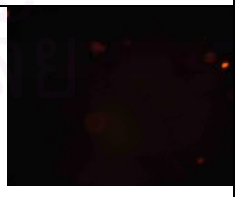
10 pmol	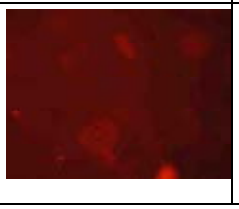	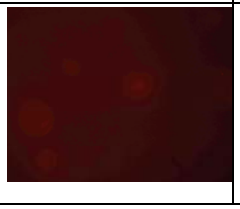	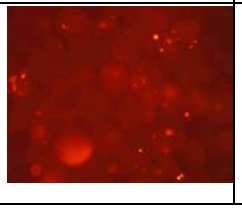	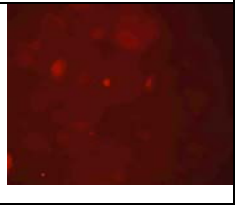

The results of the some experiment with the probe (**P4**) with 5'-TTGGGGAAGGGAA-3' and 5'-TTGGGGGAGGGAA-3' as complementary and single mismatch DNA targets are shown in **Table 3.12**.

Table 3.12 Fluorescence image of experiments using the PNA probe TMR-O-SLE 2 (P4)

Quantity	Control	Complementary	Single mismatch	Non-complementary
100 pmol	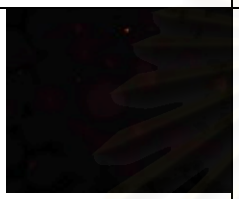	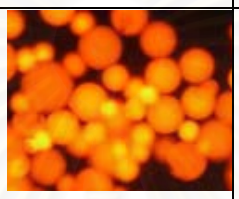	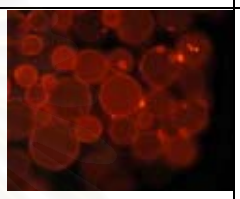	
10 pmol				

From the **Table 3.11** and **Table 3.12** it is clear that discrimination of single-base mismatch targets are possible with these 13-mer mixed base PNA probes. It was found that the minimum amounts of the **P3** and **P4** sequences that can be clearly discriminate between complementary and single base mismatch were 10 and 100 pmol respectively. This is not unexpected considering the T_m differences in each case. The higher sensitivity of **P4** compared to **P3** could be explained by the higher melting temperature of **P4** (T_m = 70.0 ^{O}C) compared to **P3** (T_m = 61.0 ^{O}C). This contributed to the higher binding affinity between **P4** and DNA target than that between **P3** and DNA target. The sensitivity the detection to distinguish between complementary and single base mismatch was much lower than the T_9 (T_m = 74.0-76.0 ^{O}C) case. Although these levels of sensitivity in both cases are probably not yet sufficient for analysis of real DNA samples, attempts have been made to do so.

The hybridization specificity in was attempted with double-stranded DNA samples obtained from two human individuals by PCR one carry a complementary and the other carry a single mismatch DNA sequence to **P4**. (The samples were kindly provided by Mr. Jeerawat Nakkuntod,and Dr. Nattiya Hirankarn of Lupus Research

Unit, Department of Microbiology, Faculty of Medicine, Chulalongkorn University). The quantity of TMR-mixbase (**P4**) used was 10 pmol.

Table 3.13 Detection of TMR mixed base PNA (**P4**) with real sample.

Quantity	Complementary	Single mismatch
10 pmol (2 sec)		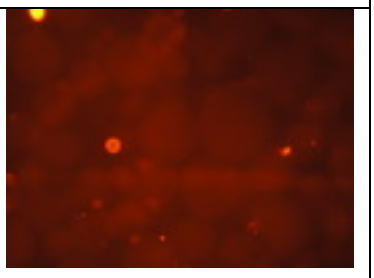
10 pmol wash 3% MeCN (2 sec)	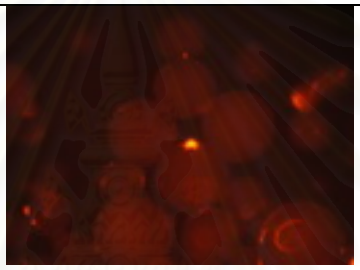	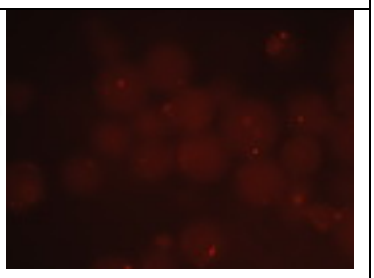

The result showed that the differences between complementary and single mismatch DNA targets were not yet sufficient to allow unambiguous analysis of the DNA sequence. A greater difference was observed after washing the support with 3% acetonitrile in water, but again the difference was not clear enough to make a conclusion. It is possible that the sensitivity of the technique is not yet sufficient. Furthermore, salts and protein residues in the real DNA samples may interfere with the hybridization of PNA·DNA.

Work in the future should aim to improve the sensitivity of the detection by re-designing the sequence to improve the $T_{m,}$ or to use approaches such as molecular beacons [43] that would enhance the difference between the hybridized and unhybridized state of PNA.

3.3.5.2 Towards development of multicolor DNA sequence detection system.

In order to increase the reliability of the DNA sequence detection, more than one fluorescent labeled probes are required. In principle, to detect the base sequence at a particular position, four probes corresponding to A, T, C and G should be required. However, for detection of SNP, two probes are usually sufficient since two polymorphisms are most commonly observed. Ideally, the two probes must have identical sequence except for one base and they must be labeled with different fluorophore exhibiting different emission wavelength but the molar extinction coefficient must be close to each other. Earlier experiments showed that TMR labeled PNA exhibited a good sensitivity and specificity to differentiate between complementary and single base mismatch DNA target so this label was chosen as the first label. Next, the second label must be identified.

Fluorescein was first chosen as the next label to investigate. In the first experiment, the carboxyfluorescein labeled PNA Flu-T_9-LysNH_2 (synthesized by Miss Boonjira Boontha) was used as PNA probe model. the DNA dA_9 (complementary) and dT_9 (non complementary) were used as DNA targets. All experiments were carried out at 500 pmol of DNA target. After the usual hybridization-absorption-washing cycles, the support was visualized under fluorescence microscope using the filterset that was the closest match to fluorescein excitation and emission (WBV). The results are shown in **Table 3.14**.

Table 3.14 Fluorescence microscope image of experiments using the PNA probe Flu-T_9-LysNH_2.

Quantity	Complementary (dA_9)	non complementary (dT_9)
500 pmol	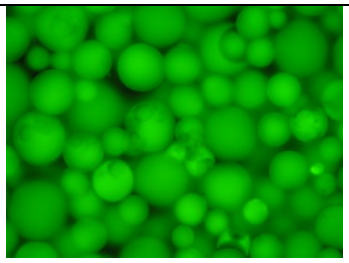	

From the **Table 3.14**, it was found that the Flu-T_9-LysNH_2 probe can clearly differentiate between complementary and non complementary DNA target. Therefore, it is possible that this label can be used as the second fluorescent labeling group and it was chosen for further optimization. Next, the effectiveness of carboxyfluorescein labeling group, in differentiation between complementary and single base mismatch in DNA target was studied. In this experiment, the carboxyFlu-O-T_8A-SerNH_2 (**P5**) was used as a probe, dA_8T and dA_9 were used as DNA targets at 100 pmol.

Table 3.15 The result of sensitivity (**P5**) with complementary DNA and single mismatch.

Quantity	complementary	single mismatch
100 pmol	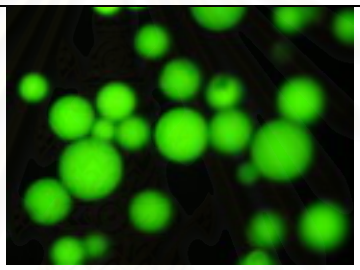	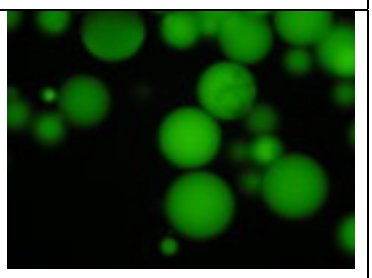

Disappointingly, a rather high background was observed in the case of single mismatch target. It was found that addition of acetonitrile to the washing medium can reduce the non-specific absorption. To study the effect of acetronitrile, the solid support was washed with different acetronitrile containing medium. In this experiment the carbxyflu-O-TTTTATTTT-SerNH_2 (**P5**) and dA_8T (complementary) were used as PNA and DNA model respectively at 100 pmol. This was found that 20% acetronitrile/H_2O was the most suitable condition to eliminate the non-specific absorption.

In order to find the detection limit, the amounts of the PNA (**P5**) and DNA (dA_9, dA_8T) probes were systematically decreased. The results are as shown in **Table 3.16**. (All photographs were taken using identical parameters: shutter speed – 1 sec, F stop - 4.8 ; ISO - 80. Identical filter sets were used in all experiments.)

Table 3.16 Detection limit in differentiation between dA8T and dA9 using the PNA probe **P5**.

Quantity	Complementary	Single mismatch
500p		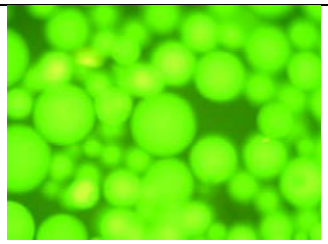
100p	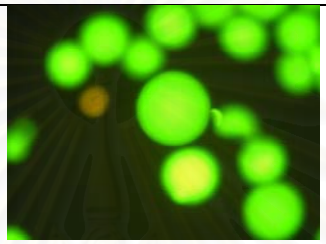	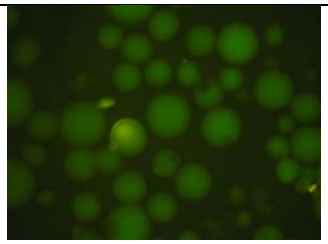
10p	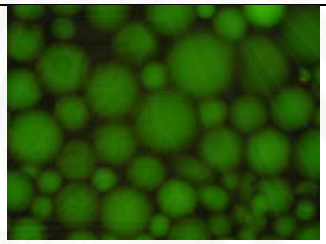	
5p		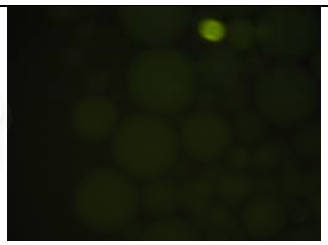
1p		

The data in **Table 3.16**, showed that the minimum quantity of carboxyfluorescein-labeled T_8A PNA **P5** that can differentiate between complementary and single base mismatch DNA target was 10 pmol. Therefore this labeled had intrinsically lower sensitivity when compared to TMR label.

From the results shown above, it can be concluded that the fluorescein labeled PNA probe can differentiate between complementary and single base mismatch DNA

down to 10 pmol level. However, this labeled PNA it can generate a high background absorption because of its structure consisted of the negatively charged carboxyfluorescein group which can be electrostatically absorbed onto the anion exchange support. In order to eliminate the non-specific absorption without the need for washing with acetonitrile, a neutral fluorescein analogue previously introduced by Nielsen [34] was studied. The structures of both labels are compared in **Table 3.17**.

Table 3.17 Structures of carboxyfluorescein and neutral fluorescein labels.

carboxyfluorescein	neutral fluorescein
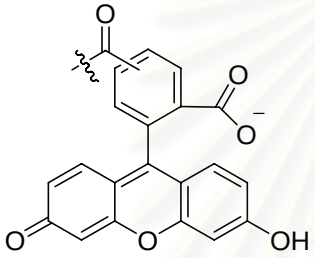	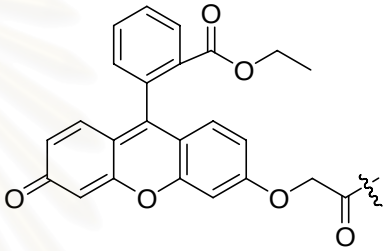

The label can be synthesized according to a literature procedure [30]. The carboxylic group of this neutral fluorescence was activated by pentafluorophenyl ester for attachment at the N-terminal of PNA sequence. The neutralFlu-O-TTTTATTTT-SerNH_2 (**P7**) was used as model to differentiate between complementary and single base mismatch DNA target. The results are shown in **Table 3.18**.

Table 3.18 Fluorescence image of experiments using the PNA probes **P7** and **P5**.

Quantity	Complementary dA_8T	Single mismatch dA_9
NeutralFlu-O-T_8-SerNH_2 10 pmol	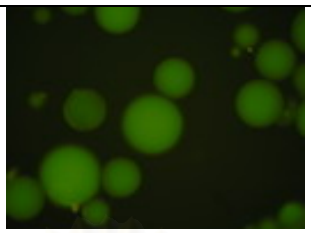	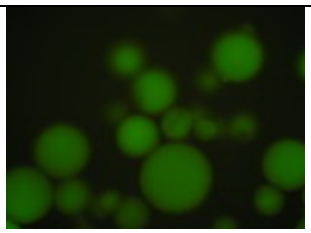
CarboxyFlu-O-T_8A-SerNH_2 10 pmol	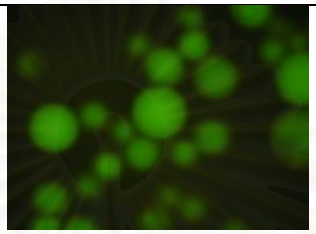	

From the **Table 3.18**, it can be conduced that this new labeled PNA probe, despite its neutrality, can be absorbed onto the solid support, generating a high background fluorescent. In addition, the ability of this labeled PNA for distinguishes between complementary and single base mismatch was less than of carboxyfluorescein-labeled PNA. The lower sensitivity compared to carboxyfluorescence might be due to its low quantum yield. Moreover the synthesis and purification of neutral fluorescence labeling group were also complicated. From these reasons, other labels were next investigated.

Atto520 labeled PNA (**P10**) was next tested. This probe can be used to distinguish between complementary and single base mismatch DNA. Unfortunately, the Atto520 labeling group showed the emission wavelength which is close to that of TMR, therefore both cannot be used together.

Five additional fluorescent labeled PNA probes (**P8-P11, P16**), were studied for their ability to distinguish between complementary and non complementary DNA targets at 10 pmol level by fluorescence microscopy. The results are summarized in **Table 3.19**

For DNS label, the PNA probe used was **P16** with a T_9 sequence. The DNA dA_9 for complementary, dA_8T for single mismatch and dT_8A for non-complementary sequences were used as models. The same PNA sequences TTTTATTTT labeled with pyrene (**P9**) and NBD (**P8**) were used as probes in combination with the same set of DNA targets. Finally the Atto425 labeled PNA with a sequence of dTTTTGTTTT

(**P11**) was used as another probe in combination with dAAAACAAAA, dAAAAAAAAA and dTTTTGTTTT as complementary, single mismatch and non-complementary DNA respectively.

Table 3.19 Fluorescence images of experiments using PNA probes labeled by other fluorophores (DNS, Pyr, NBD, Atto425).

Ac-Ser-Lys(DNS)-TTTTTTTTT-SerNH$_2$(**P16**)			
No DNA	Complementary dA_9	Single mismatch dA_4TA_4	Non complementary dT_4AT_4
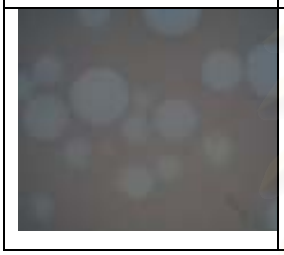	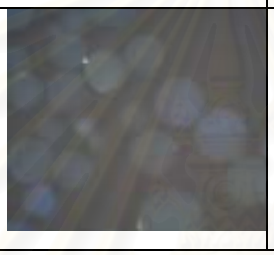		

Pyr-O-TTTTATTTT-SerNH$_2$(**P9**)			
No DNA	Complementary dA_8T	Single mismatch dA_9	Non complementary dT_8A
	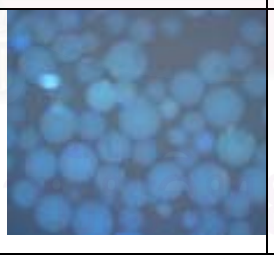		

NBD-O-TTTTATTTT-SerNH$_2$(**P8**)			
No DNA	Complementary dA_8T	Single mismatch dA_9	Non complementary dT_8A
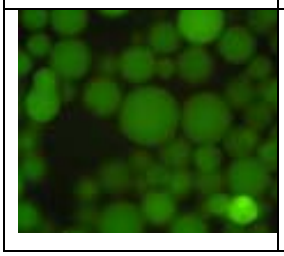		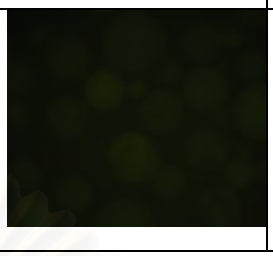	

Atto425-O-TTTTGTTTT-SerNH$_2$(**P11**)			
No DNA	Complementary dA_8C	Single mismatch dA_9	Non complementary dT_8G
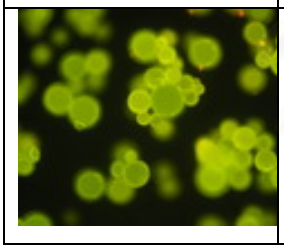	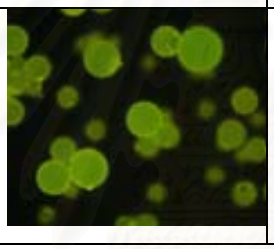	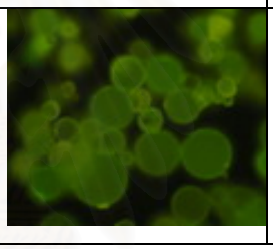	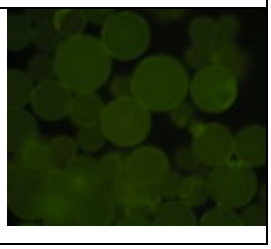

From the **Table 3.19**, this was found that all PNA probes (**P8-P11, P16**) failed to clearly discriminate between complementary and non-complementary (single base mismatch and full mismatch) at 10 pmol level. It is possible that these labeling groups have too low quantum yield and/or molar extinction coefficient (see **Table 3.2**). It is also possible that the absorption and/or emission of these labels do not match with the filter sets available in the current fluorescent microscope.

The results above showed that carboxyfluorescein is the most suitable label to be used in combination with TMR in two-color detection of DNA sequences. The TMR-T_9 probe **P2** and the carboxyFlu-T_8A probe **P5** were therefore chosen as models for the next preliminary experiments.

An equimolar mixture of the two probes (10 pmol each) was separatedly hybridized with dA_9 (complementary to TMR-T_9, single mismatch to Flu-T_8A) and dA_8T (complementary to Flu-T_8A, single mismatch to TMR-T_9). After the usual hybridization-absorption-washing cycle (with additional wash with 20% acetonitrile

to remove non-specifically bound fluorescein-labeled PNA), the supports in both cases were visualized under fluoresecence microscope using filter sets for TMR (WIG) and Flu (WBV). The results are shown in **Table 3.20**. When observed under TMR filter set (WIG), the red color appears only when the dA_9 (complementary with TMR-T_9 PNA) was present. Likewise, the green color was observed only when the dA_8T (complementary with Flu-dT_8A PNA).

Table 3.20 The result of sensitivity with complementary and single mismatch DNA of two probes

Quantity	**WIG**	**WBV**
No DNA	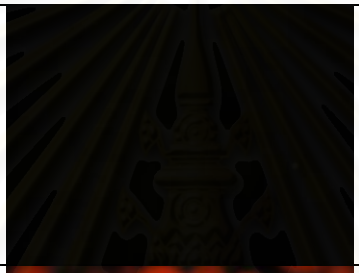	
dA_9 (match with TMR)		
dA_8T (match with Flu)		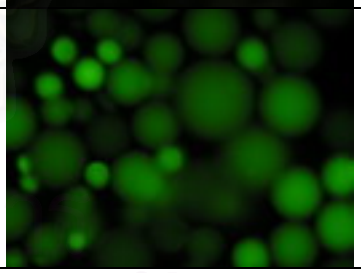

The results showed that both **P2** and **P5** can detect the difference between complementary and single mismatch DNA targets at 10 pmol level. It is therefore, in principle, possible to use two differently labeled probes for two-color detection of DNA sequence. Works remained to be done apart from increasing the sensitivity is to determine the generality of the test over a range of PNA and target DNA sequences before the test can be carried out practically with real DNA samples.

CHAPTER IV

CONCLUSION

In this research, PNA labeled with tetramethylrodamine (TMR), carboxyfluorescein, neutral fluorescein, FITC, dansyl, pyrene, Atto425, Atto520, NBD have been successfully synthesized by solid phase synthesis. These probes have been successfully used in combination with anion exchange solid support for DNA sequence determination. This method relied on the interaction between negatively charge of PNA·DNA hybrid and positively charged of anion exchange.

A variety of anion solid supports were tested. Q-sepharose was selected as the support because it showed a low non-specific absorption, high ionic capacity and wide working pH range. Among all fluorescence PNA probes tested, TMR and carboxyfluorescein labeled PNA probes showed better efficiencies compared to other labeled PNA probes. So, these two probes were selected for detection of DNA sequences hybridization.

It was observed that TMR-labeled PNA can differentiate between complementary and single base mismatch 9-base DNA target at 1 - 10 pmol levels when observed under fluorescence microscope. The mixed base 13mer TMR-labeled PNAs are less efficient, and lower sensitivities are obtained (10-100 pmol levels) in analysis of 13-base DNA targets.

Carboxyfluorescein labeled 9 mer PNA can differentiate between complementary and single base mismatch DNA targets at 10 pmol level, which is somewhat less sensitive when compared to TMR label.

Combination of two PNA probes labeled with two different fluorophores (TMR and carboxyflu) have also been successfully used in detection of DNA targets having a single different base in a multicolor format.

REFERENCES

1. Kool, E. T.; Morales, J. C.; Guckian, K.M. Mimicking the structure and function of DNA: insights into DNA stability and replication. *Angrew. Chem. Int. Ed.* **2000**, 39, 991-997.
2. Nielsen, P. E.; Egholm, M.; Berg, R. H.; Buchardt, O. Sequence-selective recognition of DNA by strand displacement with a thymine-substituted polyamide. *Science*, **1991**, *254*, 1497-1500.
3. Egholm, M.; Buchardt, O.; Christensen, L.; Behrens, C.; Freier, S. M.; Driver, D. A.; Berg, R. H.; Kim, S. K.; Norden, B.; Nielsen, P. E. PNA Hybridizes to complementary oligonucleotides obeying the watson- crick hydrogen-bonding rules. *Nature.* **1993**, *365*, 566-568.
4. Nielsen, P. E.; Egholm, M.; Buchardt, O. Evidence for $(PNA)_2$/DNA triplex structure upon binding of PNA to dsDNA by strand displacement. *J. Mol. Recog*. **1994**, *7*, 165-170.
5. Nielsen, P. E.; Haaima, G. Peptide Nucleic Acid (PNA). A DNA Mimic with a Pseudopeptide Backbone. *Chem. Soc. Rev.* **1997**, 73-78.
6. Peffer, N. J.; Hanvey, J. C.; Bisi, J. E.; Thomson, S. A.; Hassman, C. F.; Noble, S. A.; Basbiss, L. E. Strand-invasion of duplex DNA by peptide nucleic acid oligomer. *Proc. Natl. Acad. Sci. USA.* **1993**, *90*, 10648-10652.
7. Lesnik, E. A.; Risen, M. R.; Driver, D. A.; Griffith, M. C.; Sprankle, K.; Freier, S. M., Evaluation of pyrimidine PNA binding to ssDNA targets from nonequilibrium melting experiments. *Nucleic Acids Res.* **1997**, *25*, 568-574.
8. Hyrup, B.; Nielsen, P. E., Peptide nucleic acids (PNA): Synthesis, properties and potential applications. *Bioorg. Med. Chem*. **1996**, *4*, 5-23.
9. Uhlmann, E.; Peyman, A.; Breipohl, G.; Will, D. W., PNA: synthetic polyamide nucleic acids with unusual binding properties. *Angew. Chem. Int. Ed.* **1998**, *37*, 2796-2823.
10. Nielsen, P. E. Peptide Nucleic Acid. A molecule with two identities. *Acc. Chem. Res.* **1999**, 32, 624-630.

11. Suprapprom, C.; Srisuwannaket, C.; Sangvanich, P.; Vilaivan, T. Synthesis and oligodeoxynucleotide binding properties of pyrrolidinyl peptide nucleic acids bearing prolyl-2-aminocyclopentanecarboxylic acid (ACPC) backbones. *Tetrahedron Lett.* **2005**, *46*, 2833-2837.
12. Norden, B.; Ray, A. Peptide Nucleic Acid (PNA): Its medical and biotechnical applications and promise for the future. *The FASEB Journal*. **2000**, *14*, 1041-1059.
13. http://www.gitverlag.com. BIOforum International 5/2002, pp 242–243, GIT VERLAG GMBH & Co. KG, D-64220 Darmstadt.
14. Whitcombe, D.; Theaker, J.; Guy, S.; Brown, T.; Little, S. Detection of PCR products using self-probing amplicons and fluorescence. *Nature Biotechnology*. 1999, 17, 804-807.
15. Nikiforov, T.; Jeong, S. Detection of hybrid formation between peptide nucleic acid and DNA by fluorescence polarization in the presence of polylysine. *Anal.Biochem.* 1999, 275, 248-253.
16. http://micro.magnet.fsu.edu/primer/techniques/fluorescence/fluoresceinintro.htm
17. Bazan, G. C.; Gaylord, B. S.; Heeger, A. J. DNA detection using water-soluble conjugated polymers and peptide nucleic acid probes. *PNAS.* 2002, 99, 10954-10957.
18. Bazan, G. C.; Gaylord, B. S.; Heeger, A. J. DNA hybridization detection with water-soluble conjugated polymers and chromophore-labeled single-stranded DNA. *J. Am. Chem. Soc.* 2003, 125, 896-900.
19. Bazan, G. C.; Gaylord, B. S.; Wang, S. Fluorescein provides a resonance gate for FRET from conjugated polymers to DNA intercalated dyes. *J. Am. Chem. Soc.* 2004, 126, 5446-5451.
20. Bazan, G. C.; Liu, B.; Homogeneous Fluorescence-based DNA detection with water-soluble conjugate polymers. *Chem. Mater*. 2004, 16, 4467-4476.
21. Bazan, G. C.; Gaylord, B. S.; Massie, M. R.; Feinstein, S. C. SNP detection using peptide nucleic acid probes and conjugated polymers: Applications in neurodegenerative disease identification. *PNAS.* 2005, 102, 34-39.
22. Leclerc, M.; Boudreau, D.; Ho, H. A.; Doré, K.; Boissinot, M.; Bergeron, M. G.; Tanguay, R. M. Direct molecular detection of nucleic acids by

fluorescence signal amplification. *J. Am. Chem. Soc.* **2005**, 127, 12673-12676

23. Brandt, O.; Feldner, J.; Stephan, A.; Schröder, M.; Schnölzer, M.; Arlinghaus, H.; Hoheisel, J.; Jacob, A. PNA microarrays for hybridisation of unlabelled DNA samples. *Nucleic Acids Research.* **2003**, 31, 19.
24. Brandt, O.; Hoheisel, J. Peptide nucleic acids on microarrays and other biosensors. *Trends in biotechnology.* 2004, 22.
25. Komiyama, M.; Ye, S.; Liang, X.; Yamamoto, Y.; Tomita, T.; Zhou, J; Aburatani, H. PNA for One-base differentiating protection of DNA from nuclease and its use for SNPs detection. *J. Am. Chem. Soc.* **2003**, *125*, 3758-37-62.
26. Svanvik, N.; Kubbista, M.; Wang, D.; Westman, G. Light-up probes : Thiazole orange-conjugated peptide nucleic acid for detection of target nucleic acid in homogeneous solution. *Anal. Biochem.* **2000**, 281, 26-35.
27. Kool, E. T.; Sando, S. Quencher as leaving group: efficient detection of DNA-joining reactions. *J. Am. Chem. Soc.* **2002**, 124, 2096-2097.
28. Kool, E. T.; Sando, S.; Abe, H. Quenched Auto-ligating DNAs: Multicolor identification of nucleic acids at single nucleotide resolution. **2004**, 126, 1081-1087.
29. Kubista, M.; Svanvik, N.; Nygren, J.; Westman, G. * Free-Probe Fluorescence of Light-up Probes. *J. Am. Chem. Soc*. **2001**, 2001, 123, 803.
30. Appella, D.; Englund, E. Synthesis of γ-substituted peptide nucleic acids: A new place to attach fluorophores without affecting DNA binding. *Org Lett.* **2005**, 7, 16, 3465-3467.
31. Appella, D.; Zhang. Colorimetric detection of anthrax DNA with a peptide nucleic acid sandwich- hybridization assay. *J. Am. Chem. Soc*. **2007**, 129, 8424-8425.
32. Girard, J. E.; Baucom, P. J. DNA tTyping of human leukocyte antigen sequence polymorphisms by peptide nucleic acid probes and MALDI-TOF mass spectrometry. *Anal. Chem.* **1997**, 69, 4894-4898.
33. Tamiya, E.; Kerman, K.; Matsubara, Y.; Takamura, Y. Peptide nucleic acid modified magnetic beads for intercalator based electrochemical detection of DNA hybridization. *Science and Technology of Advanced Materials,* **2004**, 5, 351-357.

34. Dahl, O.; Lohse, J.; Nielsen, P. E.; Harrit, N. Fluorescein-conjugated lysine monomers for solid phase synthesis of fluorescent peptides and PNA oligomers. *Bioconjugate Chem.* **1997**, 8, 503-509.

35. Srisuwannaket, C. " Synthesis and DNA-binding properties of pyrrolidinyl peptide nucleic acids bearing (1S,2S)-2-aminocyclopentane carboxylic acids spacer". (Doctor of Philosophy thesis, Graduate School, Department of Chemistry, Faculty of science, Chulalongkorn University, 2004)

36. http://microscope.olympus.com/ga/applications/Fluo_Applications_E/fa_p16_E.html (1 of 2)

37. TentaGel is a trademark of Rapp Polymer GmbH, Tubingen, Germany.

38. Rink, H. Solid-phase synthesis of protected peptide fragments using a trialkoxy-diphenyl-methylester resin. *Tetrahedron Lett.* **1987**, *28*, 3787-3790.

39. Wang, S.; *p*-Alkoxybenzyl Alcohol Resin and *p*-alkoxybenzyloxycarbonyl hydrazide resin for solid phase synthesis of protected peptide fragments. *J. Am. Chem. Soc*., **1972**, *95*, 1328-1333.

40. http://www.nlv.ch/Molbiology/sites/Fluorescence 1.htm

41. http://www.atto-tec.com/ATTO-TEC.com/Products/labels.html

42. http://en.wikipedia.org/wiki/pyrene_%28data_page%29.

43. www.piercenet.com

44. http://probes.invitrogen.com/handbook/print/0101.html

45. Vilaivan, T.; Lowe, G. A Novel pyrrolidinyl PNA showing high sequence specificity and preferential binding to DNA over RNA. *J. Am. Chem. Soc.* **2002**, *124*, 9326-9327.

46. Lilley, D. M. J. Methods in Enzymology, Volume 211, DNA structures part A: synthesis and physical analysis of DNA, Academic press, inc., 389-405.

47. Blackburn, G. M.; Gart, M. S. Nucleic Acids in Chemistry and Biology, 2nd ed., New York: Oxford University Press. Inc. 446-451.

48. www.varianinc.com

49. http://www.anaspec.com/products/product.asp?id=28807

50. "Ion Exchange Chromatography: Principles and Methods", Technical Booklet Series (1999), Pharmacia Biotech, Uppsala, Sweden.

APPENDICES

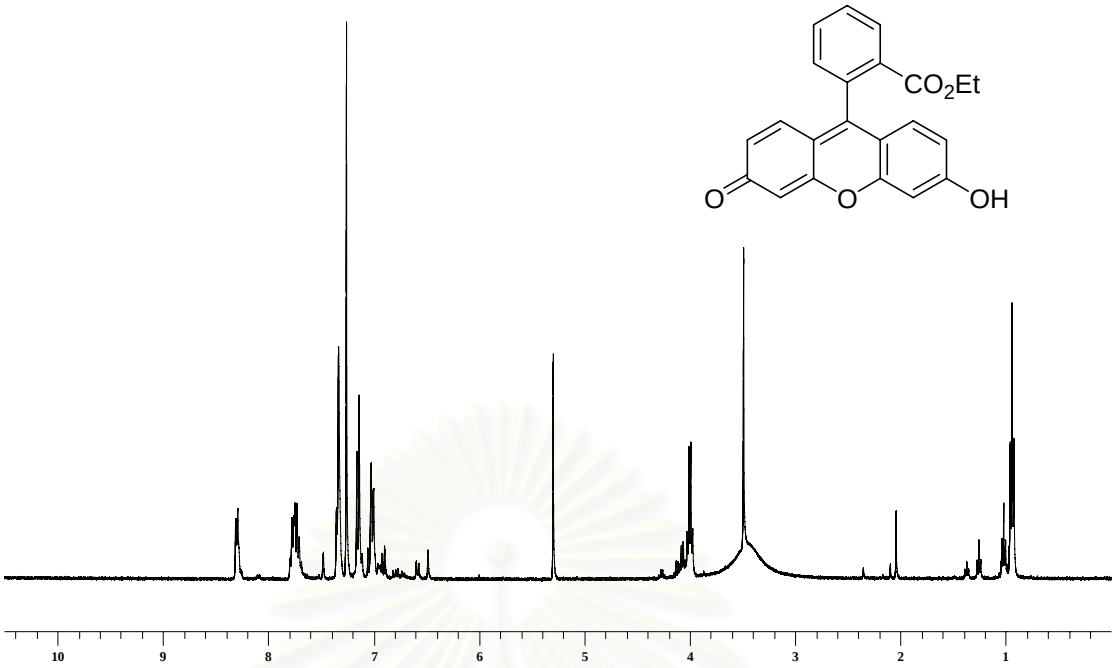

Figure A-1 ^{1}H NMR spectrum of ethyl 2-(6-hydroxy-3-oxo-3*H*-xanthen-9-yl) benzoate (**2**)

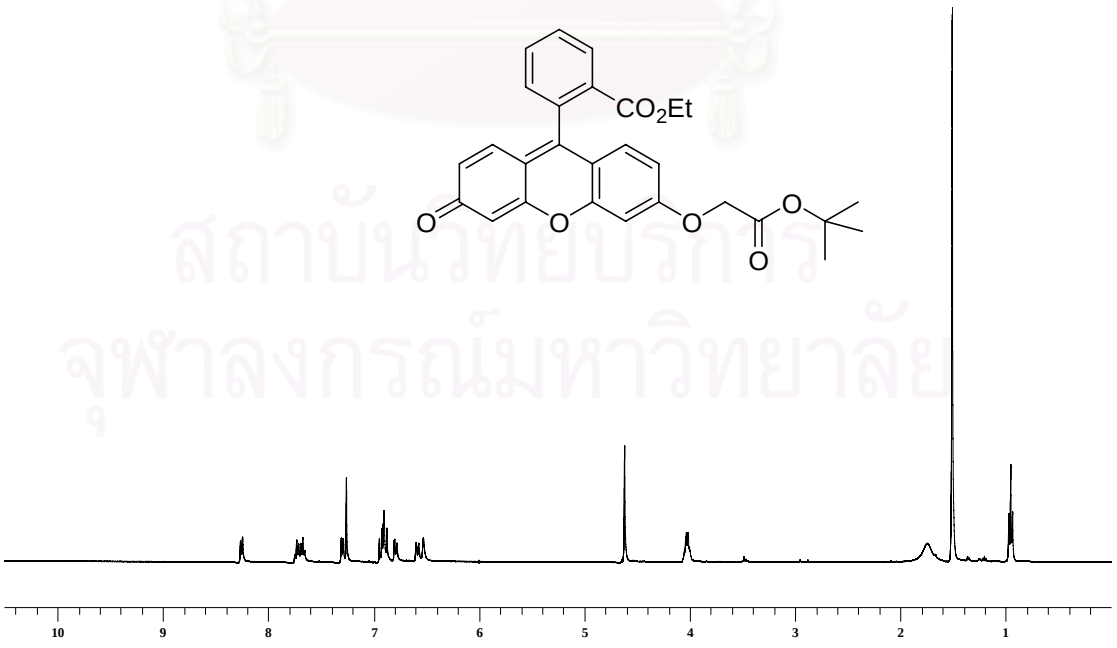

Figure A-2 ^{1}H NMR spectrum of 6-*O*-(*tert*-butyoxycarbonylmethyl)fluorescein 2-ethyl ester (**3**)

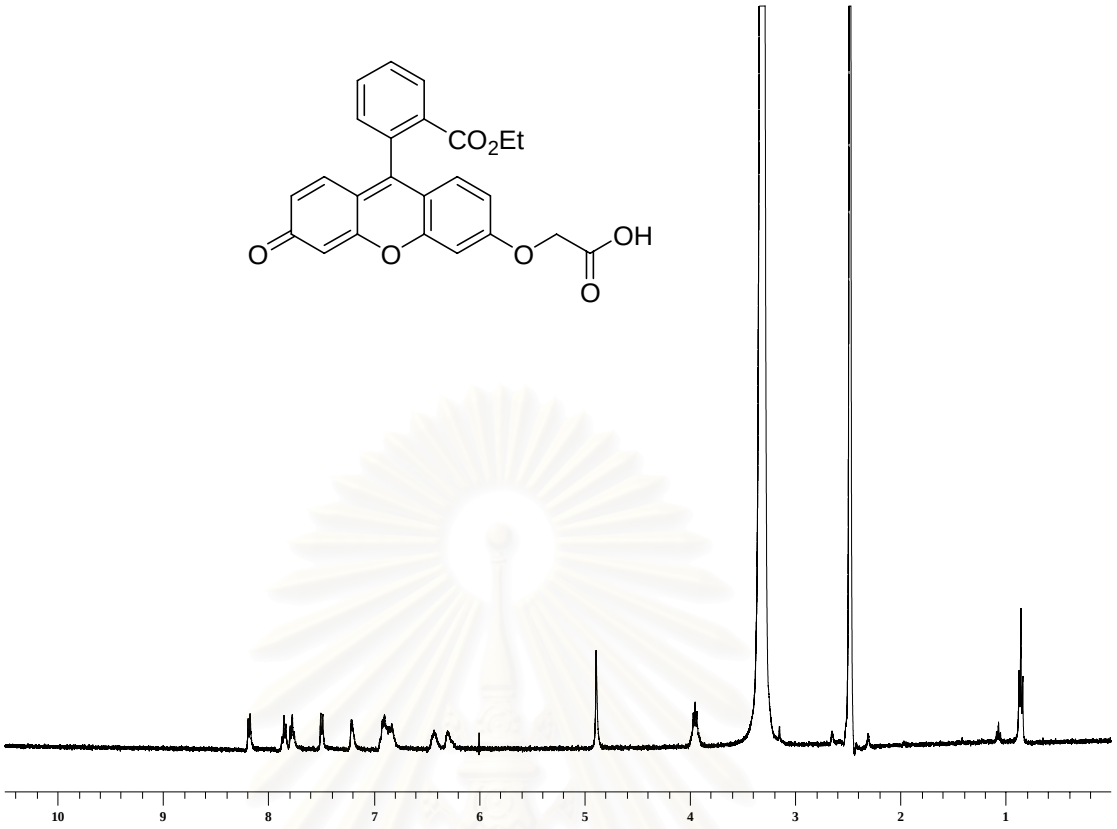

Figure A-3 ^{1}H NMR spectrum of 6-*O*-(carboxymethyl)fluorescein 2-ethyl ester (**4**)

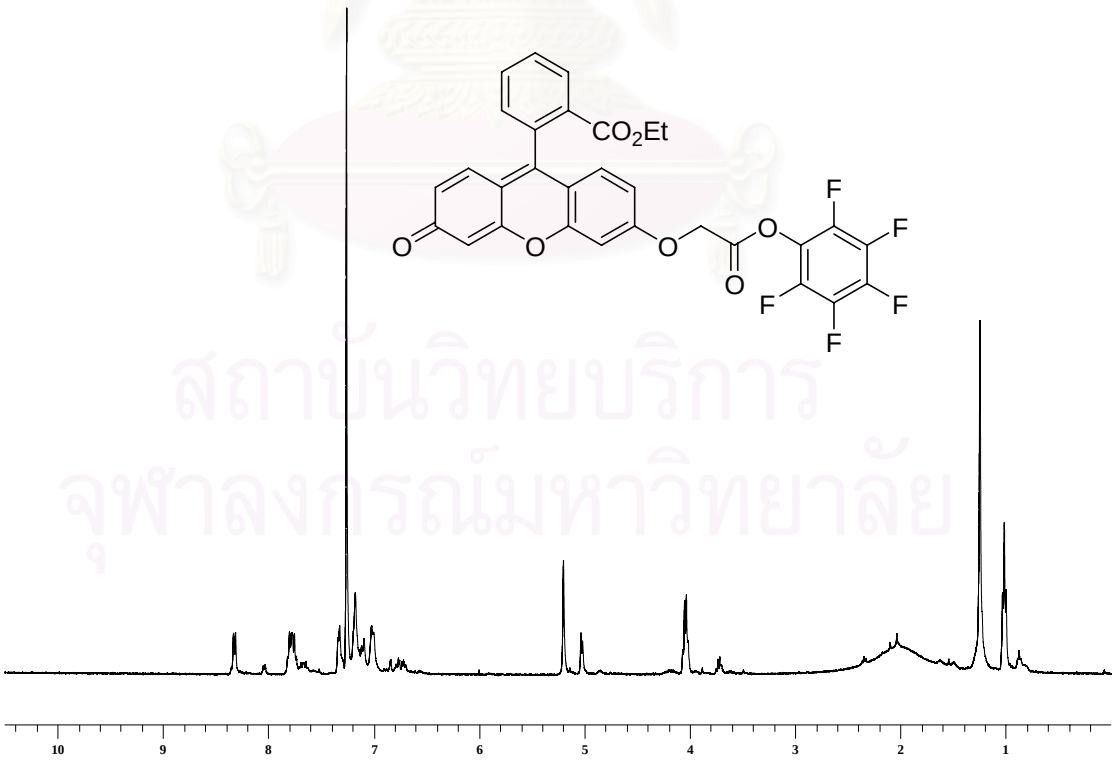

Figure A-4 ^{1}H NMR spectrum of 6-*O*-(carboxymethyl)fluorescein 2-ethyl ester pentafluorophenyl ester (**5**)

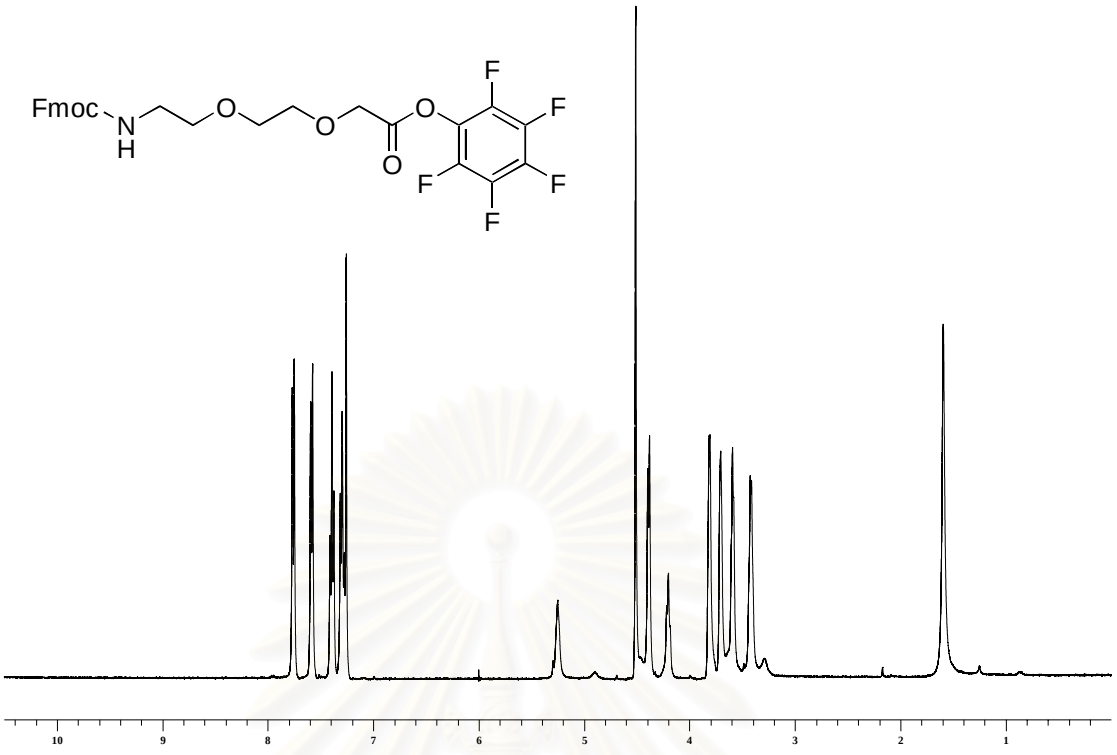

Figure A-5 ^{1}H NMR spectrum of {2-[2-(Fmoc-amino)ethoxy]ethoxy}acetic acid pentafluorophenyl ester (**7**)

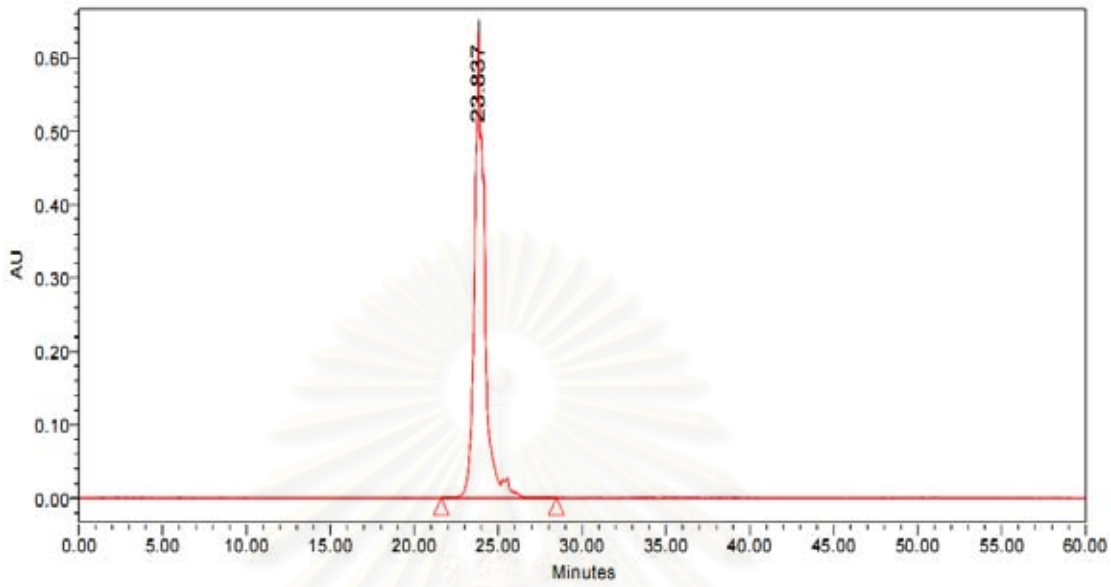

Figure B-1 : HPLC chromatogram of TMR-O-T_9-SerNH_2 (**P2**)

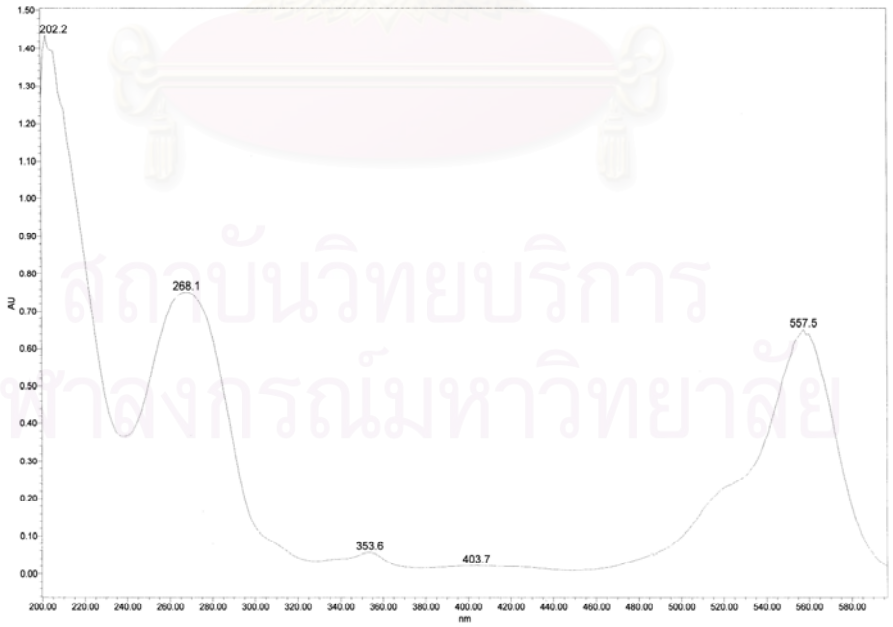

Figure B-2 : HPLC chromatogram of TMR-O-T_9-SerNH_2 (**P2**)

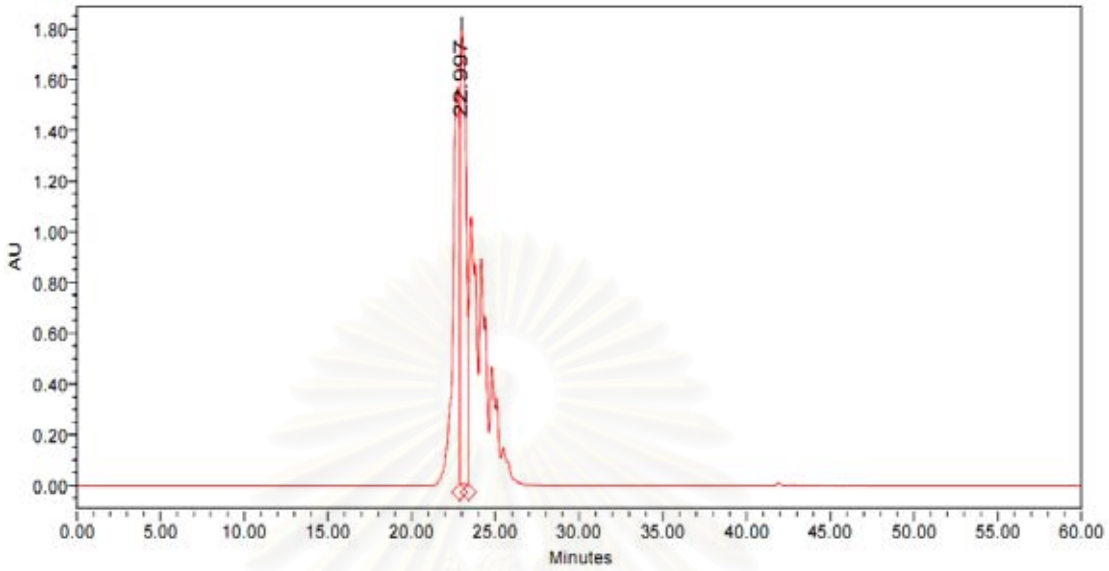

Figure B-3 : HPLC chromatogram of TMR-O-TTCCCCCTCCCAA-SerNH$_2$ (**P3**)

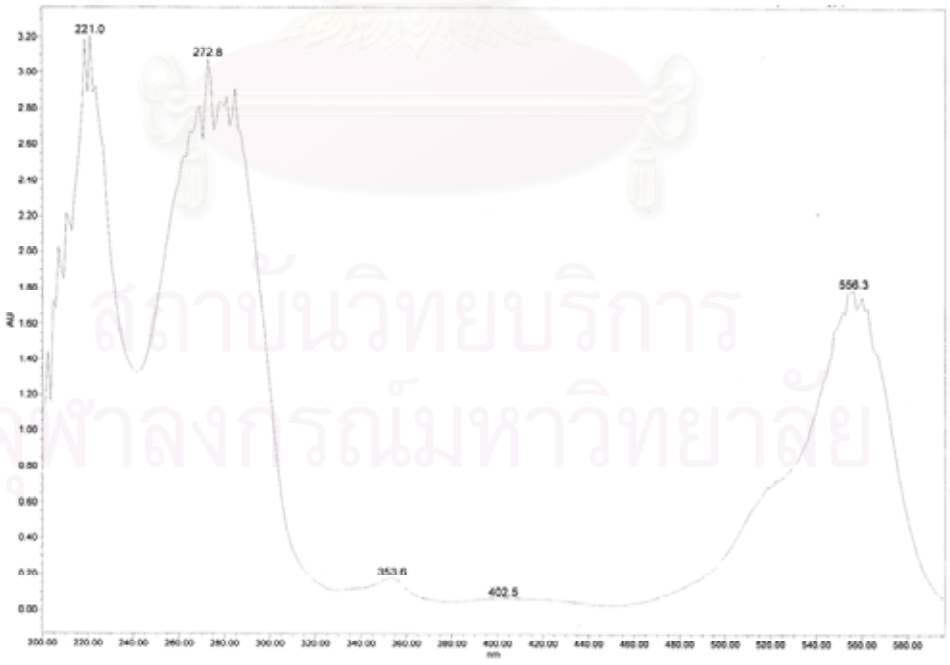

Figure B-4 : HPLC chromatogram of TMR-O-TTCCCCCTCCCAA-SerNH$_2$ (**P3**)

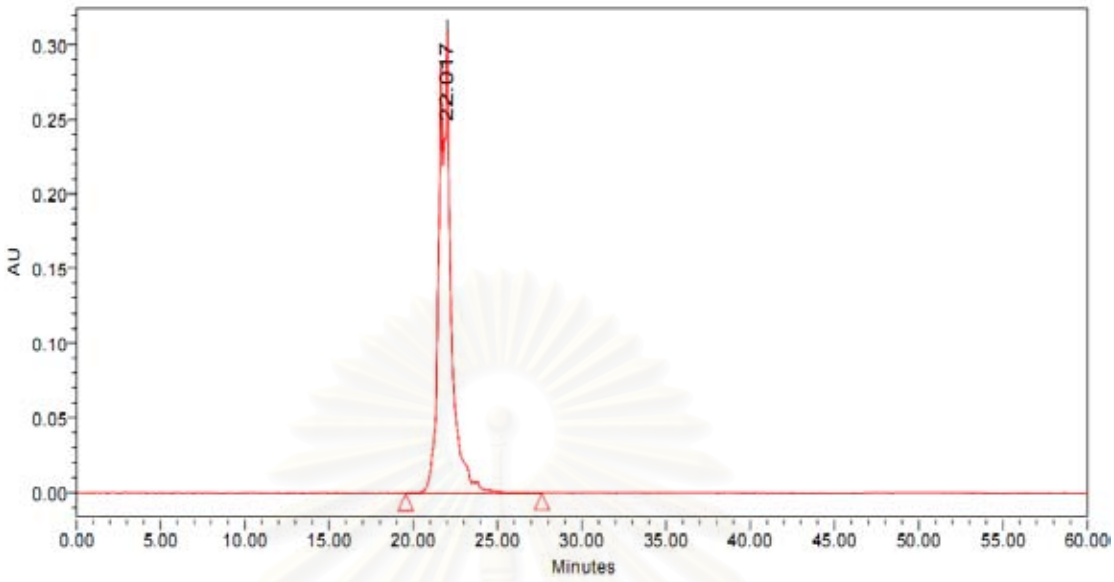

Figure B-5 : HPLC chromatogram of TMR-O-TTCCCCTTCCCAA-SerNH$_2$ (**P4**)

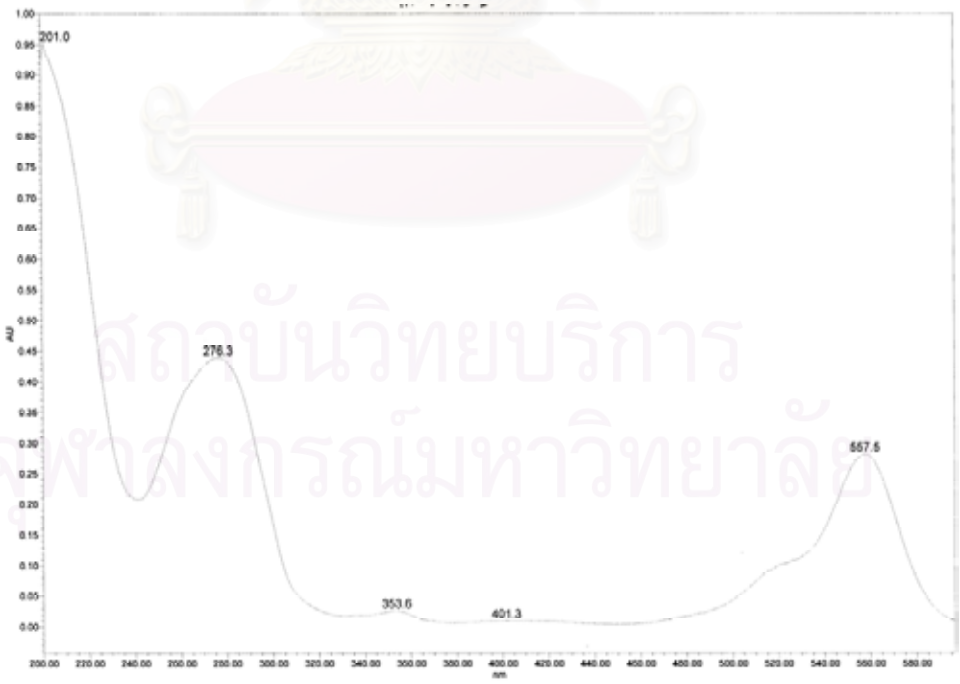

Figure B-6 : HPLC chromatogram of TMR-O-TTCCCCTTCCCAA-SerNH$_2$ (**P4**)

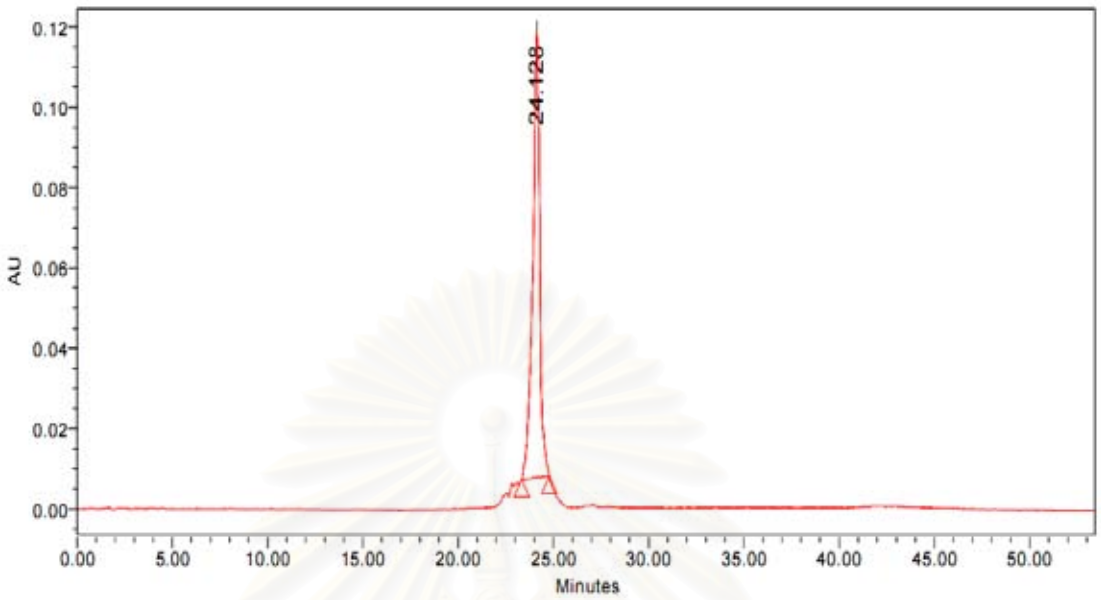

Figure B-7 : HPLC chromatogram of carboxyflu-O-T_4AT_4-SerNH_2 **(P5)**

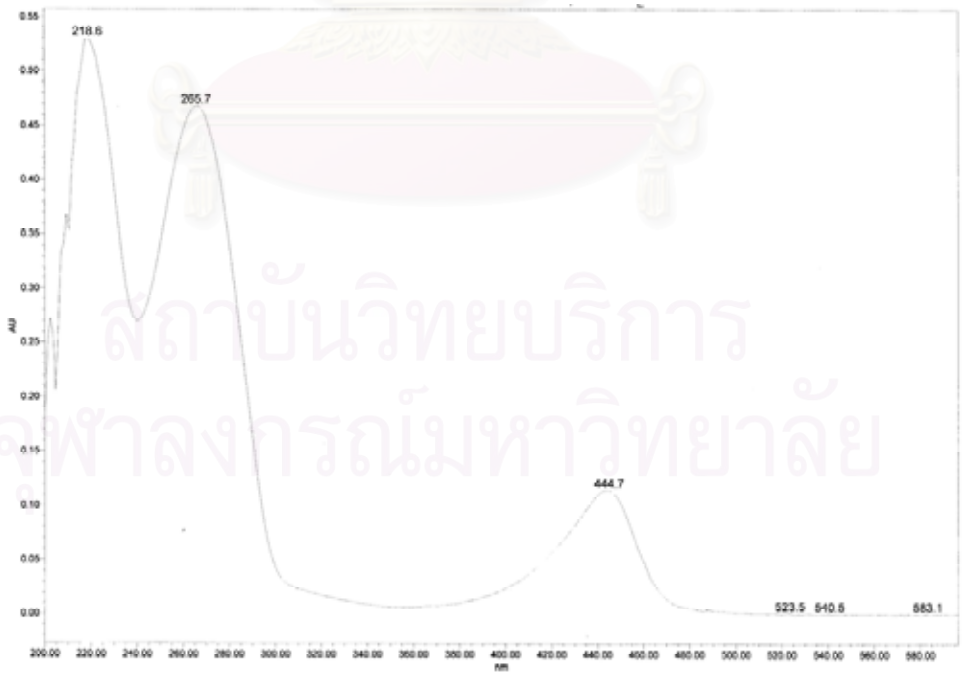

Figure B-8 : HPLC chromatogram of carboxyflu-O-T_4AT_4-SerNH_2 **(P5)**

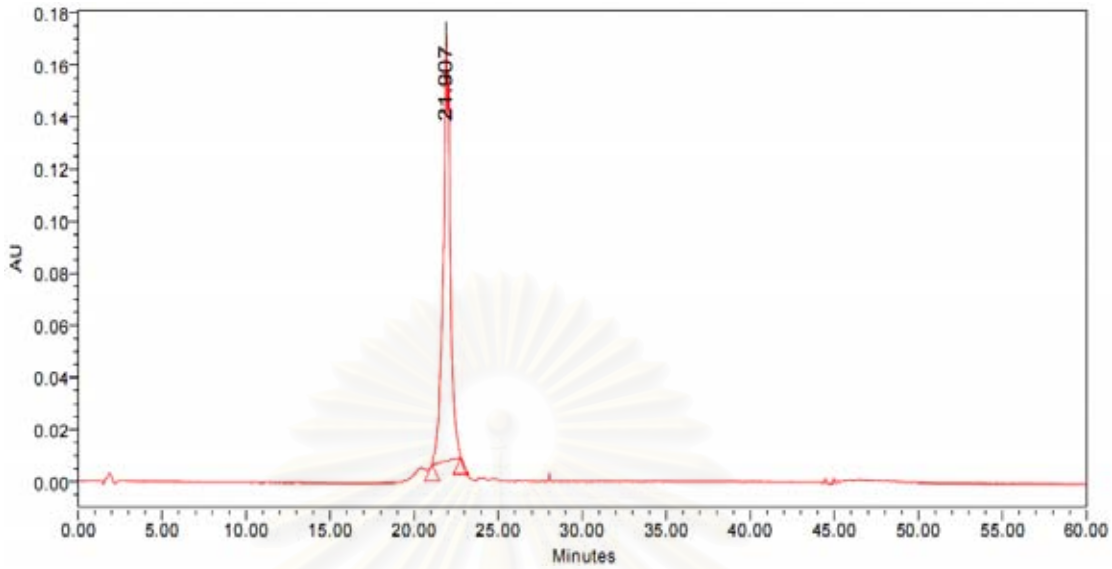

Figure B-9 : HPLC chromatogram of NeutralFlu-O-T_4AT_4-SerNH_2 **(P7)**

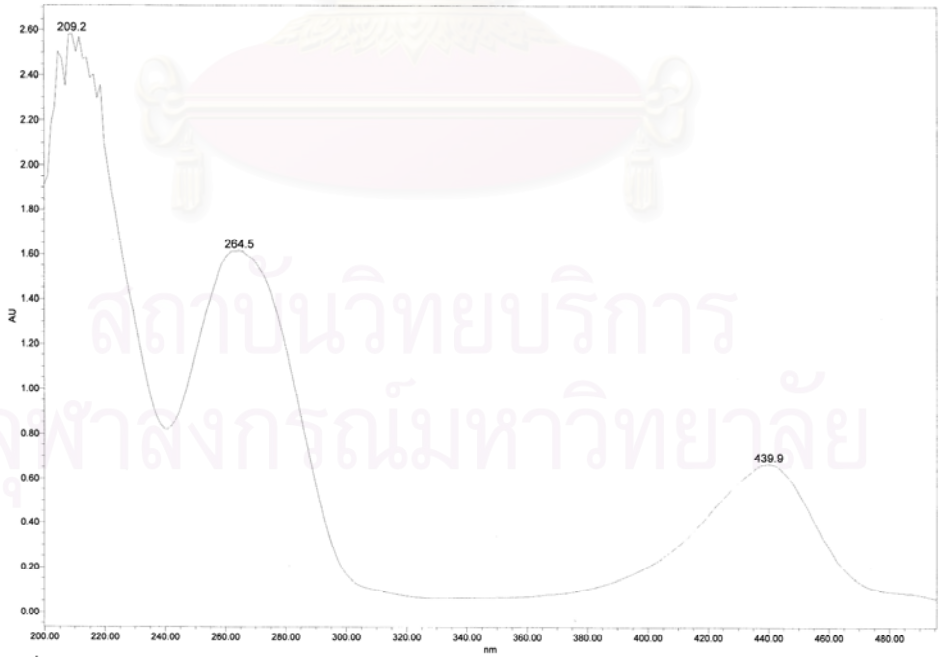

Figure B-10 : HPLC chromatogram of NeutralFlu-O-T_4AT_4-SerNH_2 **(P7)**

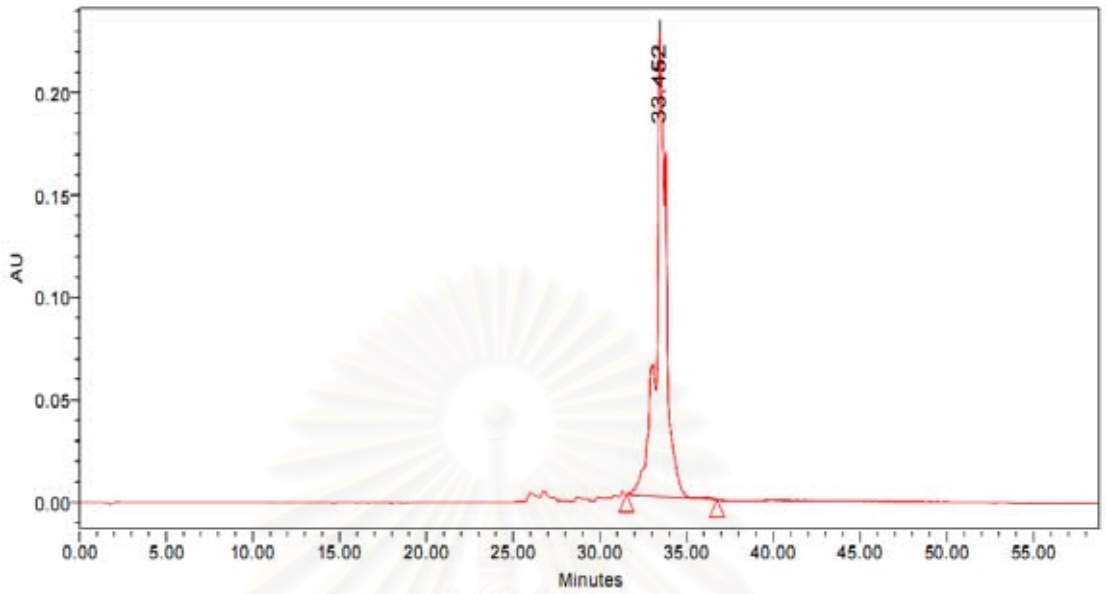

Figure B-11 : HPLC chromatogram of NBD-O- T_4AT_4-SerNH_2 **(P8)**

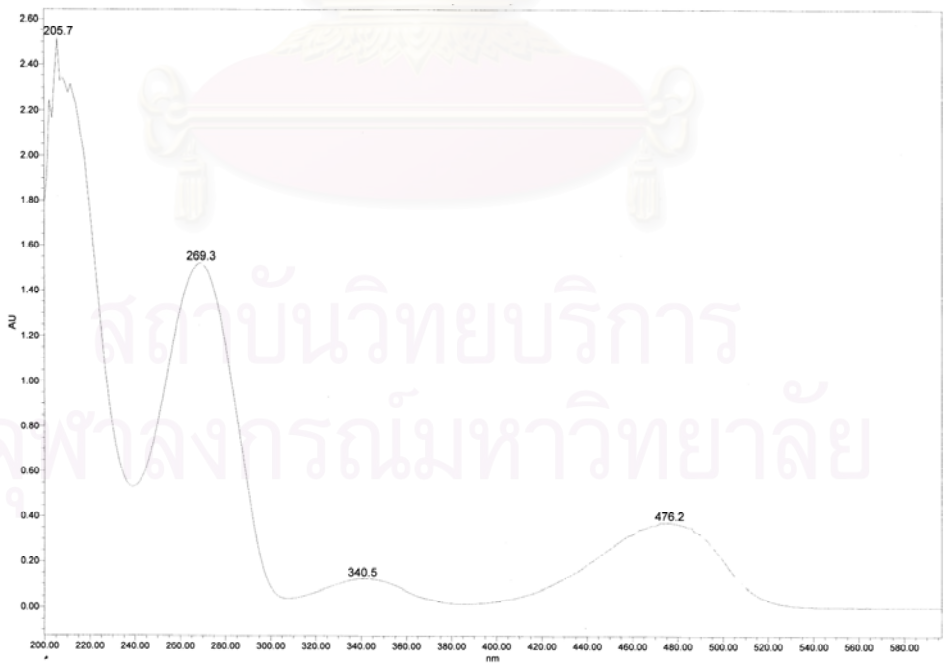

Figure B-12 : HPLC chromatogram of NBD-O- T_4AT_4-SerNH_2 **(P8)**

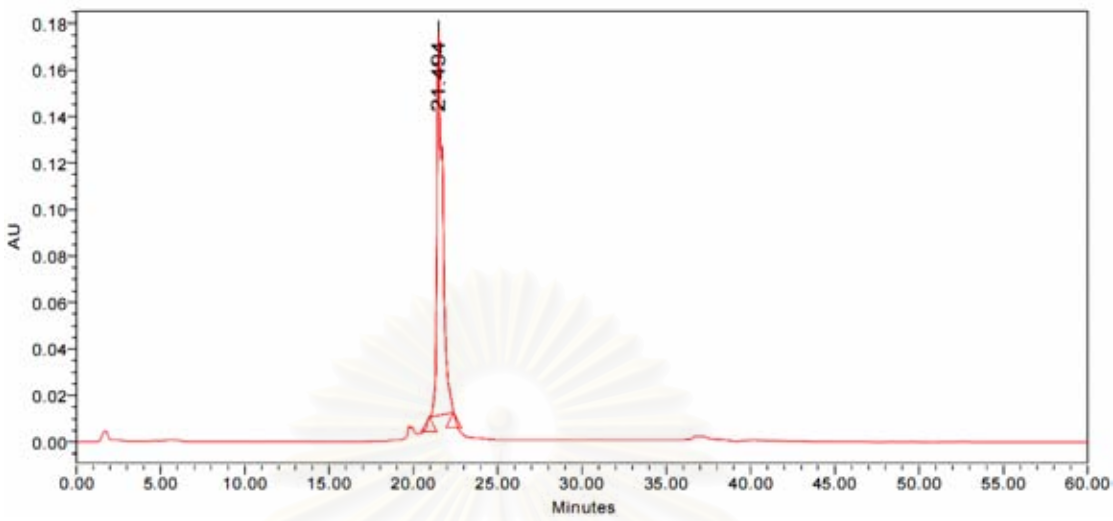

Figure B-13 : HPLC chromatogram of Pyr-O-T_4AT_4-SerNH_2 **(P9)**

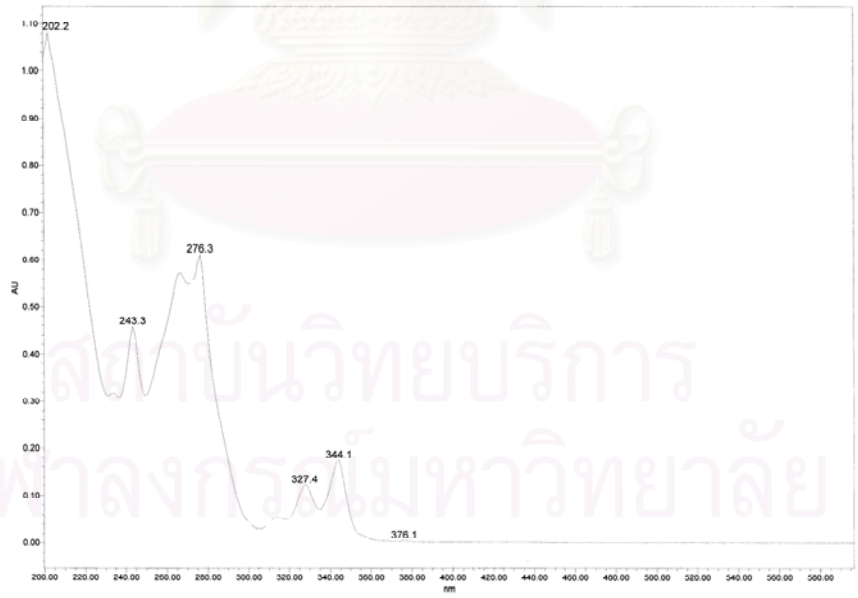

Figure B-14 : HPLC chromatogram of Pyr-O-T_4AT_4-SerNH_2 **(P9)**

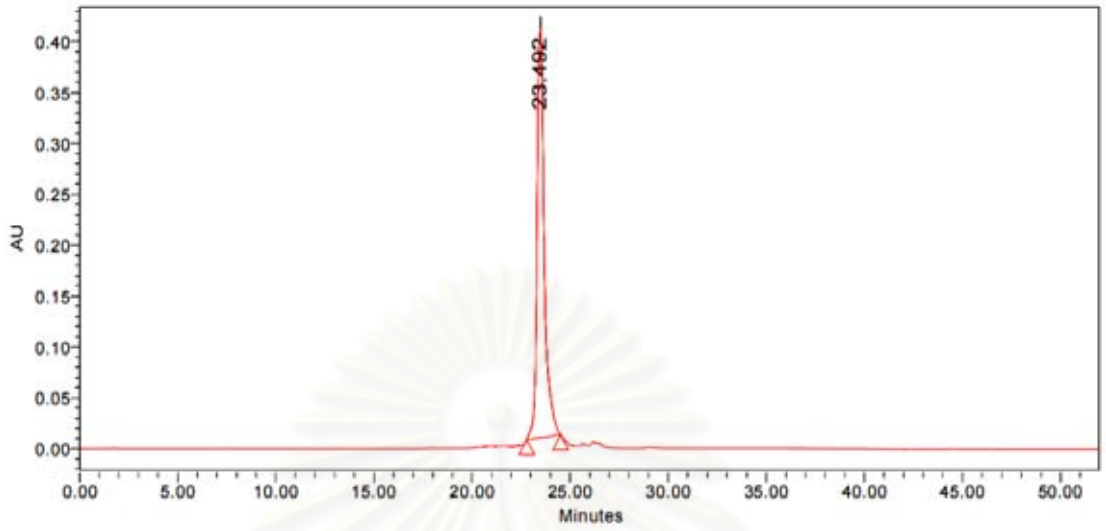

Figure B-15 : HPLC chromatogram of Atto425-O-T_4GT_4-SerNH_2 **(P11)**

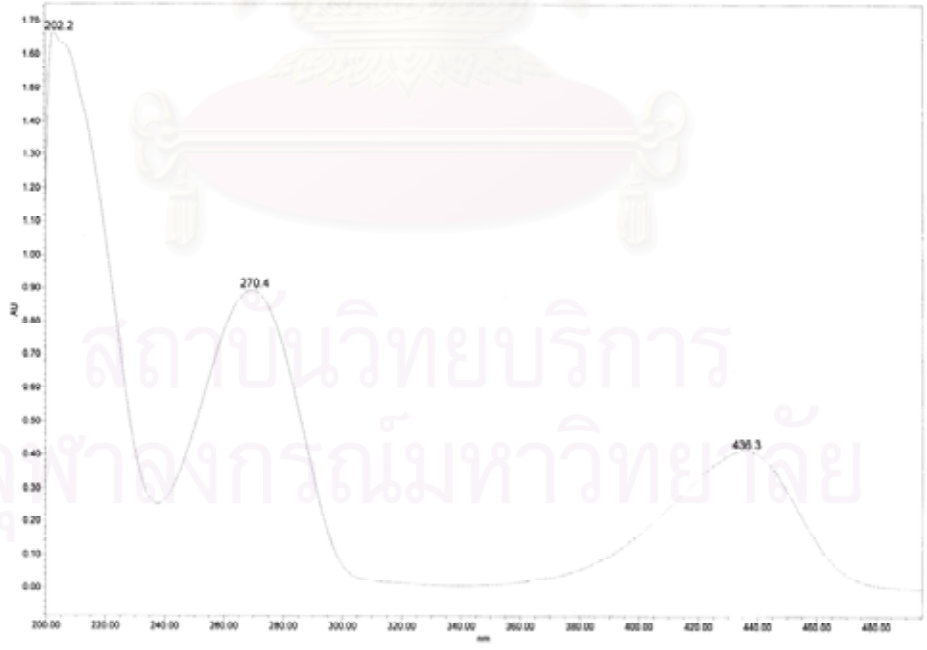

Figure B-16 : HPLC chromatogram of Atto425-O-T_4GT_4-SerNH_2 **(P11)**

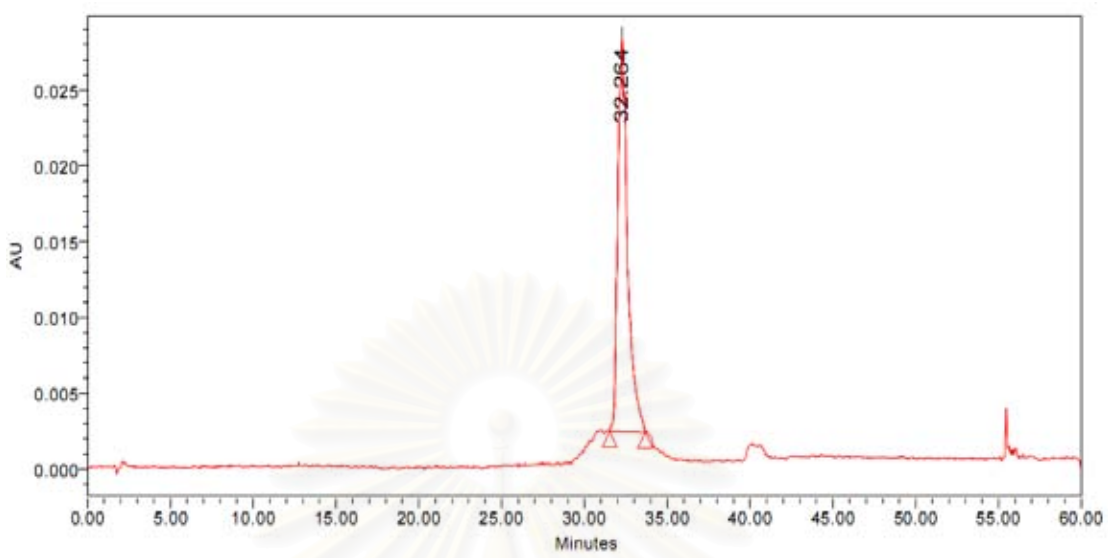

Figure B-17 : HPLC chromatogram of carboxyFlu-O-TTCCCCCTCCCAA-SerNH_2 **(P12)**

Figure B-18 : HPLC chromatogram of carboxyFlu-O-TTCCCCCTCCCAA-SerNH_2 **(P12)**

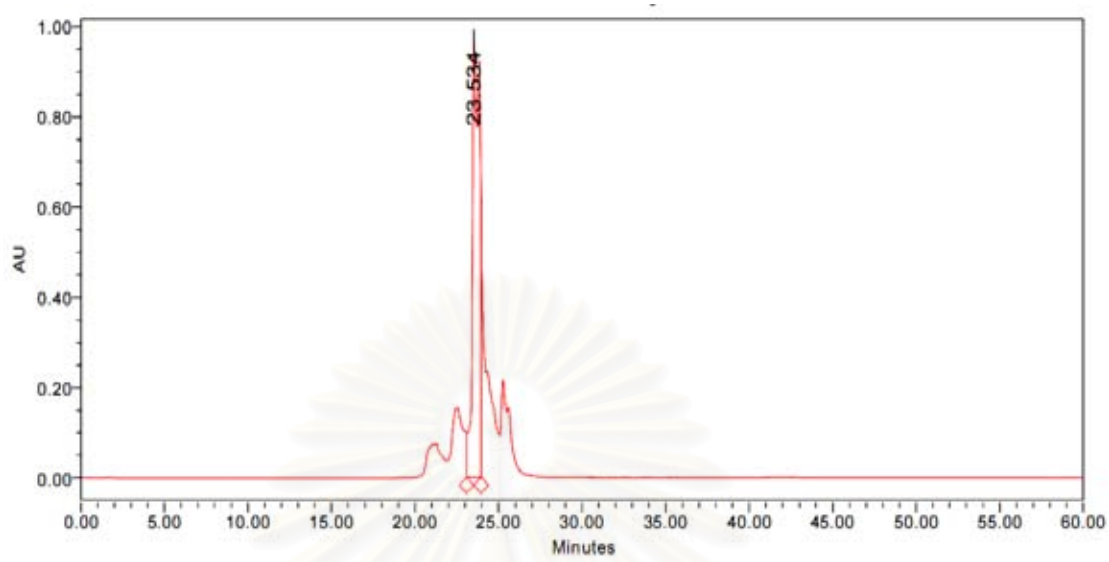

Figure B-19 : HPLC chromatogram of Neutral Flu-O-TTCCCCCTCCCAA-SerNH$_2$ **(P13)**

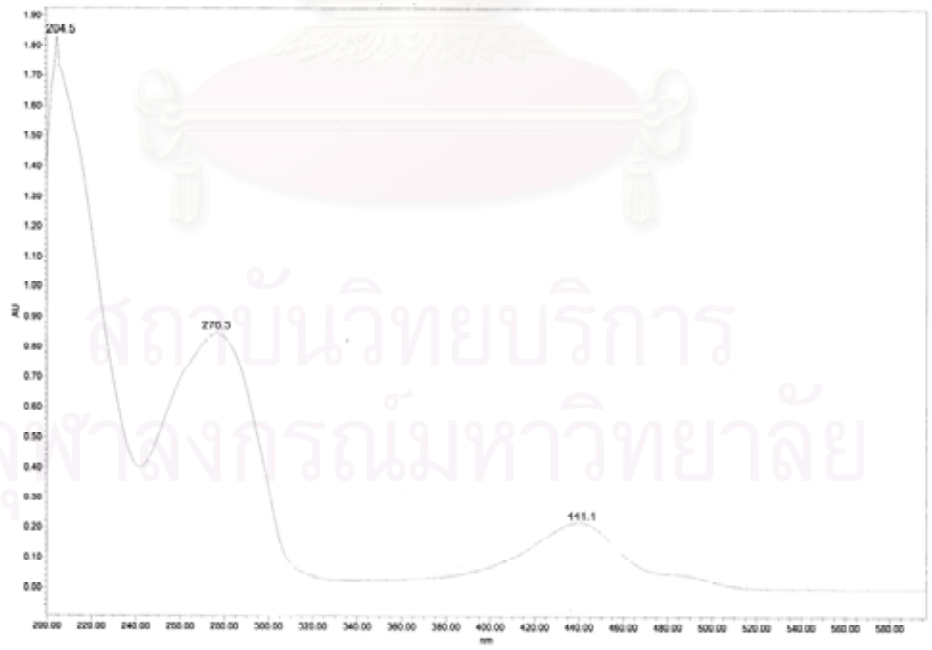

Figure B-20 : HPLC chromatogram of Neutral Flu-O-TTCCCCCTCCCAA-SerNH$_2$ **(P13)**

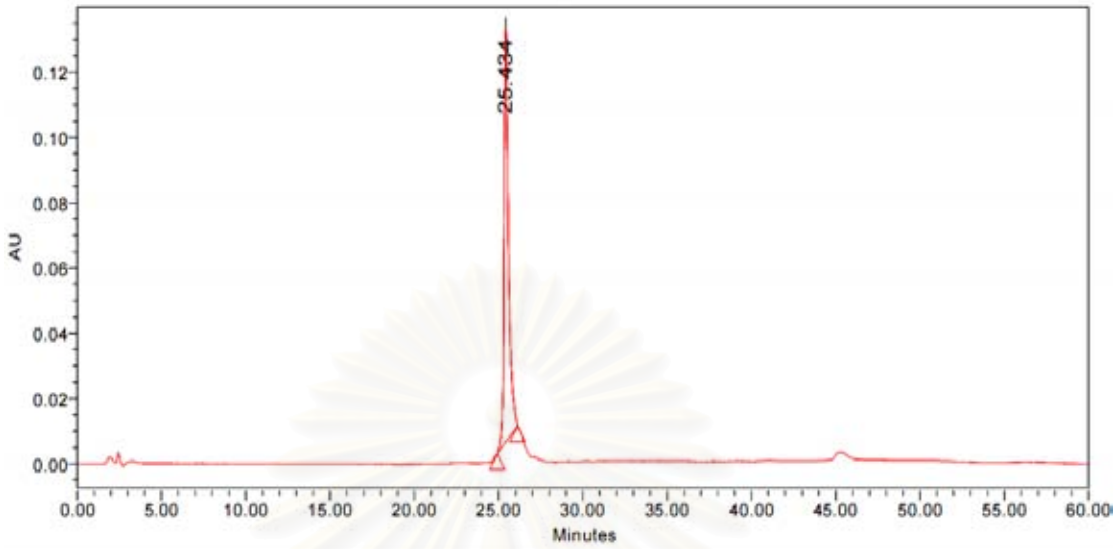

Figure B-21 : HPLC chromatogram of DNS-T_9-SerNH_2 **(P14)**

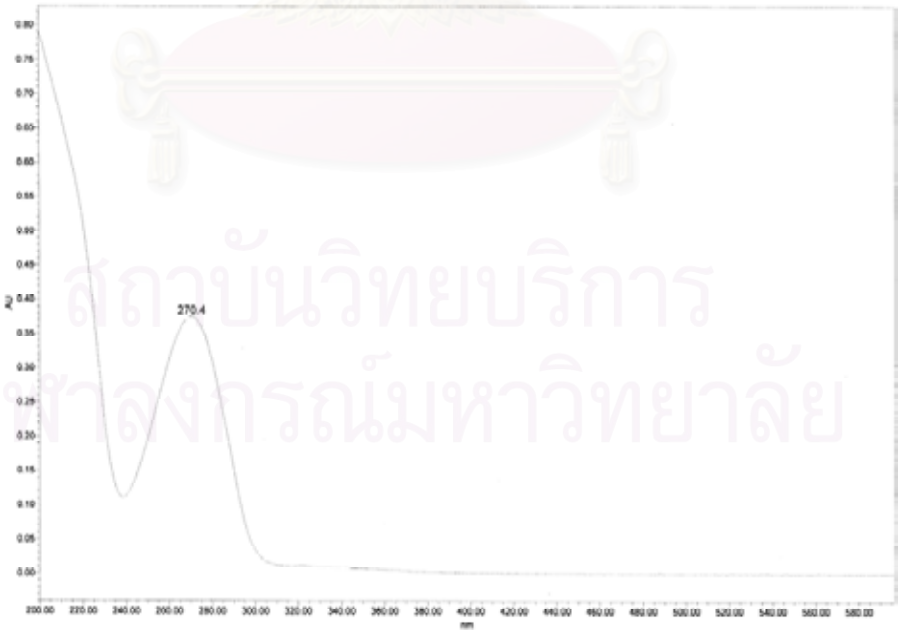

Figure B-22 : HPLC chromatogram of DNS-T_9-SerNH_2 **(P14)**

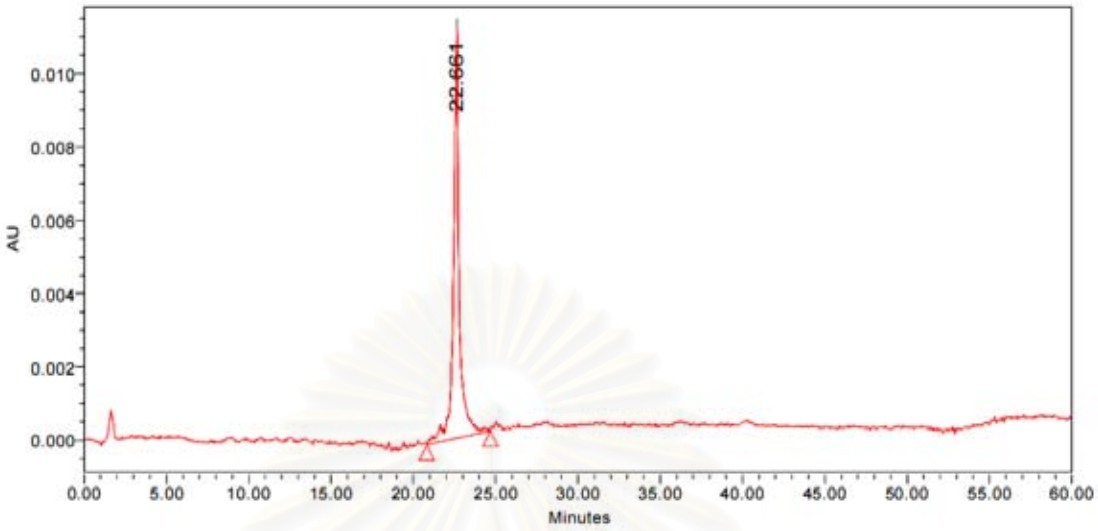

Figure B-23 : HPLC chromatogram of DNS-Ser-T_9-$SerNH_2$ **(P15)**

Figure B-24 : HPLC chromatogram of DNS-Ser-T_9-$SerNH_2$ **(P15)**

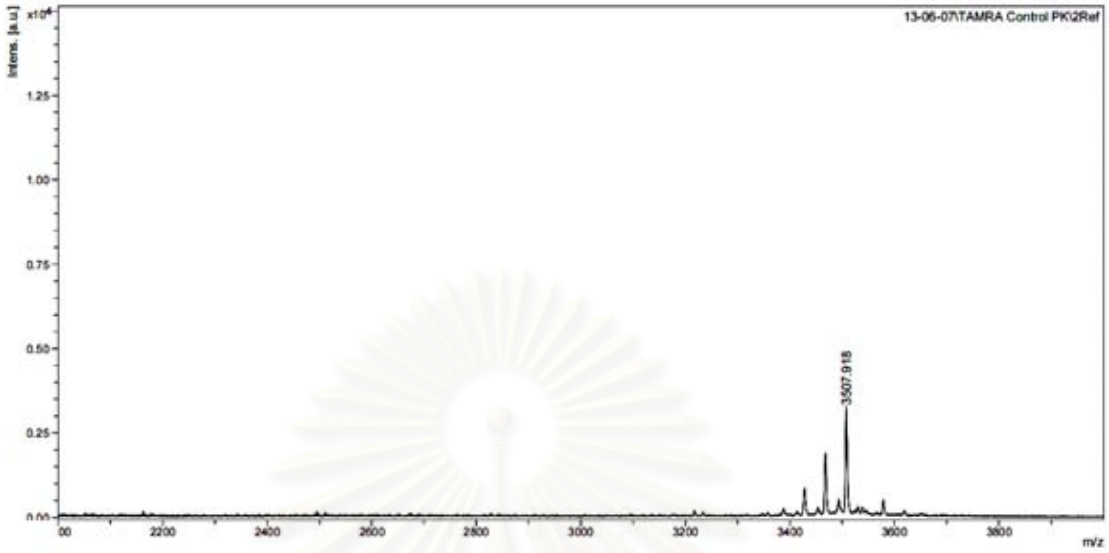

Figure C-1 : MALDI-TOF mass spectrum of TMR-T_9-SerNH_2 (**P1**)

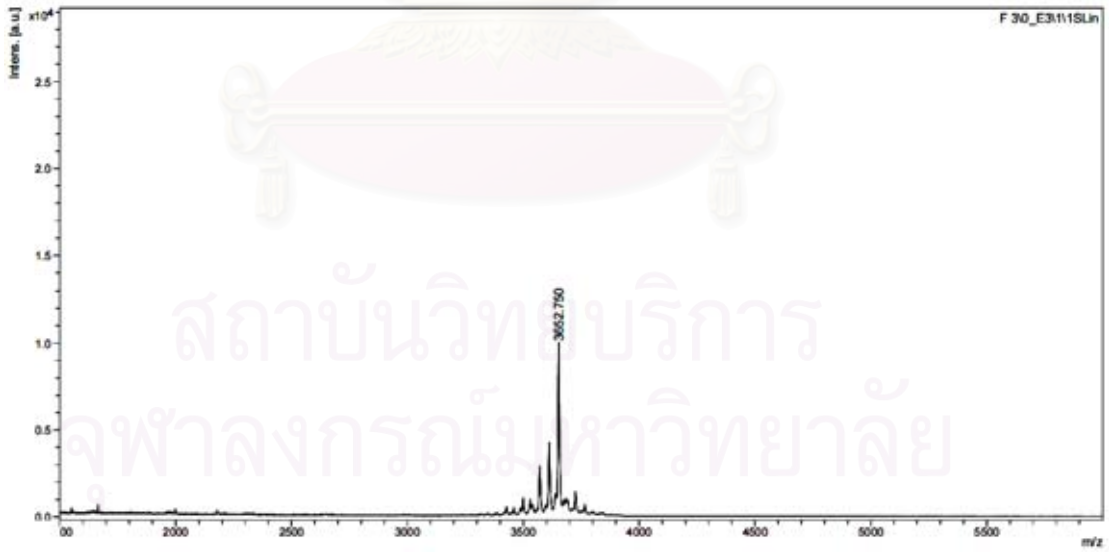

Figure C-2 : MALDI-TOF mass spectrum of TMR-O-T_9-SerNH_2 (**P2**)

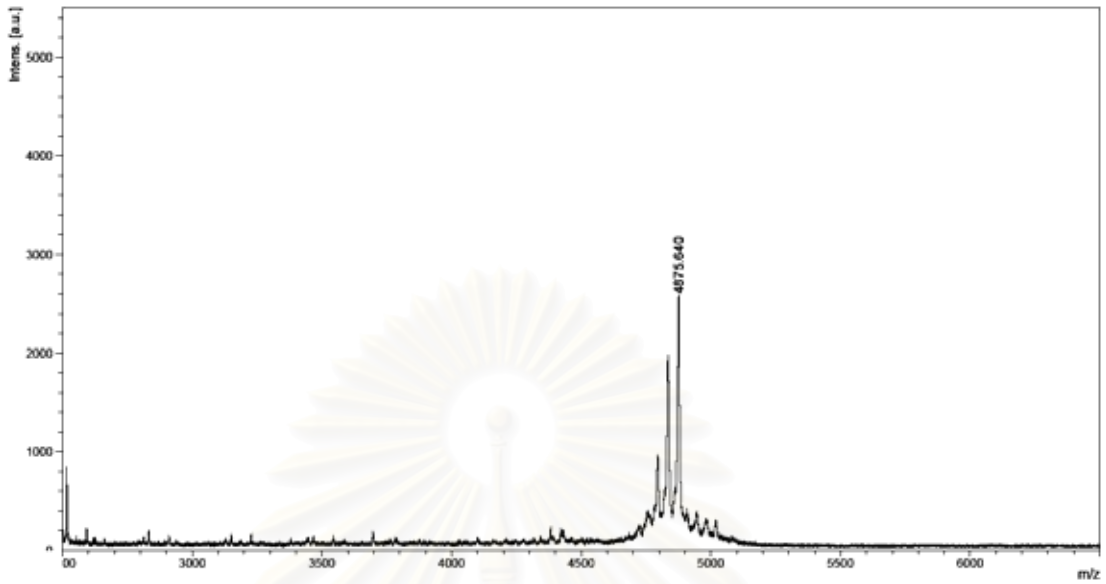

Figure C-3 : MALDI-TOF mass spectrum of TMR-O-TTCCCCCTCCCAA-SerNH_2 (**P3**)

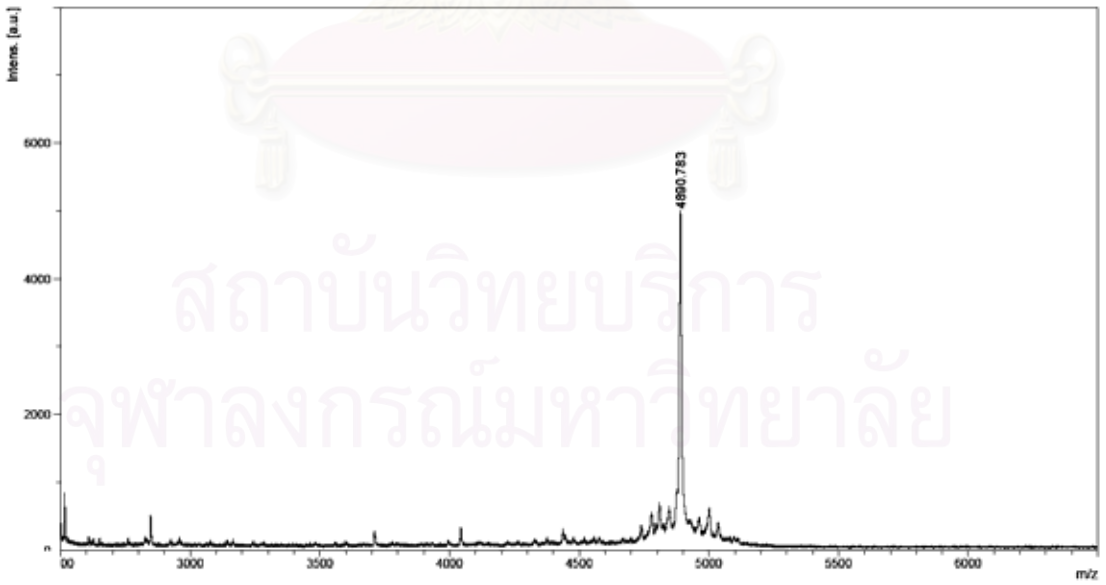

Figure C-4 : MALDI-TOF mass spectrum of TMR-O-TTCCCCTTCCCAA-SerNH_2 (**P4**)

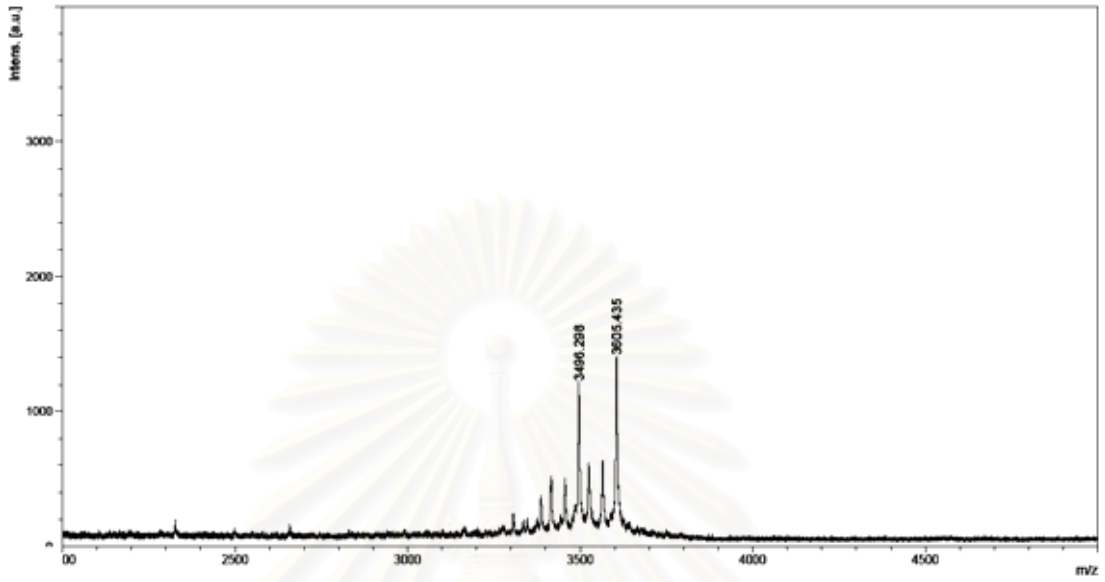

Figure C-5 : MALDI-TOF mass spectrum of carboxyflu-O-T_4AT_4-$SerNH_2$ **(P5)**

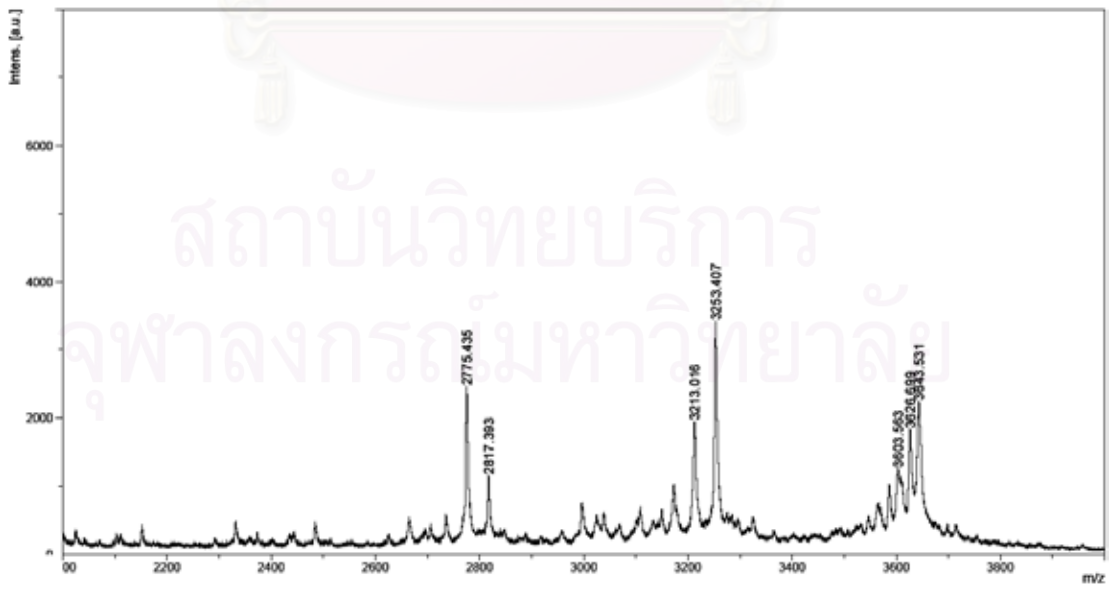

Figure C-6 : MALDI-TOF mass spectrum of FITC-O-T_4AT_4-$SerNH_2$ **(P6)**

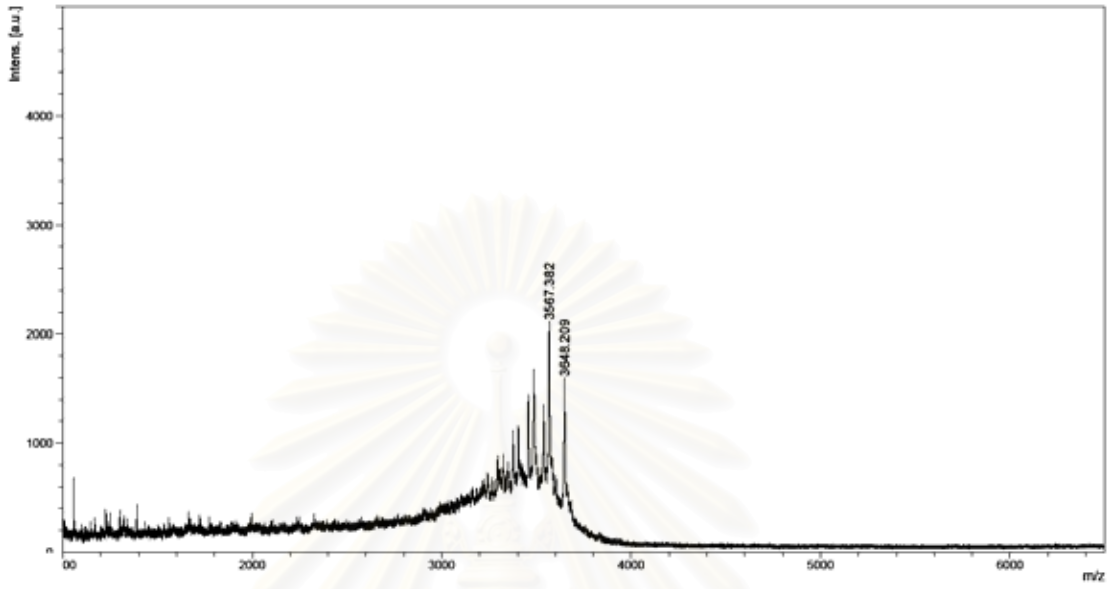

Figure C-7 : MALDI-TOF mass spectrum of NeutralFlu-O-T_4AT_4-SerNH_2 **(P7)**

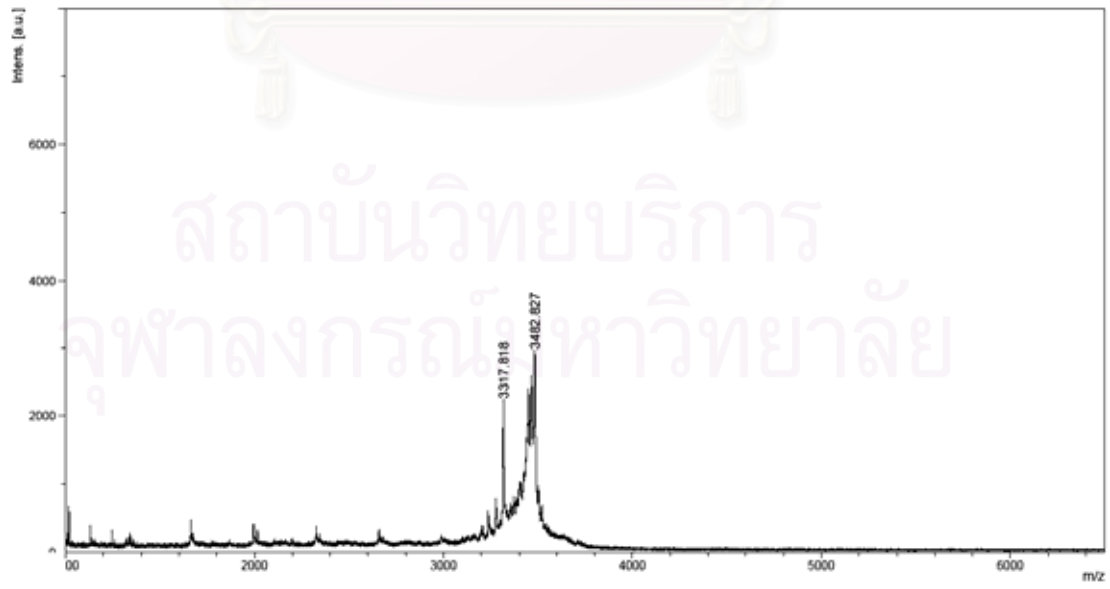

Figure C-8 : MALDI-TOF mass spectrum of NBD-O- T_4AT_4-SerNH_2 **(P8)**

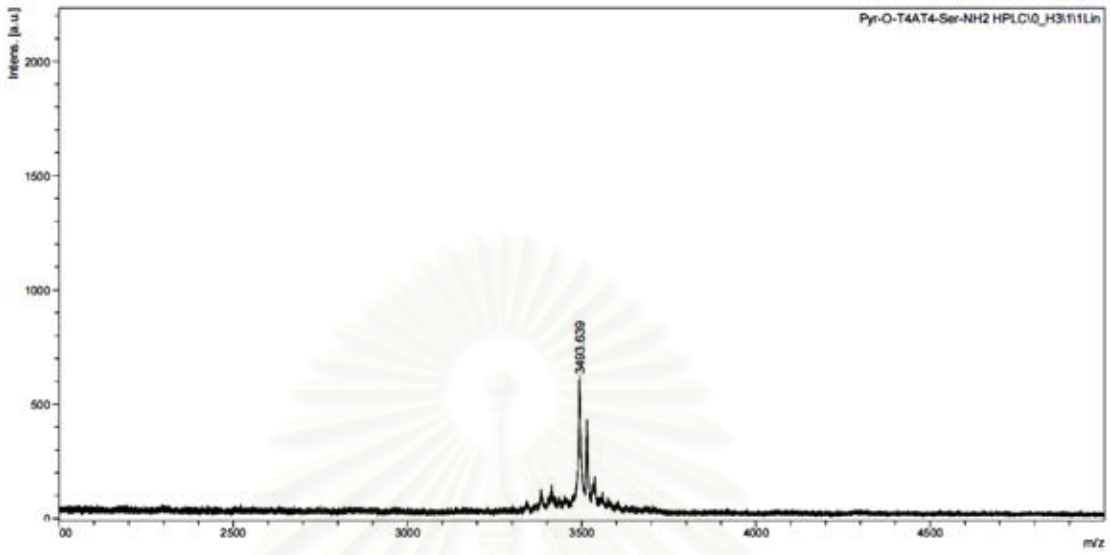

Figure C-9 : MALDI-TOF mass spectrum of Pyr-O-T_4AT_4-SerNH_2 **(P9)**

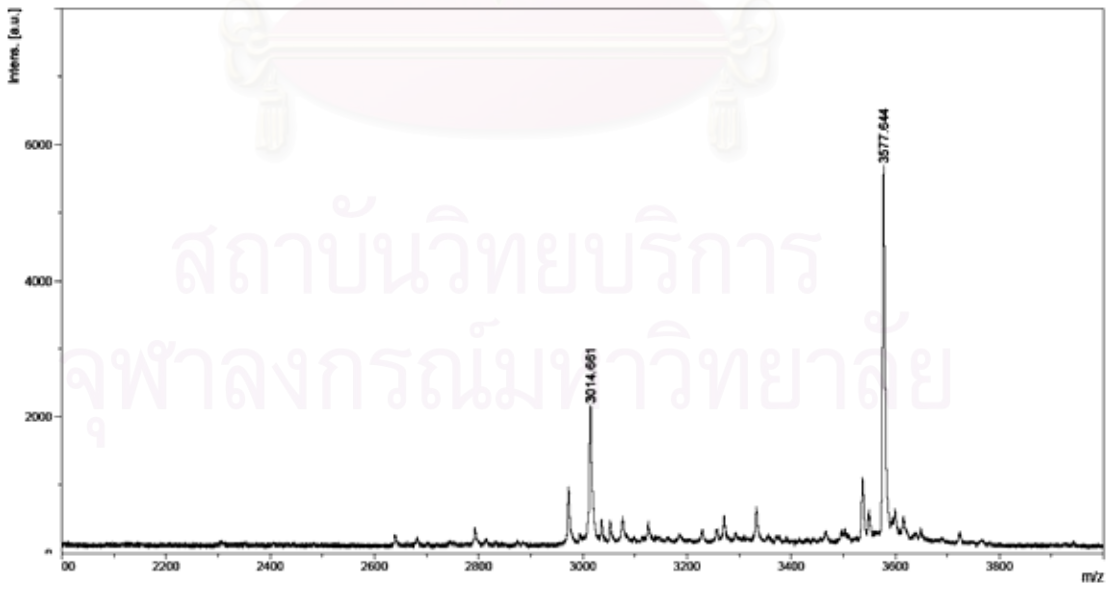

Figure C-10 : MALDI-TOF mass spectrum of Atto520-O-T_4CT_4-SerNH_2 **(P10)**

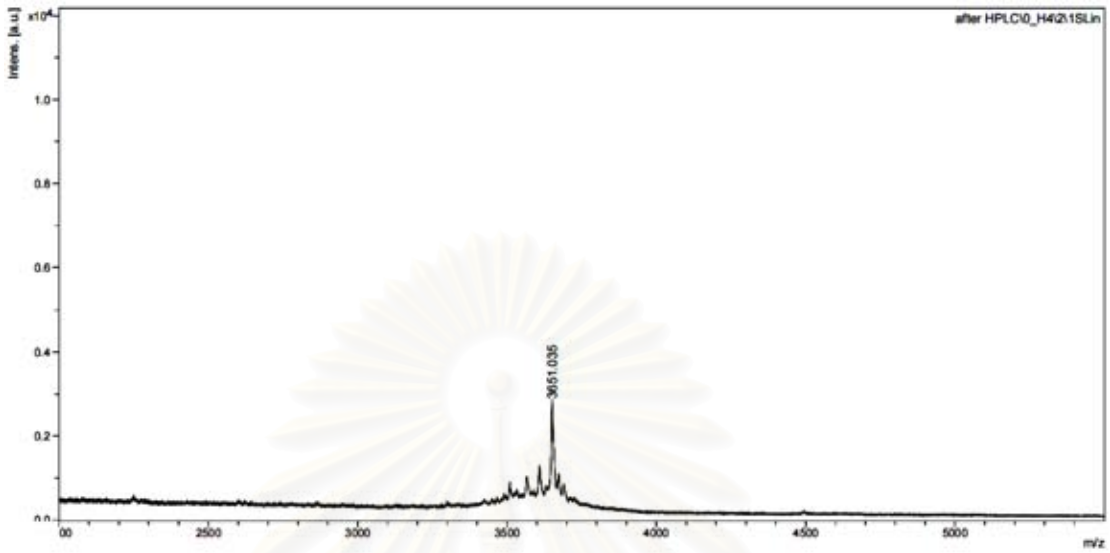

Figure C-11 : MALDI-TOF mass spectrum of Atto425-O-T_4GT_4-SerNH_2 **(P11)**

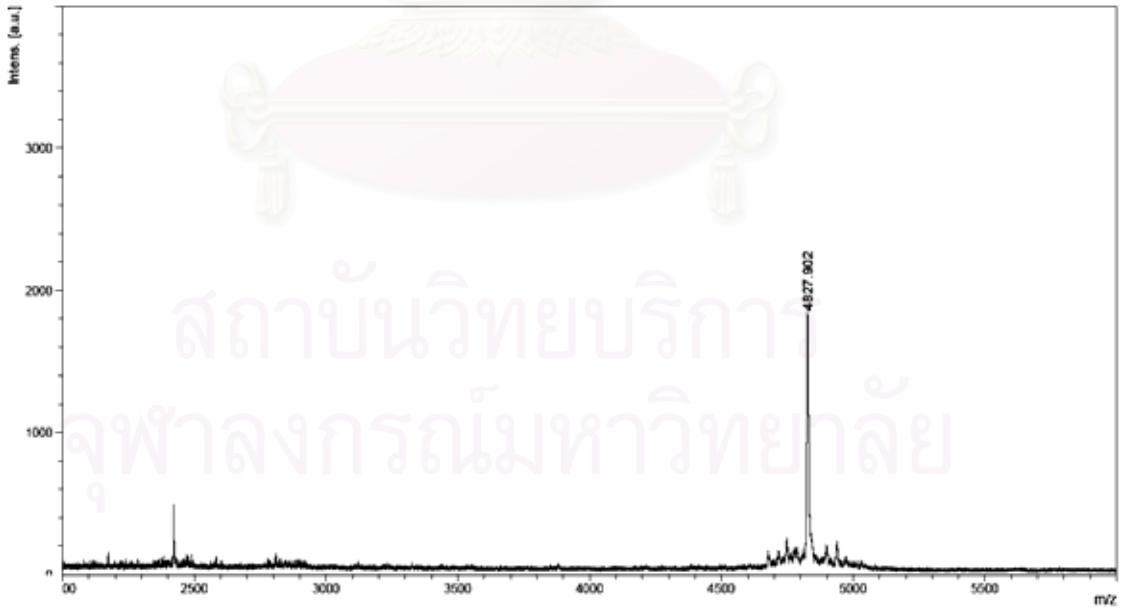

Figure C-12 : MALDI-TOF mass spectrum of carboxyFlu-O-TTCCCCCTCCCAA-SerNH_2 **(P12)**

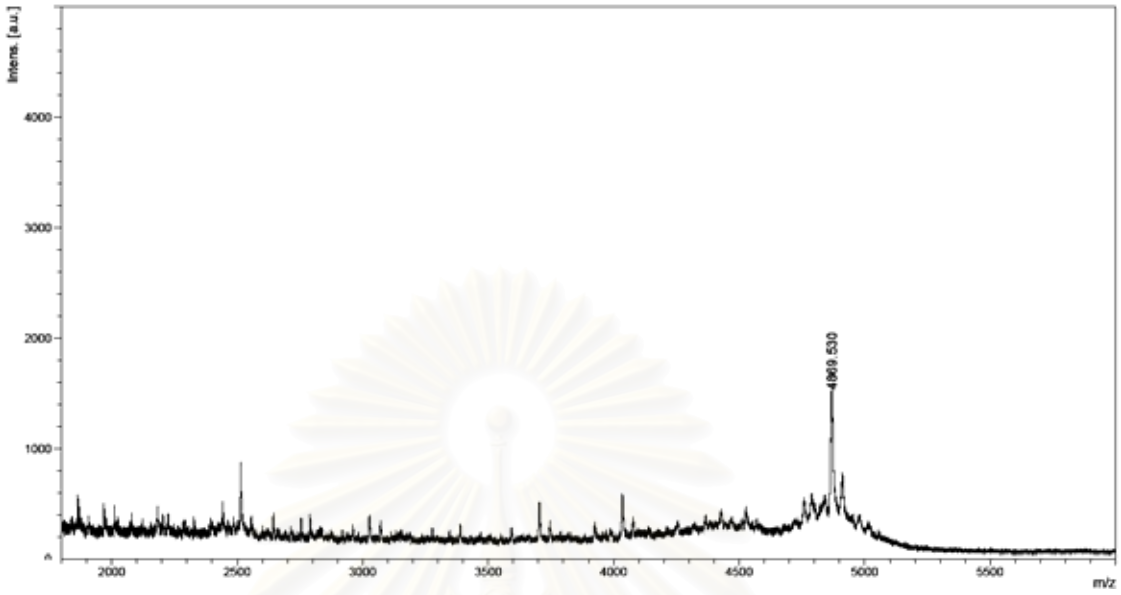

Figure C-13 : MALDI-TOF mass spectrum of Neutral Flu-O-TTCCCCCTCCCAA-$SerNH_2$ **(P13)**

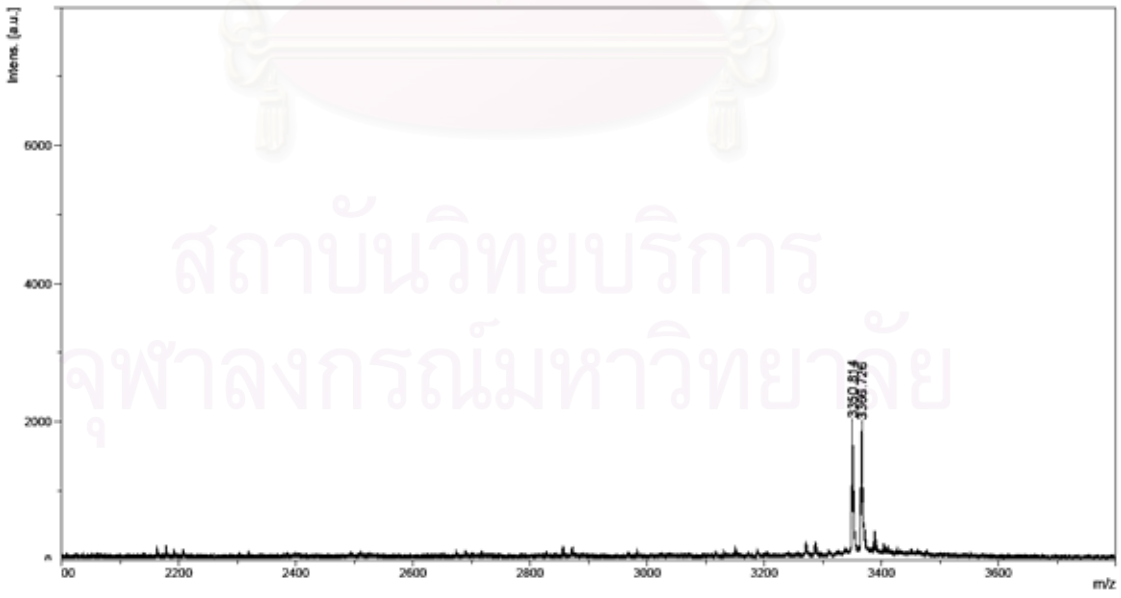

Figure C-14 : MALDI-TOF mass spectrum of DNS-T_9-$SerNH_2$ **(P14)**

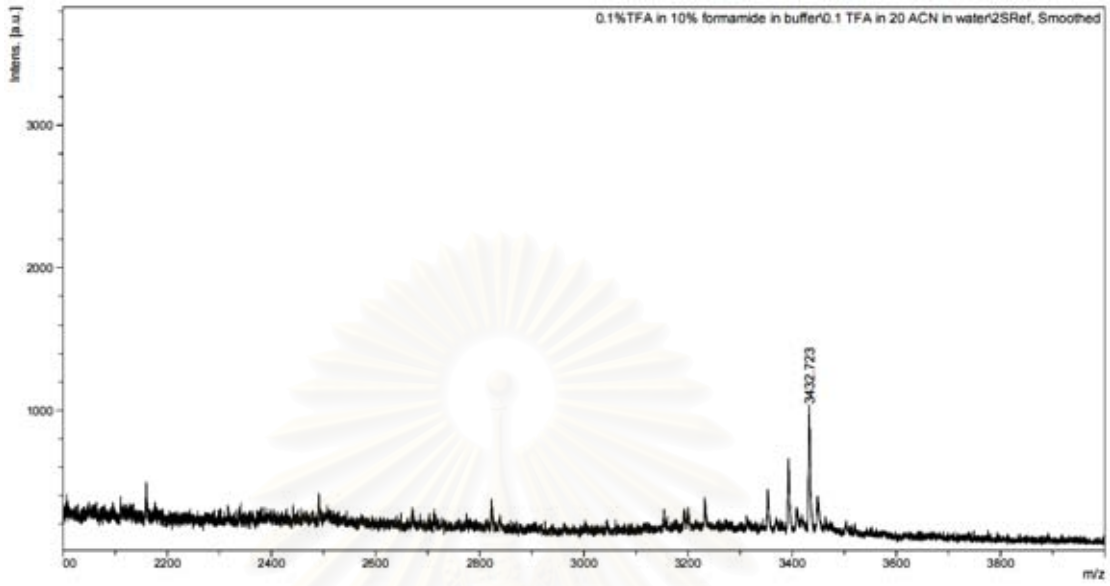

Figure C-15 : MALDI-TOF mass spectrum of DNS-Ser-T_9-SerNH_2 **(P15)**

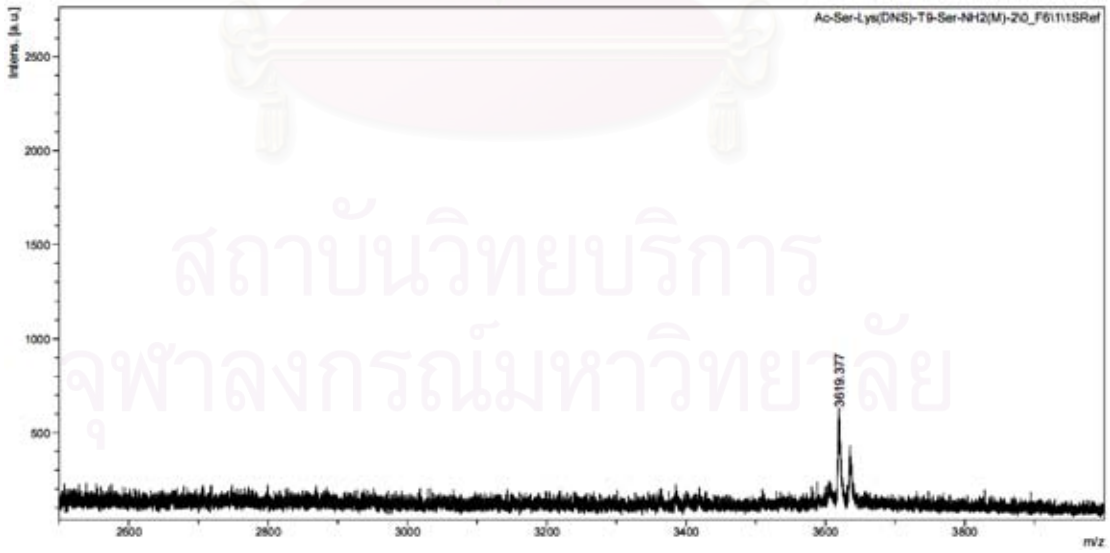

Figure C-16 : MALDI-TOF mass spectrum of Ac-Ser-Lys(DNS)-T_9-SerNH_2 **(P16)**

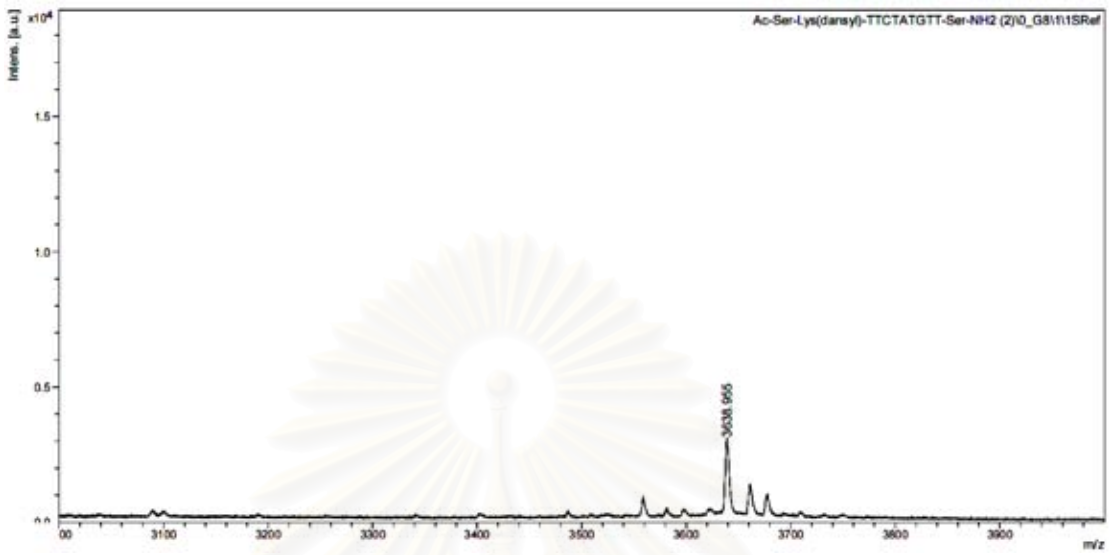

Figure C-17 : MALDI-TOF mass spectrum of Ac-Ser-Lys(DNS)-TTCTATGTT-SerNH_2 **(P17)**

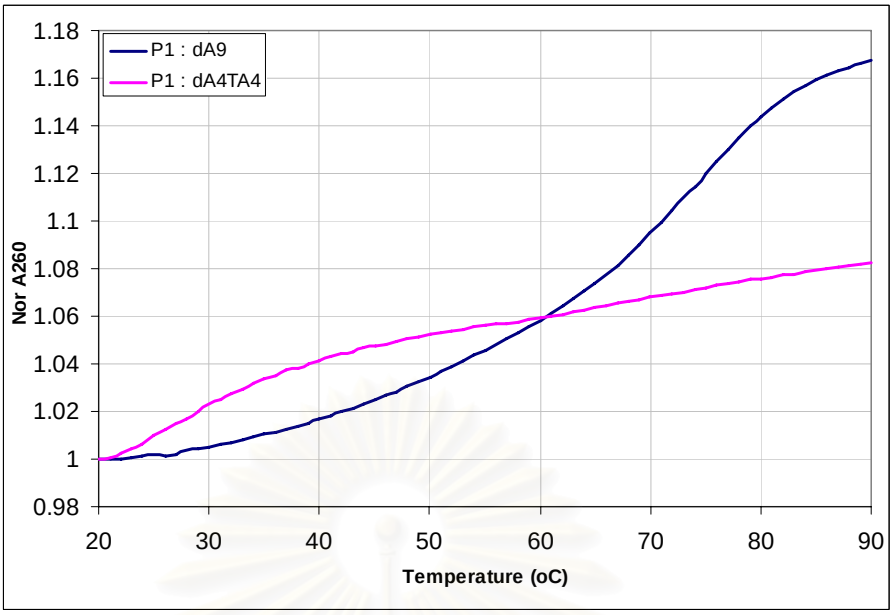

Figure D-1 T_m curves of PNA TMR-TTTTTTTTT-SerNH$_2$ (**P1**) with dA$_9$ and dA$_8$T: Condition PNA : DNA = 1:1, [PNA] = 0.1 µM, 10 mM sodium phosphate buffer, pH 7.0, heating rate 1.0 °C/min.

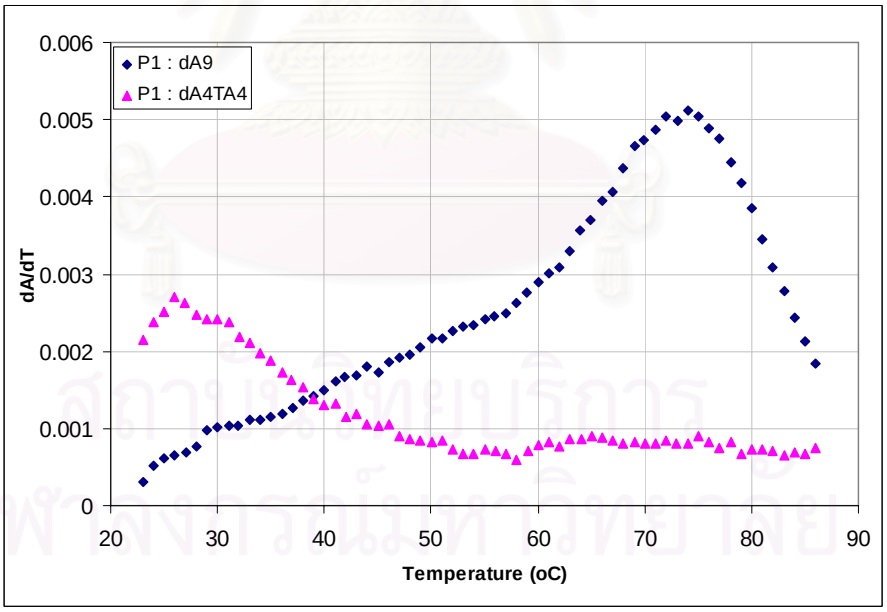

Figure D-2 First-derivative normalized UV-T_m plots between TMR-TTTTTTTTT-SerNH$_2$ (**P1**) with dA$_9$ and dA$_8$T: Condition PNA : DNA = 1:1, [PNA] = 0.1 µM, 10 mM sodium phosphate buffer, pH 7.0, heating rate 1.0 °C/min.

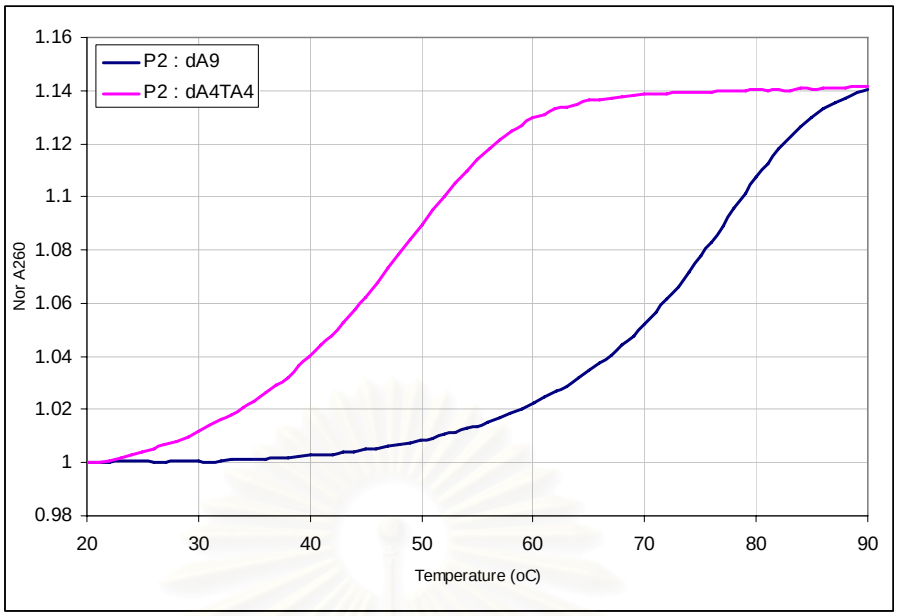

Figure D-3 T_m curves of PNA TMR-O-TTTTTTTTT-SerNH$_2$ (**P2**) with dA$_9$ and dA$_8$T: Condition PNA : DNA = 1:1, [PNA] = 0.1 µM, 10 mM sodium phosphate buffer, pH 7.0, heating rate 1.0 °C/min.

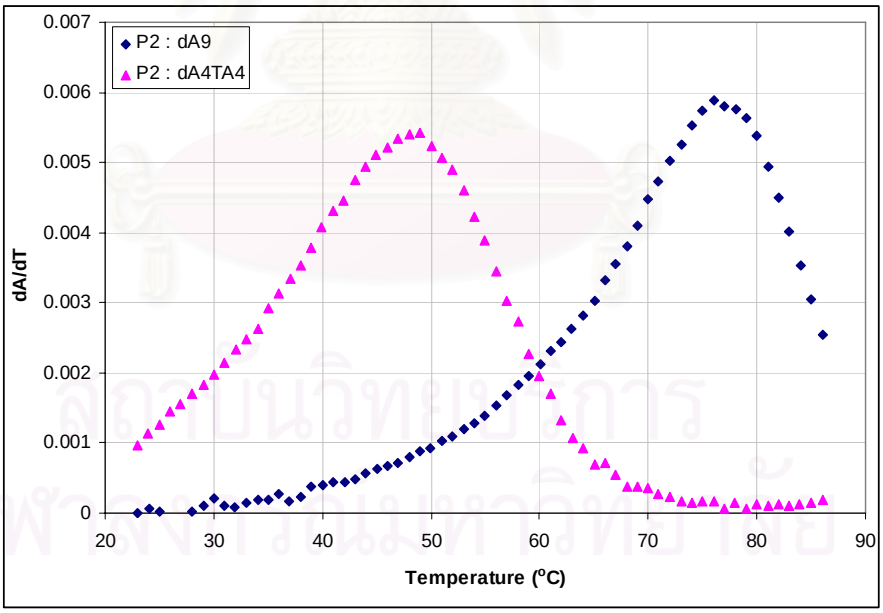

Figure D-4 First-derivative normalized UV-T_m plots between TMR-O-TTTTTTTTT-SerNH$_2$ (**P2**) with dA$_9$ and dA$_8$T: Condition PNA : DNA = 1:1, [PNA] = 0.1 µM, 10 mM sodium phosphate buffer, pH 7.0, heating rate 1.0 °C/min.

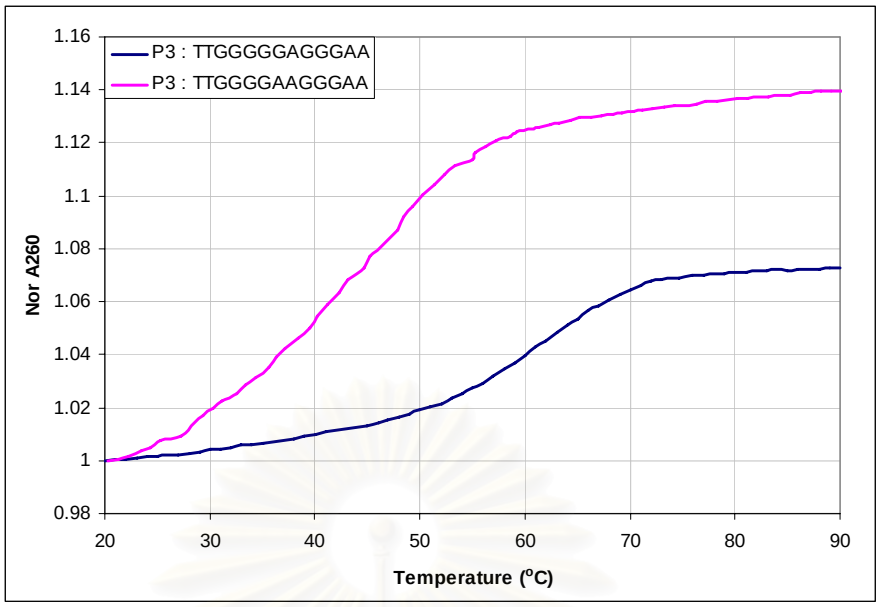

Figure D-5 T_m curves of PNA TMR-O-TTCCCCCTCCCAA-SerNH$_2$ (**P3**) with dTTGGGGGAGGGAA and dTTGGGGAAGGGAA : Condition PNA : DNA = 1:1, [PNA] = 0.1 µM, 10 mM sodium phosphate buffer, pH 7.0, heating rate 1.0 °C/min.

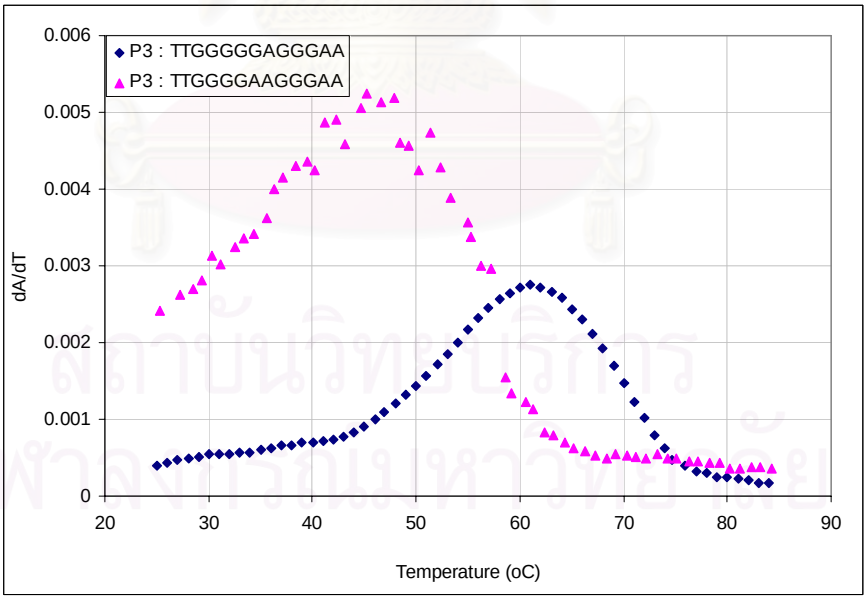

Figure D-6 First-derivative normalized UV-T_m plots between PNA TMR-O-TTCCCCCTCCCAA-SerNH$_2$ (**P3**) with dTTGGGGGAGGGAA and dTTGGGGAAGGGAA : Condition PNA : DNA = 1:1, [PNA] = 0.1 µM, 10 mM sodium phosphate buffer, pH 7.0, heating rate 1.0 °C/min.

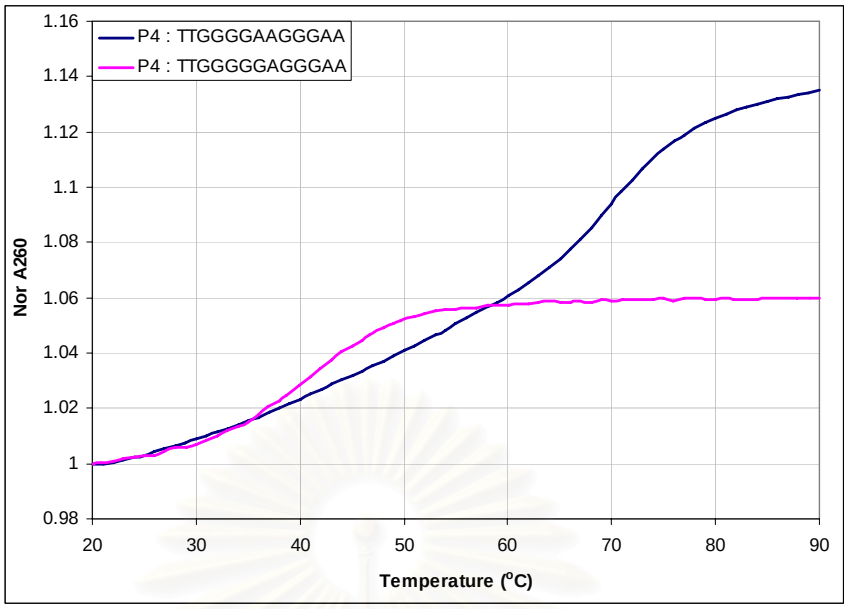

Figure D-7 T_m curves of PNA TMR-O-TTCCCCTTCCCAA-SerNH$_2$ (**P4**) with dTTGGGGAAGGGAA and dTTGGGGGAGGGAA : Condition PNA : DNA = 1:1, [PNA] = 0.1 µM, 10 mM sodium phosphate buffer, pH 7.0, heating rate 1.0 °C/min.

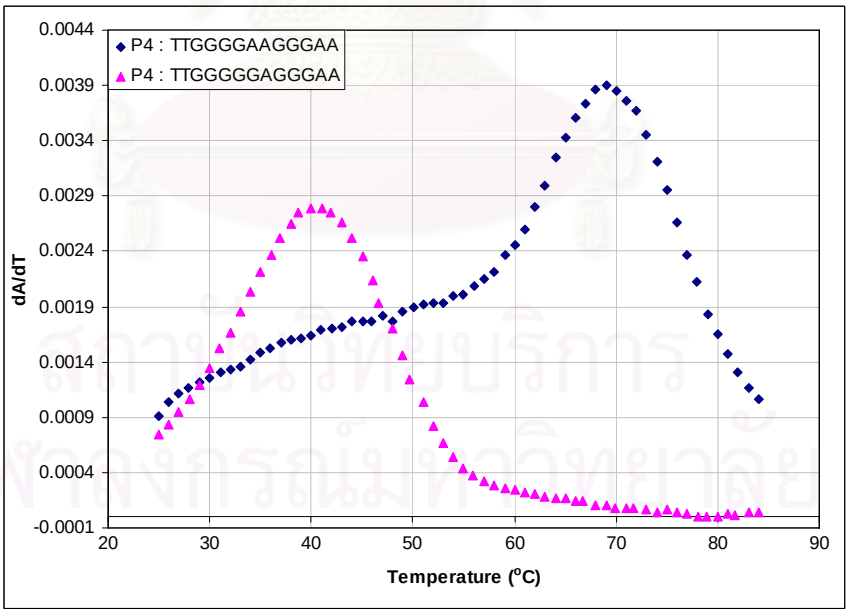

Figure D-8 First-derivative normalized UV-T_m plots between PNA TMR-O-TTCCCCTTCCCAA-SerNH$_2$ (**P4**) with dTTGGGGAAGGGAA and dTTGGGGGAGGGAA : Condition PNA : DNA = 1:1, [PNA] = 0.1 µM, 10 mM sodium phosphate buffer, pH 7.0, heating rate 1.0 °C/min.

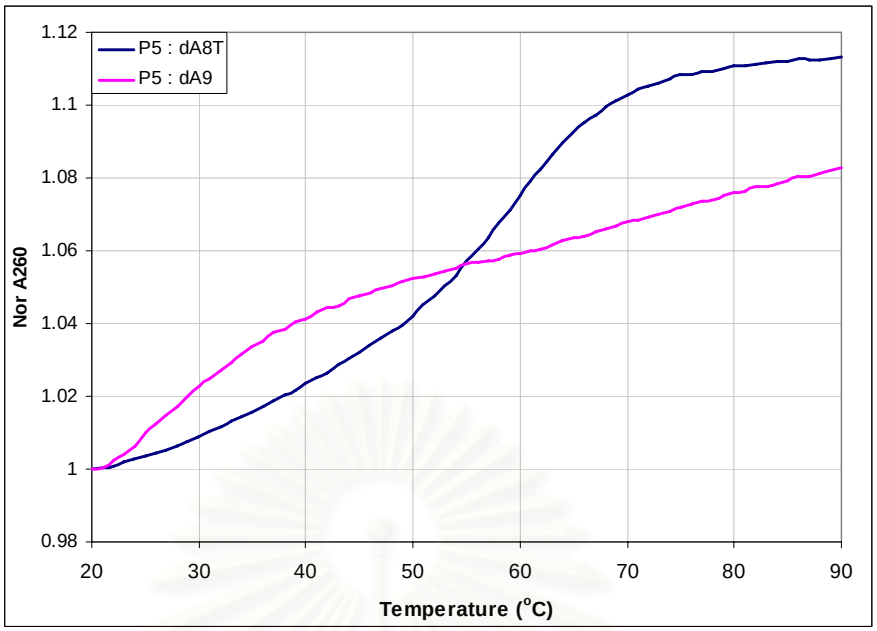

Figure D-9 T_m curves of PNA carboxyflu-O-TTTTATTTT-SerNH$_2$ (**P5**) with dA$_8$T and dA$_9$: Condition PNA : DNA = 1:1, [PNA] = 0.1 µM, 10 mM sodium phosphate buffer, pH 7.0, heating rate 1.0 °C/min.

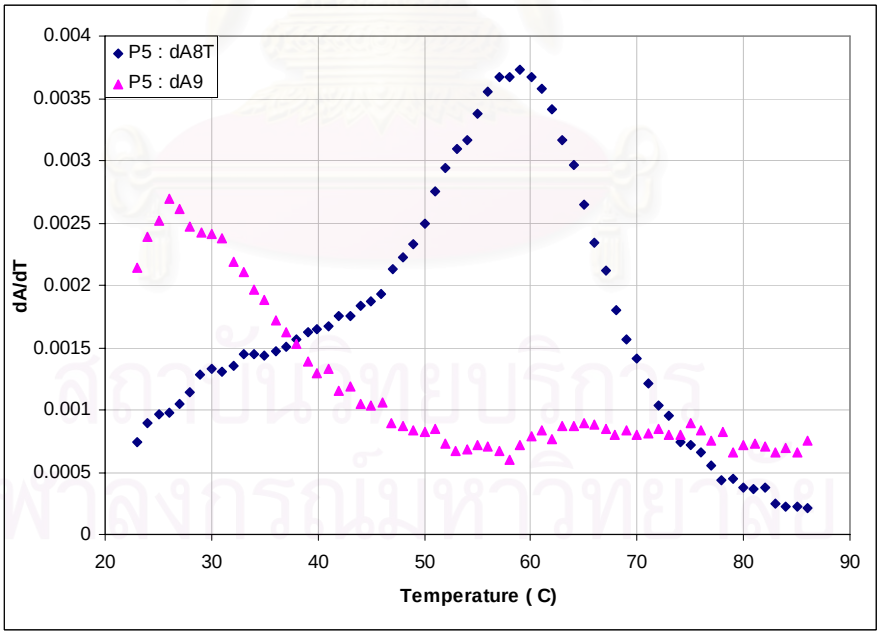

Figure D-10 First-derivative normalized UV-T_m plots between PNA carboxyflu-O-TTTTATTTT-SerNH$_2$ (**P5**) with dA$_8$T and dA$_9$: Condition PNA : DNA = 1:1, [PNA] = 0.1 µM, 10 mM sodium phosphate buffer, pH 7.0, heating rate 1.0 °C/min.

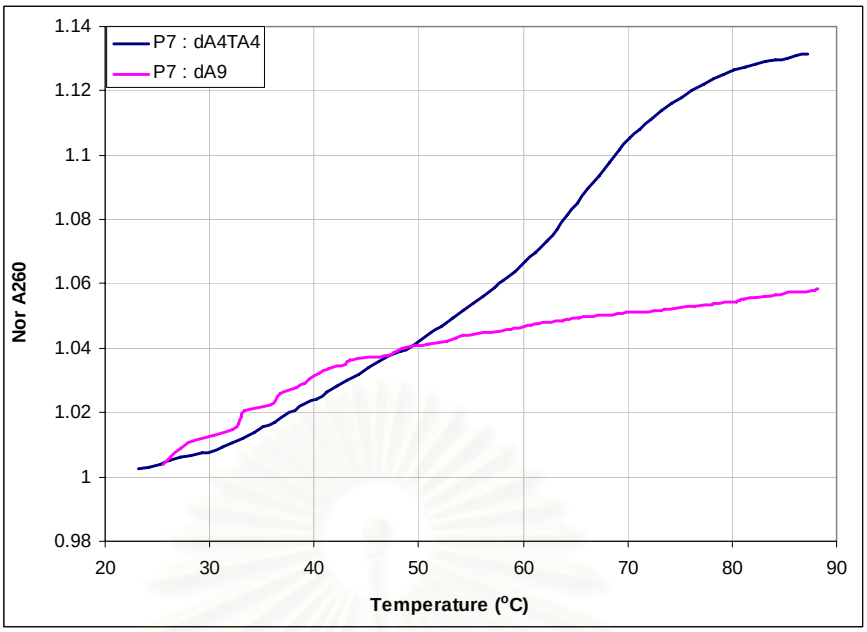

Figure D-11 T_m curves of PNA neutralflu-O-TTTTATTTT-SerNH$_2$ (**P7**) with dA$_8$T and dA$_9$: Condition PNA : DNA = 1:1, [PNA] = 0.1 µM, 10 mM sodium phosphate buffer, pH 7.0, heating rate 1.0 °C/min.

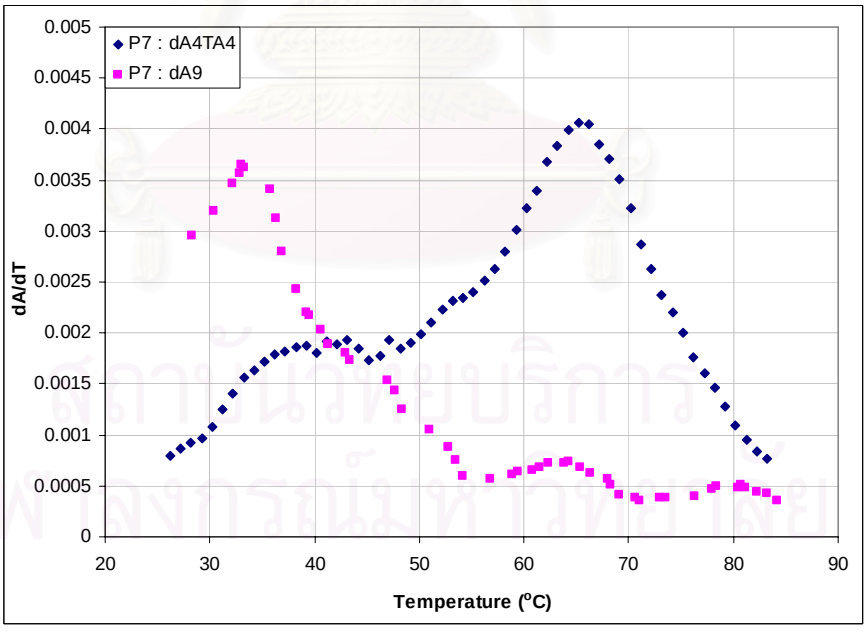

Figure D-12 First-derivative normalized UV-T_m plots between PNA neutralflu-O-TTTTATTTT-SerNH$_2$ (**P7**) with dA$_8$T and dA$_9$: Condition PNA : DNA = 1:1, [PNA] = 0.1 µM, 10 mM sodium phosphate buffer, pH 7.0, heating rate 1.0 °C/min.

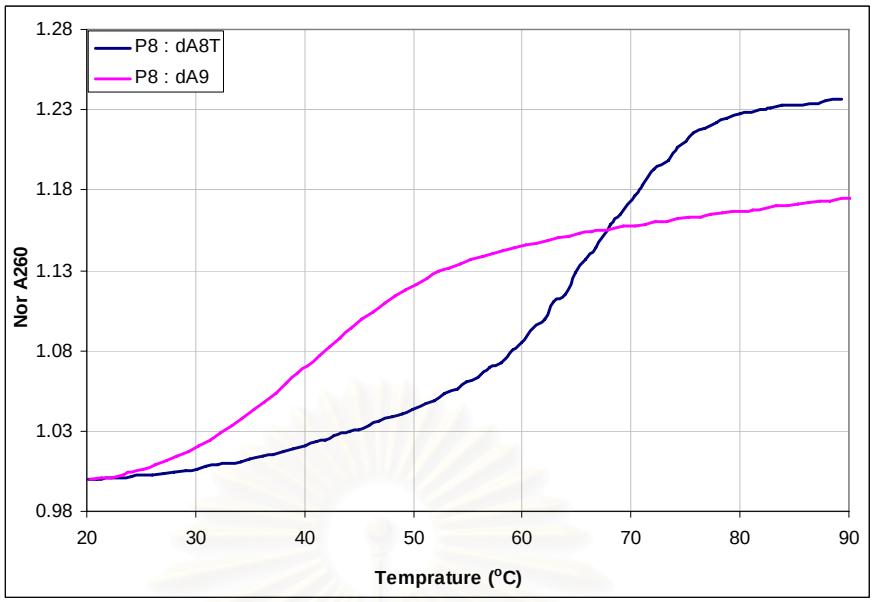

Figure D-13 T_m curves of NBD-O-TTTTATTTT-SerNH$_2$ (**P8**) with dA$_8$T and dA$_9$: Condition PNA : DNA = 1:1, [PNA] = 0.1 µM, 10 mM sodium phosphate buffer, pH 7.0, heating rate 1.0 °C/min.

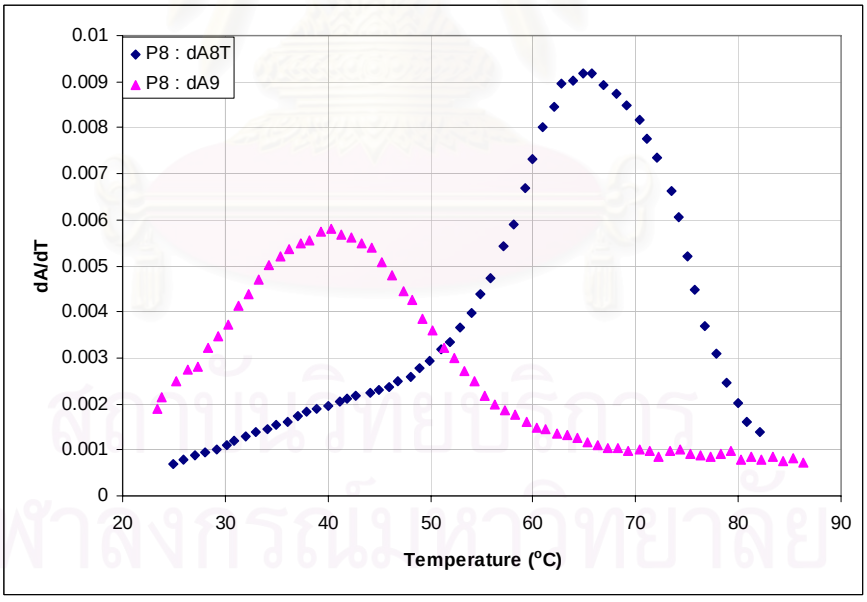

Figure D-14 First-derivative normalized UV-T_m plots between PNA NBD-O-TTTTATTTT-SerNH$_2$ (**P8**) with dA$_8$T and dA$_9$: Condition PNA : DNA = 1:1, [PNA] = 0.1 µM, 10 mM sodium phosphate buffer, pH 7.0, heating rate 1.0 °C/min.

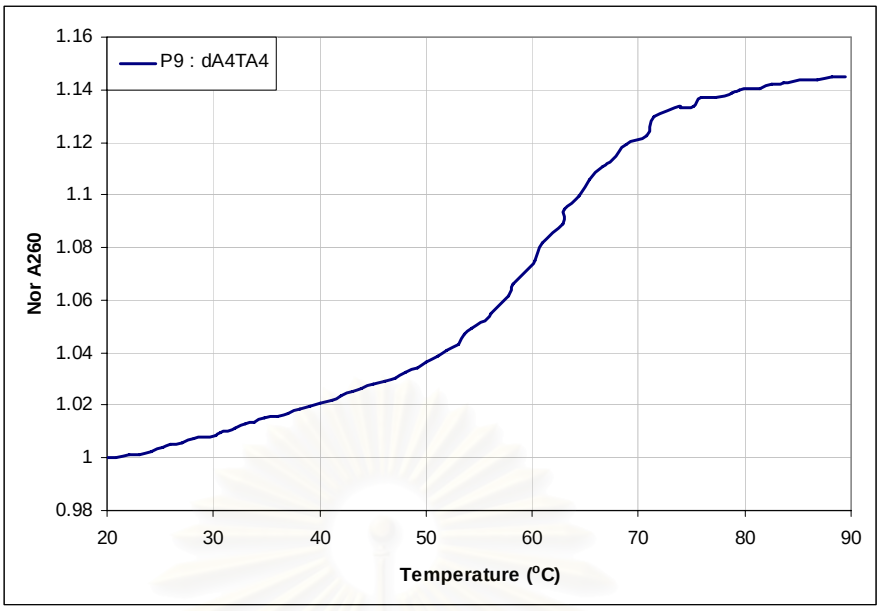

Figure D-15 T_m curves of PNA Pyr-O-TTTTATTTT-SerNH$_2$ (**P9**) with dA$_8$T : Condition PNA : DNA = 1:1, [PNA] = 0.1 µM, 10 mM sodium phosphate buffer, pH 7.0, heating rate 1.0 °C/min.

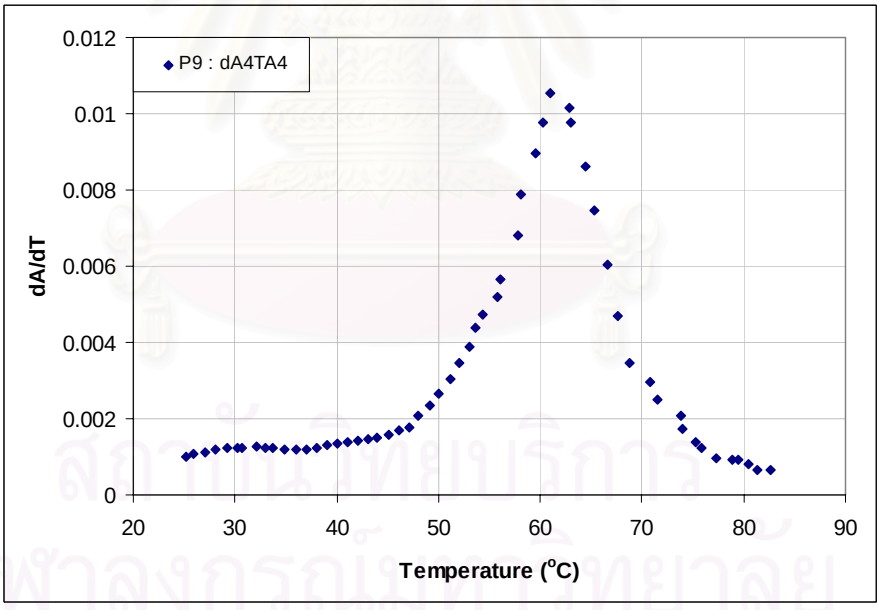

Figure D-16 First-derivative normalized UV-T_m plots between PNA Pyr-O-TTTTATTTT-SerNH$_2$ (**P9**) with dA$_8$T : Condition PNA : DNA = 1:1, [PNA] = 0.1 µM, 10 mM sodium phosphate buffer, pH 7.0, heating rate 1.0 °C/min.

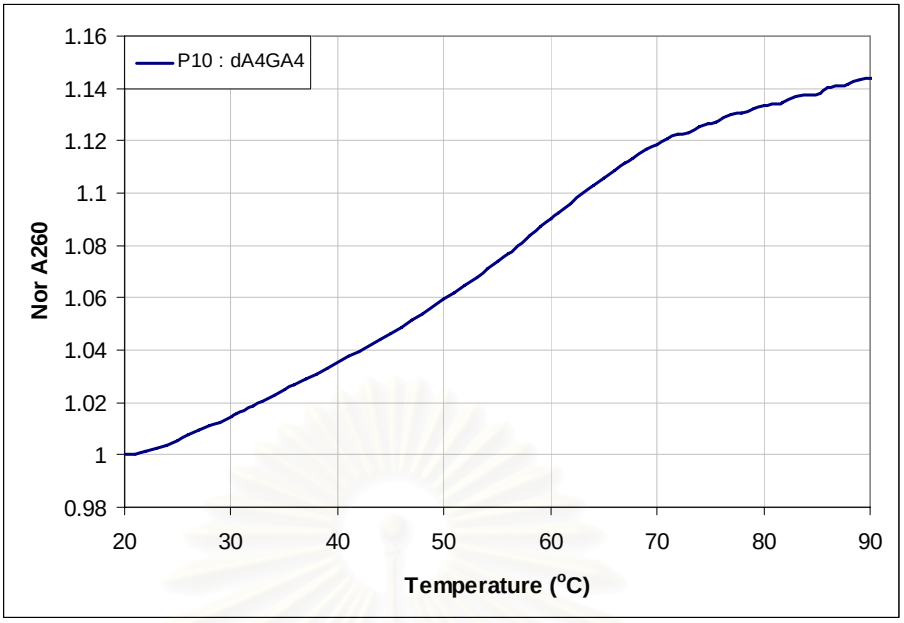

Figure D-17 T_m curves of PNA Atto520-O-TTTTCTTTT-SerNH$_2$ (**P10**) with dA$_8$G : Condition PNA : DNA = 1:1, [PNA] = 0.1 µM, 10 mM sodium phosphate buffer, pH 7.0, heating rate 1.0 °C/min.

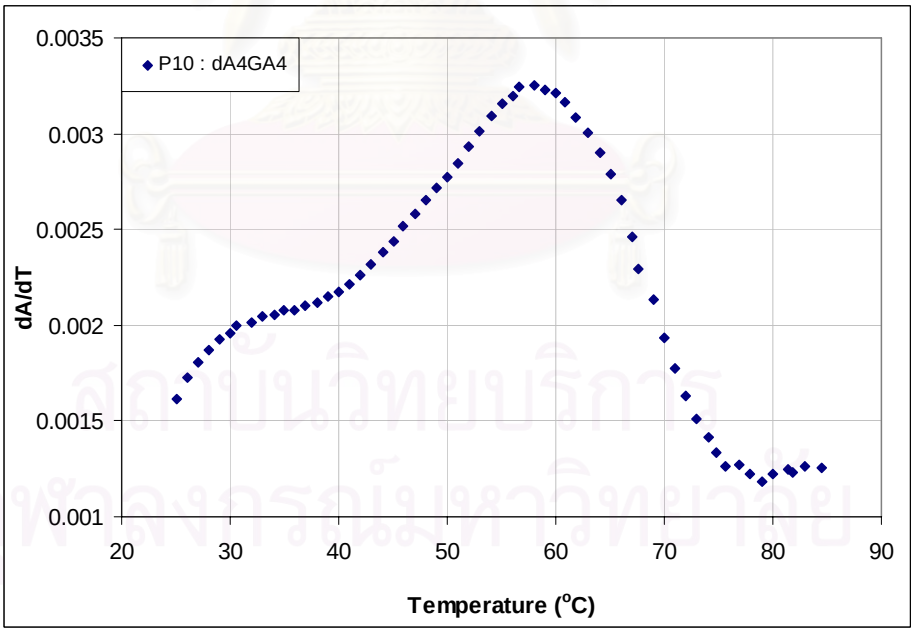

Figure D-18 First-derivative normalized UV-T_m plots between PNA Atto520-O-TTTTCTTTT-SerNH$_2$ (**P10**) with dA$_8$G : Condition PNA : DNA = 1:1, [PNA] = 0.1 µM, 10 mM sodium phosphate buffer, pH 7.0, heating rate 1.0 °C/min.

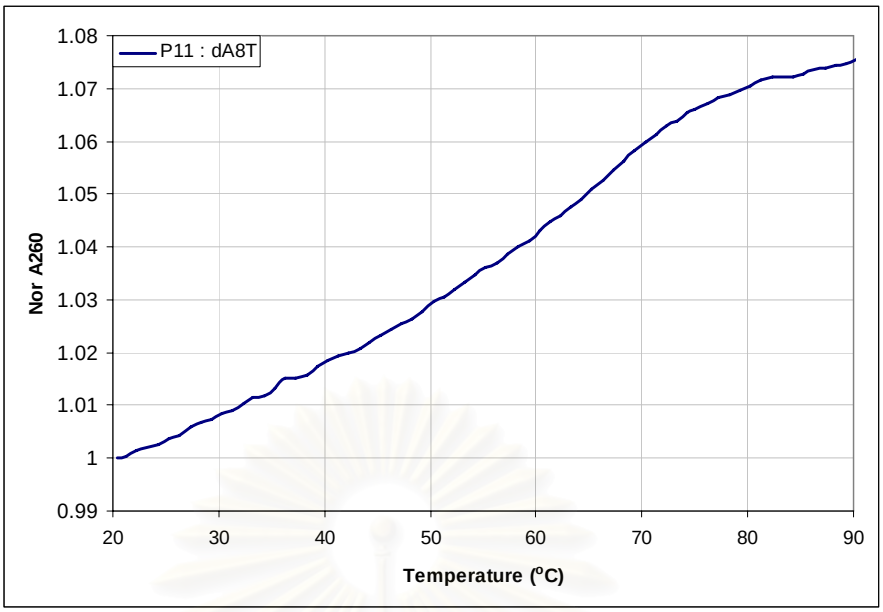

Figure D-19 T_m curves of PNA Atto425-O-TTTTGTTTT-SerNH$_2$ (**P11**) with dA$_8$C : Condition PNA : DNA = 1:1, [PNA] = 0.1 µM, 10 mM sodium phosphate buffer, pH 7.0, heating rate 1.0 °C/min.

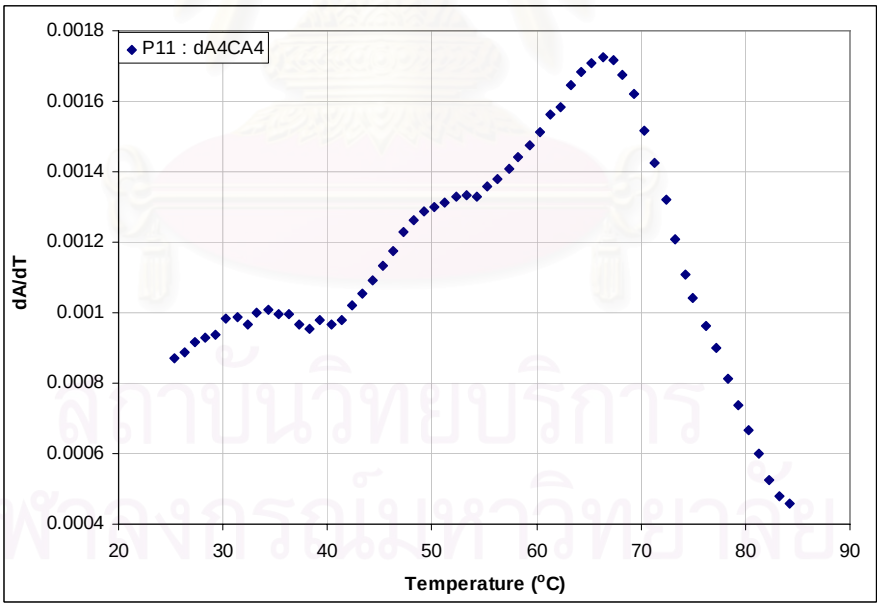

Figure D-20 First-derivative normalized UV-T_m plots between PNA Atto425-O-TTTTGTTTT-SerNH$_2$ (**P11**) with dA$_8$C: Condition PNA : DNA = 1:1, [PNA] = 0.1 µM, 10 mM sodium phosphate buffer, pH 7.0, heating rate 1.0 °C/min.

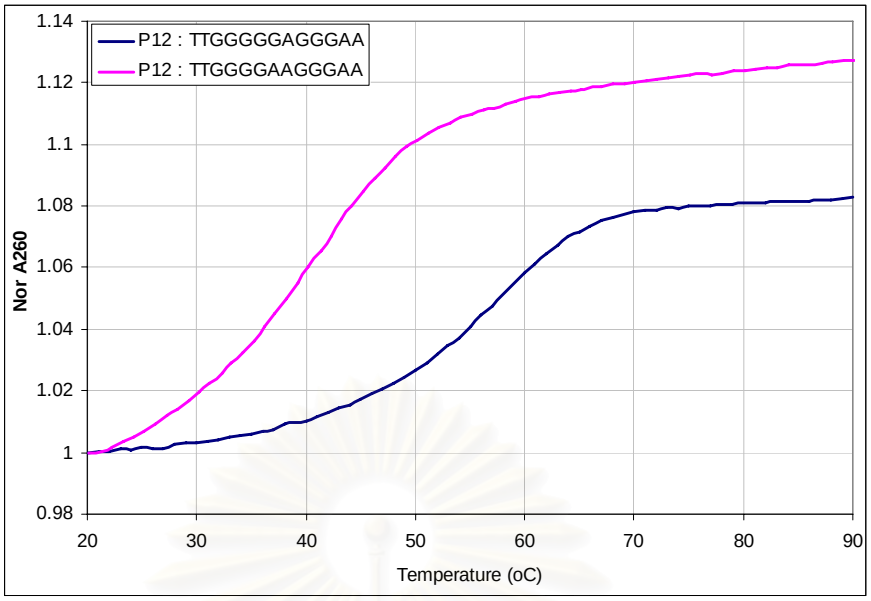

Figure D-21 T_m curves of PNA T_m curves of PNA Carboxyflu-O-TTCCCCCTCCCAA-SerNH$_2$ (**P12**) with dTTGGGGGAGGGAA and dTTGGGGAAGGGAA : Condition PNA : DNA = 1:1, [PNA] = 0.1 µM, 10 mM sodium phosphate buffer, pH 7.0, heating rate 1.0 °C/min.

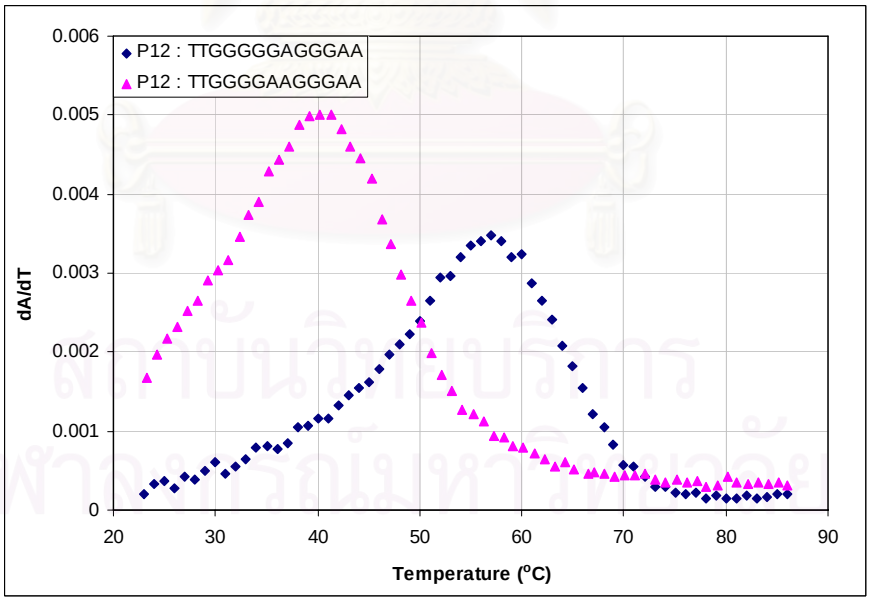

Figure D-22 First-derivative normalized UV-T_m plots between PNA Carboxyflu-O-TTCCCCCTCCCAA-SerNH$_2$ (**P12**) with dTTGGGGGAGGGAA and dTTGGGGAAGGGAA : Condition PNA : DNA = 1:1, [PNA] = 0.1 µM, 10 mM sodium phosphate buffer, pH 7.0, heating rate 1.0 °C/min.

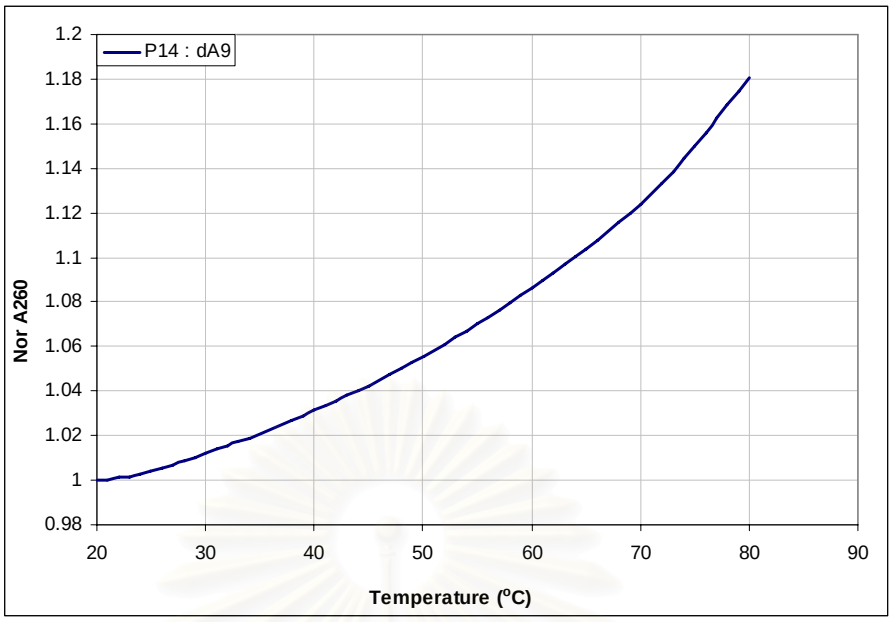

Figure D-23 T_m curves of PNA DNS-TTTTTTTTT-SerNH$_2$ (**P14**) with dA$_9$: Condition PNA : DNA = 1:1, [PNA] = 0.1 µM, 10 mM sodium phosphate buffer, pH 7.0, heating rate 1.0 °C/min.

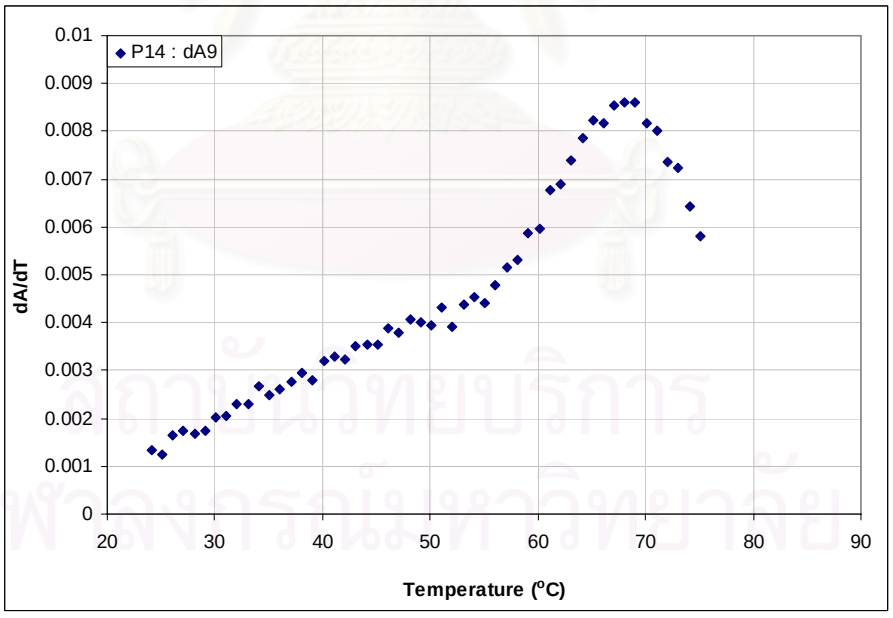

Figure D-24 First-derivative normalized UV-T_m plots between DNS-TTTTTTTTT-SerNH$_2$ (**P14**) with dA$_9$: Condition PNA : DNA = 1:1, [PNA] = 0.1 µM, 10 mM sodium phosphate buffer, pH 7.0, heating rate 1.0 °C/min.

VITAE

Pratchayaporn Korkaew was born on Febuary 08, 1979 in Sisaket, Thailand. She received Bachelor Degree of Science in Chemistry from Ramkhamhaeng University in 2005. Since 2006 she has become a student in Master Degree of Science of Chulalongkorn University studying in Department of Chemistry.